



Western Washington University  
Western CEDAR

---

WWU Graduate School Collection

WWU Graduate and Undergraduate Scholarship

---

Spring 2023

## New Synthetic Methods Based on Silicon-Tethered Nucleophilic Addition Reactions

Alexie W. Clover

---

Follow this and additional works at: <https://cedar.wwu.edu/wwuet>

New Synthetic Methods Based on Silicon-Tethered Nucleophilic Addition Reactions

By

Alexie W. Clover

Accepted in Partial Completion  
Of the Requirements of the Degree  
Master of Science

ADVISORY COMMITTEE

Dr. Gregory O'Neil, Chair

Dr. James Vyvyan

Dr. Mike Larsen

GRADUATE SCHOOL

Dr. David L. Patrick, Dean

**Master's Thesis**

In presenting this thesis in partial fulfillment of the requirements for a master's degree at Western Washington University, I grant to Western Washington University the non- exclusive royalty-free right to archive, reproduce, distribute, and display the thesis in any and all forms, including electronic format, via any digital library mechanisms maintained by WWU.

I represent and warrant this is my original work, and does not infringe or violate any rights of others. I warrant that I have obtained written permissions from the owner of any third party copyrighted material included in these files.

I acknowledge that I retain ownership rights to the copyright of this work, including but not limited to the right to use all or part of this work in future works, such as articles or books. Library users are granted permission for individual, research and non-commercial reproduction of this work for educational purposes only. Any further digital posting of this document requires specific permission from the author.

Any copying or publication of this thesis for commercial purposes, or for financial gain, is not allowed without my written permission.

Alexie W. Clover

June 2023

New Synthetic Methods Based on Silicon-Tethered Nucleophilic Addition Reactions

A Thesis  
Presented to  
The Faculty of  
Western Washington University

In Partial Fulfillment  
Of the Requirements for the Degree  
Master of Science

By  
Alexie W. Clover  
June 2023

## **Abstract**

With the recent discovery of an iodine mediated rearrangement of diallylsilanes, we set out to investigate a similar fluorine mediated rearrangement, aimed at introducing a new method for synthesizing organofluorine compounds. Interest in incorporating fluorine into organic molecules has grown significantly in recent years, primarily for medicinal applications. Since certain fluorination methods require the use of mCPBA, a common epoxidizing reagent, control experiments were performed on the reaction of several diallylsilanes with mCPBA, anticipating that a competing epoxidation of the diallylsilanes might occur. It was found that the formation of the hydroxy ester occurred through a regioselective epoxide opening from the carboxylic acid derivative of mCPBA. This was later mitigated by the addition of a basic buffer to yield the epoxysilanes. Various Lewis and Bronsted acids were screened to promote an intramolecular epoxide opening, however it was observed that Triethylamine trihydrofluoride (HF TEA) had complete regioselective fluoride ring opening of the given epoxide under mild conditions. To our knowledge this type of fluorine ring opening has not been described. Attachment of different ligands on silicon permits the tunability and activation of the so-called beta silyl effect. A range of epoxysilanes containing different groups on silicon were studied to investigate the rate, stereoselectivity, and further functionalization.

## Acknowledgments

**Research Advisor:** Dr. Gregory W. O'Neil

**Thesis Committee Members:** Dr. James Vyvyan

Dr. Mike Larsen

**Project Contributors:** Adam Jones

**Instrument Technicians:** Dr. Hla Win-Piazza

Mark Lorenz

### And Others:

A special thank you to my family who has given me unconditional love and support throughout my graduate studies. I am especially grateful to Professor O'Neil for allowing me to join his research group and for serving as my advisor. I feel fortunate to have been part of a terrific group of scientists in the O'Neil lab. Additionally, I'd like to thank Adam for all the help and fun times in the lab. And last but definitely not least, thank you Brian for the countless good times and support throughout this journey. I could not have done this without all of you!

## Table of Contents

Abstract	iv
Acknowledgements	v
List of Figures, Tables, and Schemes	vii
<b>Chapter 1: Introduction</b>	
1.1 Background	1
1.2 Iodine Mediated Rearrangement	4
1.3 Exploring Fluorine as an Additional Electrophile with Diallylsilanes	8
1.4 Importance of Fluorine Containing Compounds	8
<b>Chapter 2: Initial Discovery of Fluorohydins</b>	
2.1 Attempts at the Fluorine Mediated Rearrangement	11
2.2 Epoxidation of Allylsilanes	17
2.3 Attempts at an Intramolecular Epoxide Allylation	18
2.4 Initial Discovery of Fluorohydrin	21
<b>Chapter 3: Fluorohydrin Synthesis</b>	
3.1 Introduction to Fluorohydins	22
3.2 Optimization and Scope	25
3.3 One-pot Synthesis of Fluorohydins	30
3.4 Probing the Mechanism	32
<b>Chapter 4: Functionalization of Fluorohydins</b>	
4.1 Transformations and Tamao Oxidation	38
4.2 Conformational Analysis of the Fluorine-Silicon Interaction	44
4.3 Conclusion and Outlook	53
<b>Chapter 5: Experimentals</b>	54
<b>Crystal Data of 82</b>	66
<b>Spectra</b>	68
<b>Work Cited</b>	99

## List of Figures, Tables, and Schemes

### **Figures:**

<b>Figure 1.1.</b> The beta-silicon effect.	2
<b>Figure 1.2.</b> Reaction rates measured in 97% trifluoroethanol at 25 °C.	2
<b>Figure 1.3.</b> First and second wave of fluoro-pharmaceuticals that were brought to market.	9
<b>Figure 1.4.</b> FDA-approved PET tracers with fluorine-18 as of August 2021.	10
<b>Figure 3.1.</b> The <i>gauche</i> and <i>anomeric</i> effect due to hyperconjugation from donor-acceptor interactions.	23
<b>Figure 3.2.</b> Mosher ester 1 H NMR analysis of enantioenriched 3-silylfluorohydrins. Integration values for the $\alpha$ -fluoro hydrogen in all cases was ~1:5:1, consistent with the ee measured for the triisopropylsilyl epoxide (22%).	34
<b>Figure 4.1.</b> $^1\text{H}$ NMR of $\text{I}_2$ , MeOH with allyldiphenyl silane <b>116</b> resulting in unknown side products.	41
<b>Figure 4.2.</b> COSY NMR of $\text{I}_2$ , MeOH with allyldiphenyl silane <b>116</b> resulting in unknown side products.	42
<b>Figure 4.3.</b> Computational study regarding rotation about the Si-C-C-F bond for TMS fluorohydrin <b>91</b> .	46
<b>Figure 4.4.</b> Image of TMS fluorohydrin <b>91</b> in lowest energy <i>anti</i> conformation.	46
<b>Figure 4.5.</b> Crystal structure ORTEP image of triphenylsilyl fluorohydrin <b>82</b> .	47
<b>Figure 4.6.</b> Model systems from the Emenike group.	48
<b>Figure 4.7.</b> NMR coupling constant study using substrates <b>91</b> and <b>82</b> .	51
<b>Figure 4.8.</b> Global energy minima of DFE in the <i>gauche</i> conformation.	52
<b>Figure 5.1.</b> ORTEP of the structure with thermal ellipsoids at the 50% probability level. Disorder omitted for clarity.	67

### **Tables:**

<b>Table 1.1.</b> Reaction routes of diallylsilanes with different electrophiles	4
<b>Table 2.1.</b> Attempted fluorine rearrangement products with p-iodotoluene, selectfluor, DCM, and an HF source.	13
<b>Table 2.2.</b> Attempted fluorine rearrangement products with PhIO, DCM, and an HF source.	15
<b>Table 2.3.</b> Attempted fluorine rearrangement products with p-iodotoluene, mCPBA, DCM, and HF pyr.	16
<b>Table 2.4.</b> Attempts at intramolecular epoxide allylation with various Lewis Acids.	19
<b>Table 2.5.</b> Attempts at intramolecular epoxide allylation with non-chlorine Lewis Acids.	20
<b>Table 2.6.</b> Attempts at fluorine product <b>24</b> with deoxyfluorination Lewis Acids.	21
<b>Table 3.1.</b> Conversion of triphenyl epoxysilane <b>76</b> to triphenylsilyl fluorohydrin <b>82</b> using different solvents.	30
<b>Table 4.1.</b> Oxidation and Wittig product followed by Tamao-Fleming conditions with triphenyl and dimethylphenyl silyl.	39
<b>Table 4.2.</b> Reaction conditions for screening unveiling the masked hydroxy group using iodine.	43
<b>Table 5.1.</b> Crystallographic Data for the <b>82</b> .	67

### **Schemes:**

<b>Scheme 1.1.</b> Reactions involving diallylsilanes as useful synthetic tools.	1
<b>Scheme 1.2.</b> Domino allylation of diallylsilane with $\alpha, \beta$ -unsaturated ketones.	3
<b>Scheme 1.3.</b> Mechanism of Domino allylation of diallylsilane with $\alpha, \beta$ -unsaturated ketones.	3

<b>Scheme 1.4.</b> Intramolecular iodine mediated rearrangement of diallyldiphenylsilane.	5
<b>Scheme 1.5.</b> Elimination of diallyldimethylsilane to form allyliodide.	5
<b>Scheme 1.6.</b> Further transformations of the iodine mediated rearrangement product.	6
<b>Scheme 1.7.</b> Iodine rearrangement followed by asymmetric dihydroxylation synthesis of enantioenriched and diastereomeric cyclic silyl ethers.	7
<b>Scheme 1.8.</b> Elimination of iodine from diastereomeric compound <b>19</b> to cyclic allylsilane <b>21</b> .	7
<b>Scheme 1.9.</b> Fluorine mediated rearrangement from pre-existing work from the O’Neil group.	8
<b>Scheme 2.1.</b> Difluorination of alkenes <b>25</b> and <b>27</b> with the proposed mechanism.	12
<b>Scheme 2.2.</b> Difluorination and aryl migration using PHIO.	14
<b>Scheme 2.3.</b> Difluorination using mCPBA as catalyst oxidant.	16
<b>Scheme 2.4.</b> Epoxide openings from 3-chlorobenzoic acid of diallyldimethylsilane <b>10</b> and <b>49</b> .	17
<b>Scheme 2.5.</b> Regioselective ring opening of trimethylepoxysilane with different acids.	18
<b>Scheme 2.6.</b> The initial discovery of allyldiphenyl fluorohydrin from HF•TEA.	21
<b>Scheme 2.7.</b> Opposite regioselectivity of fluorohydrins from selectfluor with allylsilanes.	22
<b>Scheme 3.1.</b> Epoxide openings of <b>65</b> and <b>67</b> under harsh conditions to yield fluorohydrins <b>66</b> and <b>68</b> .	24
<b>Scheme 3.2.</b> Reaction of epoxide <b>69</b> with HF•TEA resulting in by-products and optimization.	25
<b>Scheme 3.3.</b> Oxone epoxidation of different allylsilanes with corresponding yields and reaction run times.	27
<b>Scheme 3.4.</b> Fluorohydrin synthesis from epoxysilanes with an explanation of regioselectivity and structures of byproducts.	29
<b>Scheme 3.5.</b> One-pot synthesis of fluorohydrins from the Sedgwick group.	31
<b>Scheme 3.6.</b> One-pot synthesis of fluorohydrins from allylsilanes.	32
<b>Scheme 3.7.</b> Shi epoxidation of allylsilanes to give epoxysilanes.	33
<b>Scheme 3.8.</b> Enantioenriched epoxysilanes and their corresponding fluorohydrin with an assessment of fluorohydrin enantiopurity by conversion to the Mosher ester derivative.	33
<b>Scheme 3.9.</b> Grubbs metathesis with allylsilanes to yield substituted 4-(silyl)but-2-en-1-ol of <b>97</b> and <b>98</b> in 55% and 87% yield, respectively.	35
<b>Scheme 3.10.</b> One-pot reactions with 4-(silyl)but-2-en-1-ol to yield <b>99</b> and <b>100</b> with slight retention of stereochemistry.	36
<b>Scheme 3.11.</b> Formation of $\alpha$ -substituted allylsilanes with subsequent epoxidation followed by HF•TEA.	37
<b>Scheme 4.1.</b> Protection of fluorohydrin <b>59</b> and Tamao conditions for transformation of masked hydroxy group.	40
<b>Scheme 4.2.</b> Allyldiphenyl silane <b>116</b> reacting of I <sub>2</sub> and MeOH resulting in unknown side products.	40
<b>Scheme 4.3.</b> Treatment of silane <b>119</b> with Tamao conditions, unfortunately recovering starting material.	42
<b>Scheme 4.4.</b> Protection of fluorohydrin <b>80</b> followed by One-pot Tamao conditions to synthesize <b>121</b> .	44
<b>Scheme 4.5.</b> Possible explanation to elimination during the one-pot Tamao oxidations.	52

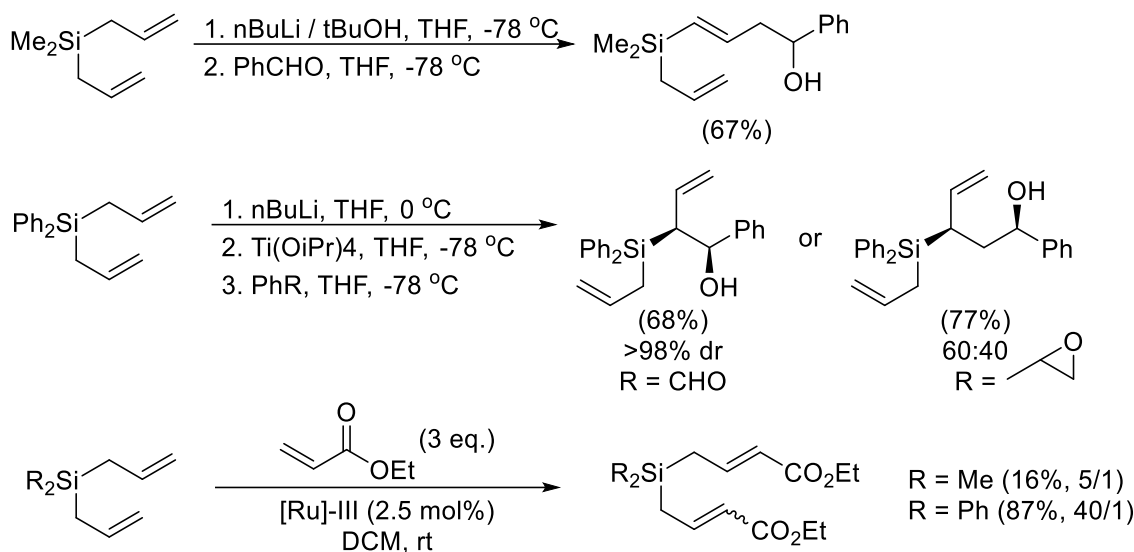
## Chapter 1. Introduction

### 1.1 Background

The formation of carbon-carbon bonds is of great importance in synthetic organic chemistry.

Organosilanes have proven to be an invaluable tool for this feat. Examples include the Sakurai allylation and the Mukaiyama aldol reaction.<sup>1,2</sup> Many reactions of this nature have been documented, however the use of diallylsilanes for this purpose remains a largely underexplored area for synthetic chemists. Current carbon-carbon bond forming reactions involving diallylsilanes range from the coupling of carbonyls,<sup>3,4</sup> epoxides,<sup>4</sup> and cross metathesis<sup>5</sup> (Scheme 1.1). Unlike the Sakurai allylation reaction, which is driven by the stabilization of a carbocation, these are some reactions that proceed without the utilization of the  $\beta$ -silyl effect.

**Scheme 1.1.** Reactions involving diallylsilanes as useful synthetic tools.



The  $\beta$ -silyl effect is a type of hyperconjugation where silicon stabilizes a positive charge on a carbon in the  $\beta$ -position.<sup>6</sup> The C-Si  $\sigma$  orbital in **1** can donate electron density to the empty p-orbital in the  $\beta$  position **2** to stabilize the resulting carbocation (Figure 1.1). This effect can also present itself as a destabilizing force for a bond at this position (i.e. C-X  $\sigma$ ). In this case, the C-Si  $\sigma$  orbital is able to donate electron density into the C-X  $\sigma^*$  orbital **3** thus weakening the bond. This effect is maximized when the two groups are antiperiplanar to each other.<sup>7</sup> This combination of C-X  $\sigma$  bond destabilization and  $\beta$ -carbocation stabilization increases the kinetics for heterolysis at this position.

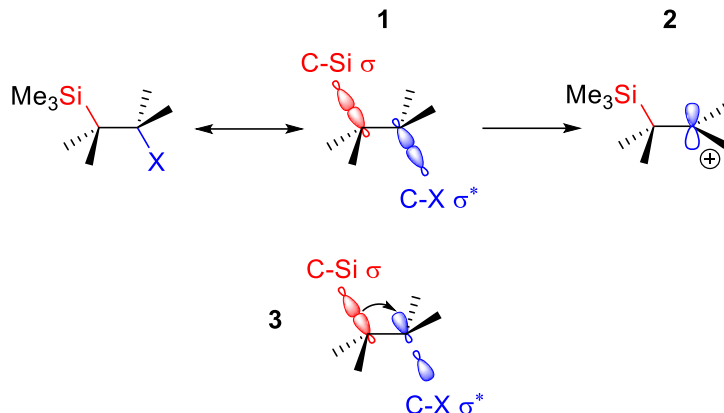


**Figure 1.1.** The beta-silicon effect.

Lambert et al. studied the impact silicon has on the rate for an S<sub>N</sub>1 reaction between trifluoroacetates and ethanol.<sup>8</sup> The results demonstrated the accelerating effect that silicon has on an S<sub>N</sub>1 reaction rate, especially if the leaving group is positioned antiperiplanar (Figure 1.2). With the leaving group  $\beta$  and trans to silicon, the observed reaction rate is just under 10 orders of magnitude larger than the compound lacking silicon. While Lambert saw the largest effects on rate for the trans orientation of the leaving group and silyl groups, the cis conformation still had a reaction rate 5 orders of magnitude larger than the non-silyl compound. Lambert attributed this reduced reaction rate to a lessening of the beta-silyl effect for the cis, as the strength of hyperconjugation is highly dependent on the dihedral angle.<sup>6,8</sup> In the anti-configuration, the rate enhancement effect of silicon is  $\sim 10^{10}$  with  $10^8$  being attributed to hyperconjugation and  $10^2$  from the inductive effects of the silicon bond. In the cis-configuration, the rate enhancement is much lower ( $\sim 10^4$ ) as the hyperconjugation effects are drastically reduced to  $10^2$  while the inductive effects stay nearly identical at  $10^2$ .

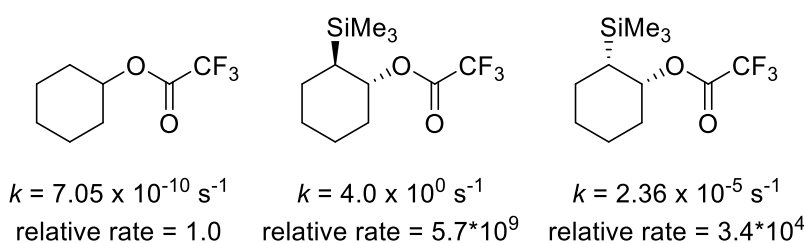
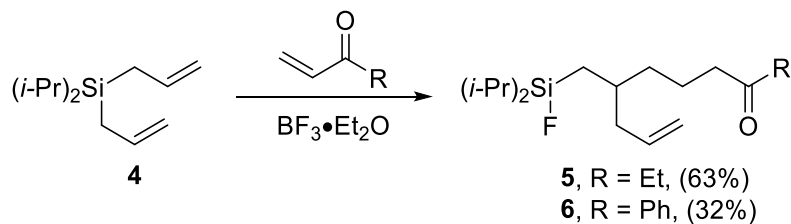


**Figure 1.2.** Reaction rates measured in 97% trifluoroethanol<sub>(aq)</sub> at 25.0°C.

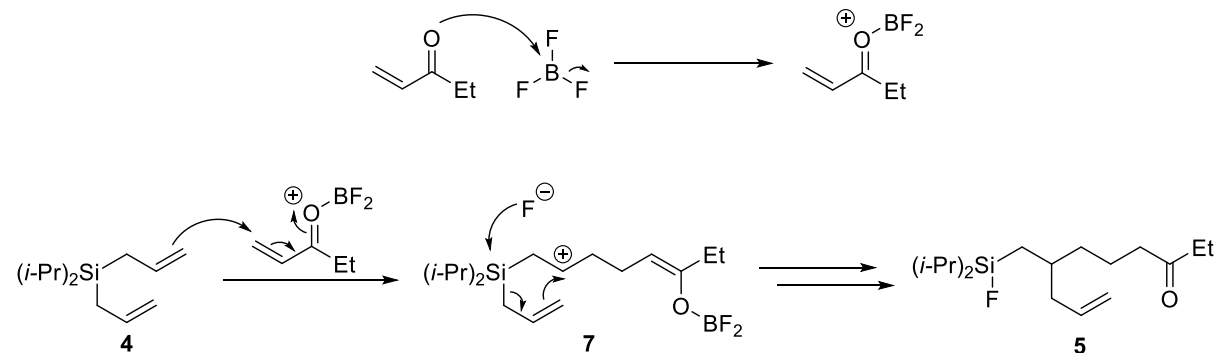
This  $\beta$ -silyl effect can be expanded to diallylsilanes and has been shown to promote intramolecular rearrangements to form a new carbon-carbon bond along with a stereocenter.<sup>9</sup> This way relatively simple starting materials are efficiently transformed into more complex structures which also hold further functionalization sites. The first report of an intramolecular diallylsilane rearrangement was from the Akiyama et al. group in 1998 showed the domino allylation of diallylsilanes to  $\alpha,\beta$ -unsaturated ketones (Scheme 1.2). For their reaction,  $\text{BF}_3\bullet\text{Et}_2\text{O}$  was used with diallyldiisopropylsilane **4** along with several  $\alpha,\beta$ -unsaturated ketones. In their case, the diallyldiisopropylsilane proved optimal for this conversion to take place and had the best yield with the ethyl ketone **5** as opposed to the phenyl ketone **6**.

**Scheme 1.2.** Domino allylation of diallylsilane with  $\alpha,\beta$ -unsaturated ketones.



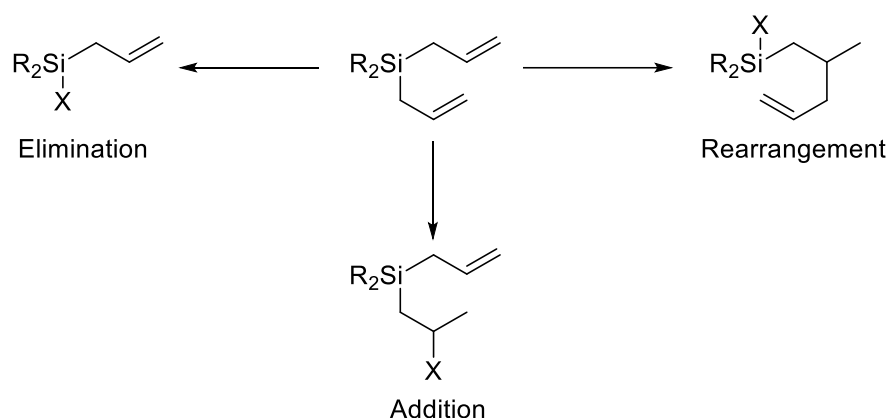
The mechanism was thought to proceed through intermediate **7** containing a carbocation at the  $\beta$ -silyl position (Scheme 1.3). The  $\beta$ -silyl effect stabilizes the carbocation through hyperconjugation with silicon thereby promoting the reaction.<sup>6</sup> After one of the allyl groups reacts with the enone, the second allyl group undergoes an intramolecular allylation to form the final product **5**.

**Scheme 1.3.** Mechanism of Domino allylation of diallylsilane with  $\alpha,\beta$ -unsaturated ketones.



A similar diallylsilane rearrangement was documented by the Shainyan group.<sup>10</sup> The addition of a Brønsted-acid was used to promote the rearrangement of diallyldiphenylsilane **8** to fluorosilane **9** (Table 1.1). The success of these rearrangements depended on the nature of substituents on silicon. According to their study, diallyldimethylsilane **10** led to either elimination or the double elimination resulting in the formation of difluorodimethylsilane. Interestingly, having one chloromethyl substituent on silicon **11** suppressed elimination and gave the desired rearrangement product. Sterically, methyl and chloromethyl groups are very similar, however substitution of silicon with these groups yielded different results. Therefore, an electronic effect is most likely responsible for the competition between rearrangement and elimination. This suggests that the more electron donating nature of a methyl substituent favors the elimination product.

**Table 1.1.** Reaction routes of diallylsilanes with different electrophiles.



HX R', R''	AcOH	CF <sub>3</sub> COOH	BF <sub>3</sub> · 2AcOH	CF <sub>3</sub> SO <sub>3</sub> H
Ph, Ph ( <b>8</b> )	No Reaction	Addition	Rearrangement ( <b>9</b> )	Rearrangement
Me, Me ( <b>10</b> )	No Reaction	Elimination	Double Elimination <sup>a</sup>	Elimination <sup>b</sup>
Me, ClCH <sub>2</sub> ( <b>11</b> )	No Reaction	Addition	Rearrangement + Elimination	Elimination + Rearrangement

<sup>a</sup> At 25–40 °C.

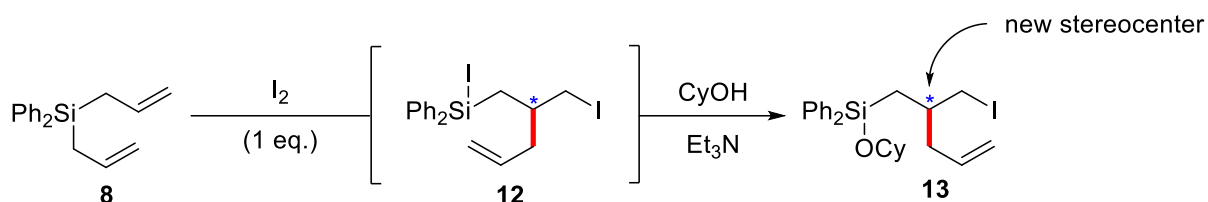
<sup>b</sup> At -40 °C.

## 1.2 Iodine mediated rearrangement of diallylsilanes

More recently in 2017, the O’Neil group reported the rearrangement of diallylsilanes with molecular iodine. Without isolation of the resulting iodosilane intermediate **12**, the addition of an amine base and an alcohol gave the corresponding iodosilylether products **13** in good yields (Scheme 4).

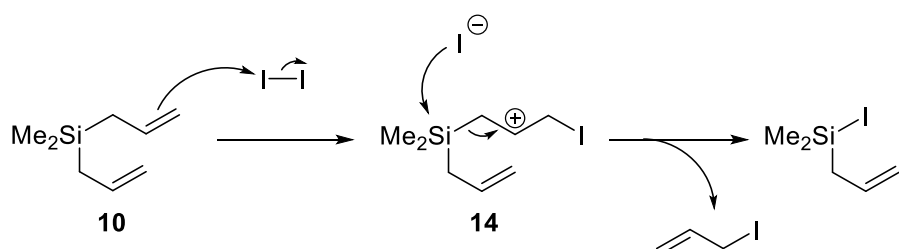
1.4).<sup>11</sup> The initial discovery of this reaction came from the investigation of activatable silanes for nucleophilic additions into carbonyls. In an attempt to synthesize allylcyclohexyloxysilacyclobutane with the addition of catalytic iodine, a trace amount of what seemed to be the rearrangement product **13** appeared (Scheme 1.4). The use of stoichiometric iodine significantly increased the yield of rearranged product. Further optimizations included testing different solvents and different diallylsilanes. Ultimately, the best results came from using diallyldiphenylsilane **8** with 1 equivalent of iodine in DCM as solvent at room temperature.

**Scheme 1.4.** Intramolecular iodine mediated rearrangement of diallyldiphenylsilane.



In this reaction, diallyldimethylsilane **10** gave the lowest conversion along with the highest percentage of allyl iodide formation. This was believed to result from both a steric and electronic effect. Sterically, the smaller methyl group could favor attack at silicon by liberated iodide upon formation of the carbocation intermediate **14** (Scheme 1.5). Electronically, this is consistent with Shainyan's Brønsted-acid promoted rearrangement, the more electron-donating methyl favors elimination.<sup>10</sup>

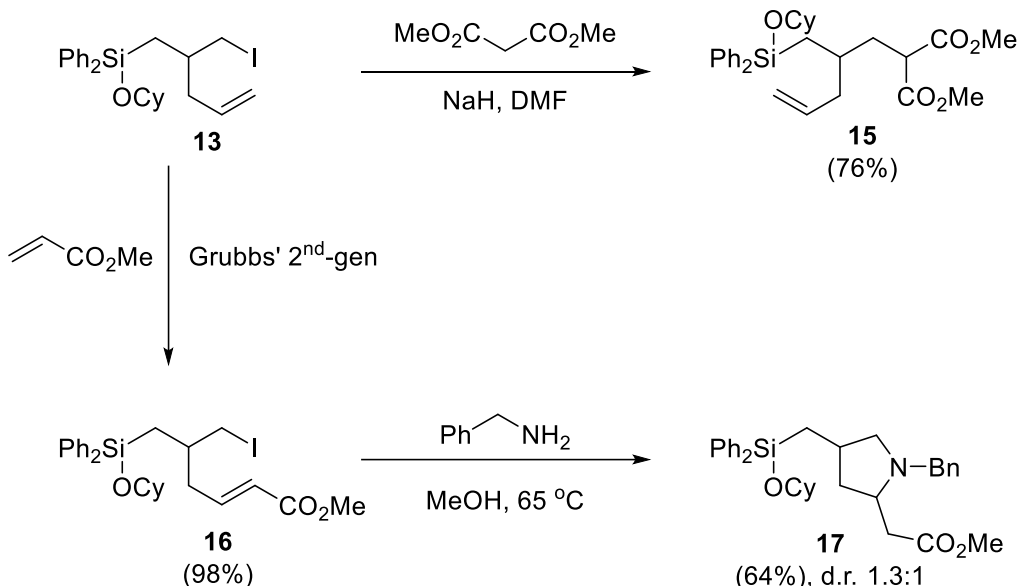
**Scheme 1.5.** Elimination of diallyldimethylsilane to form allyliodide.



It is notable that the iodine mediated rearrangement product has proven to be a versatile synthetic intermediate (Scheme 1.6). For instance, compound **13** could be alkylated with dimethylmalonate to produce the silyl diester **15**. Additionally, the O'Neil group was able to

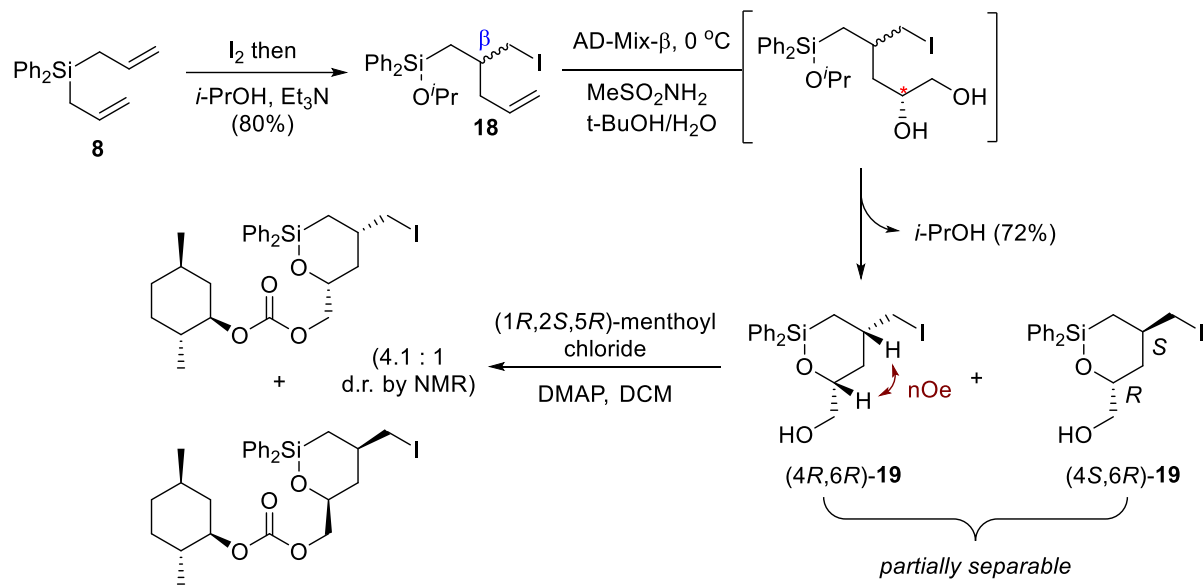
transform **13** into a complex silylmethyl-functionalized pyrrolidine **17**. This annulation was achieved via cross-metathesis of the original alkene then treating **16** with benzylamine.

**Scheme 1.6.** Further transformations of the iodine mediated rearrangement product.



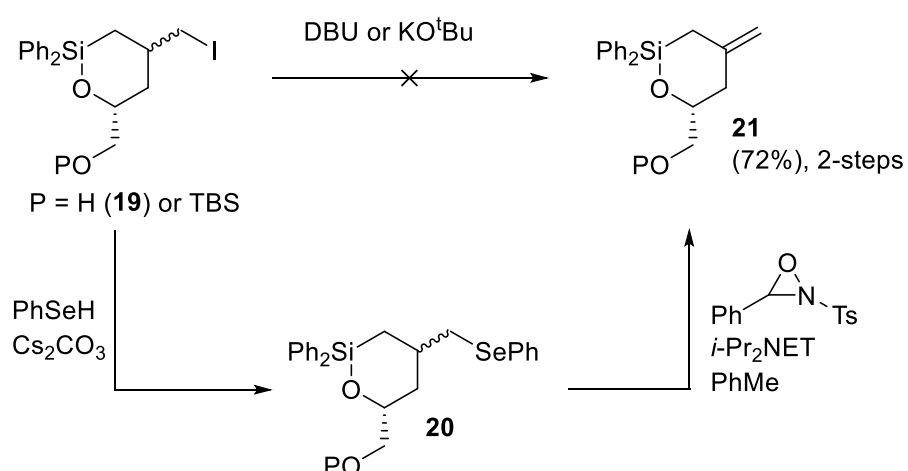
As another example demonstrating the value of iodine-promoted diallylsilane rearrangement products, the synthesis and reactions of enantioenriched oxasilacycles were also reported.<sup>12</sup> Here the iodine mediated rearrangement product **18** was taken into an asymmetric dihydroxylation reaction producing a diastereomeric 6-membered ring **19** (Scheme 1.5). This led to a 1:1 mixture of 4R,6R- and 4S,6R-diasteromers as expected. However, the diastereomers were partially separable by chromatography on silica. Moreover, NMR analysis allowed for the differentiation of the cis and trans diastereomers with NOESY spectroscopy, the 4R,6R-isomer having a characteristic cross peak between protons at C4 and C6, indicating relative proximity through space whereas in the trans product the signal is not observed. Upon addition of (1R,2S,5R)-menthoyl chloride, the enantiomeric excess (ee) of 4R,6R-**19** was determined to be 60% ee by NMR analysis.

**Scheme 1.7.** Iodine rearrangement followed by asymmetric dihydroxylation synthesis of enantioenriched and diastereomeric cyclic silyl ethers.



With difficulty separating the two diastereomers even after chromatography a new plan emerged. Instead, this mixture could be converted to a single enantiomer through the elimination of iodine. Although the initial plans to eliminate iodine with potassium tert-butoxide (KO<sup>t</sup>Bu) or 1,8-diazabicyclo [5.4.0] undec-7-ene (DBU) failed, a two-step reaction was successful (Scheme 1.6). The use of PhSeH and Cs<sub>2</sub>CO<sub>3</sub> on oxasilacycles **10** led to the selenoether **11** followed by selenoxide elimination to yield the desired product **12** which holds allylsilane moiety.

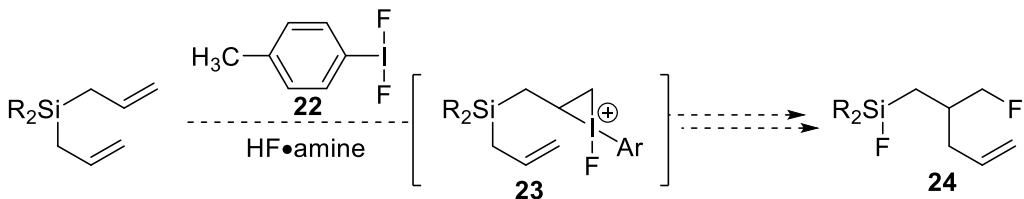
**Scheme 1.8.** Elimination of iodine from diastereomeric compound **19** to cyclic allylsilane **21**.



### 1.3 Exploring Fluorine as an Additional Electrophile with Diallylsilanes

With relatively little research done on diallylsilanes the original scope of this thesis was to explore additional electrophiles that could yield a similar rearrangement product. In particular, the development of a fluorine mediated rearrangement was of significant interest due to the value of organofluorine compounds in various disciplines.<sup>13</sup> As seen from the iodine mediated product previously, the resulting fluorosilane compound **24** could prove useful in further transformations similar to products from the iodine mediated rearrangement. Others like the Gilmour group have demonstrated the difluorination of olefins.<sup>14</sup> Their work involves the exploitation of a hypervalent iodine catalyst. In this case, an aryliodonium difluoride **22**, which forms *in situ*, activates the olefin producing cationic intermediate **23**. Given the previous work done with the iodine mediated rearrangement, we question whether this intermediate could undergo an intramolecular allylation via a similar mechanism to obtain the fluorinated product **24** (Scheme 1.7).

**Scheme 1.9.** Fluorine mediated rearrangement from pre-existing work from the O’Neil group.



In order to investigate this possibly new avenue for organofluorine compounds several diallylsilanes along with multiple different conditions were attempted. This rearrangement unfortunately proved rather difficult and never yielded any of the desired product. However, some of these experiments require the use of meta-chloroperoxybenzoic acid (mCPBA) a common epoxidizing agent to synthesize the aryliodonium species *in situ*.<sup>15</sup> Naturally, one could imagine background reactions happening with diallylsilanes in the presence of mCPBA. This avenue was then explored in further detail to determine to what extent this would interact.

### 1.4 Importance of Fluorine Containing Compounds

The incorporation of fluorine into organic compounds is ever increasing interest due to its success in pharmaceuticals and unique properties.<sup>16</sup> The first fluoro-pharmaceutical was

Fludrocortisone, Florinef, which came to the market in 1954. Florinef is a corticosteroid containing a fluorine atom and is used for treating adrenogenital syndrome, adrenal insufficiency, and postural hypotension.<sup>16</sup> The second significant historical group of fluoro-pharmaceutical was the fluoroquinolones, including ciprofloxacin, norfloxacin, and levofloxacin all introduced in the 1980s. These fluoroquinolones are potent antibacterial agents which inhibit the activity of DNA gyrase and topoisomerase. With the success of the fluorinated corticosteroid and the fluoroquinolones, the rise of fluoro-pharmaceuticals has steadily risen over the last 50 years. Globally, In the past three decades, the total number of fluoro-pharmaceuticals (191 drugs) accounted for 18% of the total pharmaceuticals (1072 drugs) and 22% of small molecule drugs (839 drugs).<sup>16</sup>

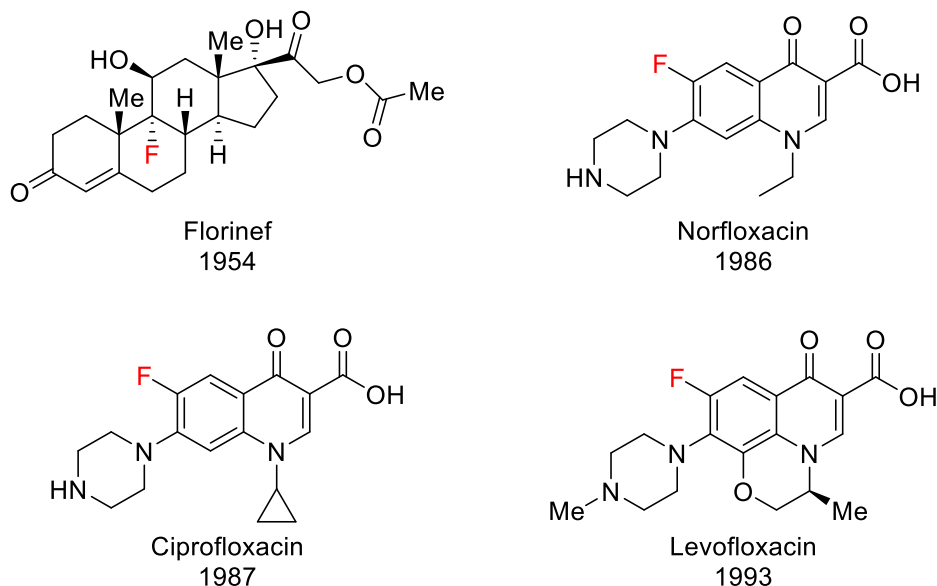


**Figure 1.3.** First and second wave of fluoro-pharmaceuticals that were brought to market.

An additional field in which this is growing is using radiolabeled fluorine-18.<sup>13</sup> Positron-emission tomography (PET) is a noninvasive imaging method that allows for *in vivo* studies that give information about metabolism, receptor concentration, and transport across cell membranes. This in turn allows for the possibility of early diagnosis of disease by screening for unusual changes. Fluorine-18 is one of the various radionuclides that have been used in PET tracers. With a half-life of 109.7 minutes, which is longer than other radionuclides such as carbon-11, nitrogen-13, and oxygen-15, can allow for multistep synthesis along with shipment of the PET tracer. The favorable half-life is

also short enough to reduce radiation exposure to the patient as opposed to iodine-124 which is 4.2 days.<sup>17</sup> Labeled fluorine-18 has been successfully used for more than 30 years, and as of August 2021 there are 16 FDA-approved PET tracers, of which 10 contain fluorine-18.<sup>13</sup> This clear advantage of using fluorine-18 as a radiolabel has made this an exciting new opportunity for organic chemists to have a lasting impact on improving human health.

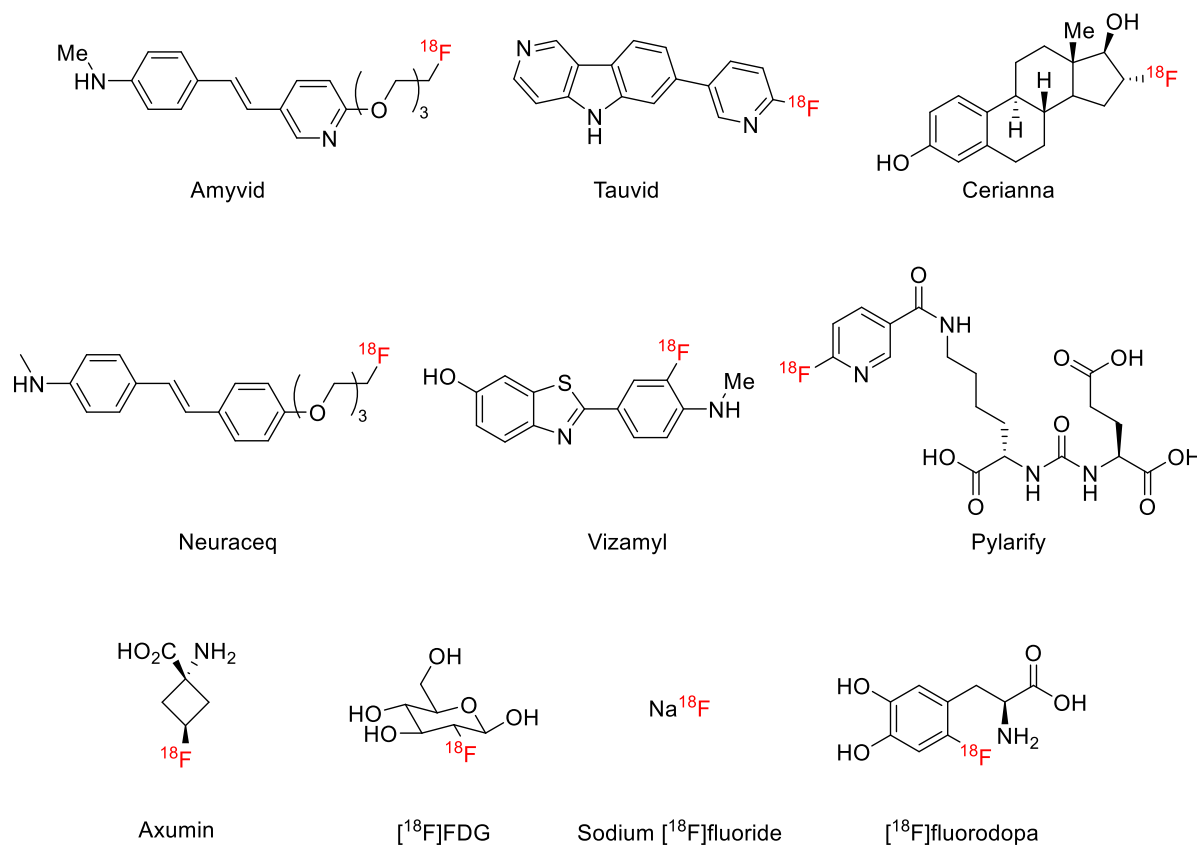


**Figure 1.4.** FDA-approved PET tracers with fluorine-18 as of August 2021.

The incorporation of fluorine has been shown to improve drug potency by affecting pK<sub>a</sub>, hydrophobic interactions and lipophilicity, and modulating conformation (which is described in further detail later in the thesis).<sup>17</sup> It has also been used to tune metabolism, such as replacing labile hydrogens for a fluorine atom can slow down metabolism by fixing fluorine on an aromatic ring that would otherwise be prone to oxidation. The introduction of fluorine into systems also lowers the pK<sub>a</sub> which can result in less toxic drugs. An example of this is that it is believed that kidney toxicity is directly related to the number of basic amines present which allow binding to the ribosomal site.<sup>18</sup> These basic amines are key factors in the antibacterial pharmacophore. Results show that upon

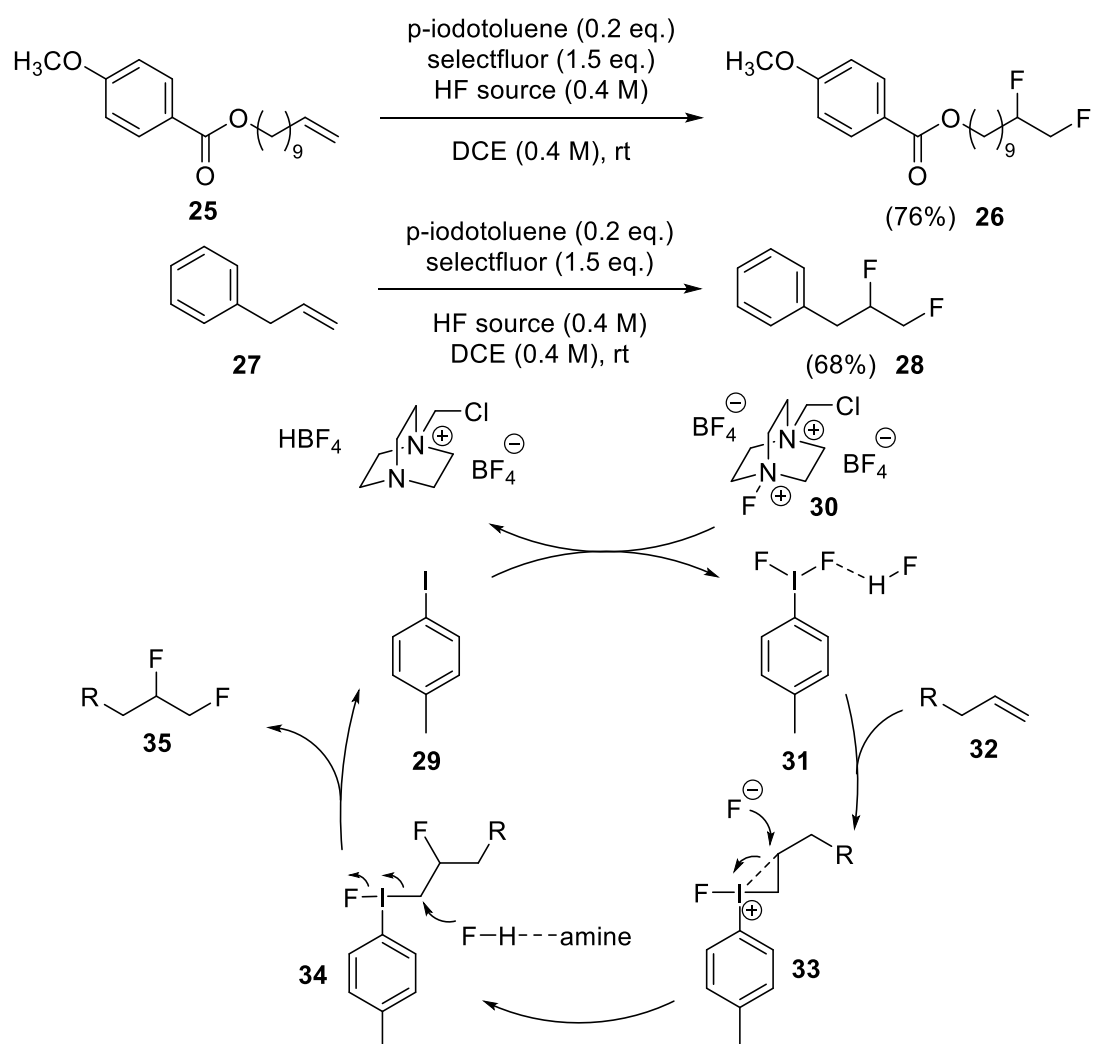
addition of electron-withdrawing substituents adjacent to the amide provides an ability to lower the amine pK<sub>a</sub>. Among a hydroxy group, fluorination, and difluorination substituents the difluorination derivative had the best results with 2-fold less toxicity towards humans. Permeability is also a major factor when considering the lead optimization of orally bioavailable compounds.<sup>17</sup> Adding fluorine into organic compounds increases lipophilicity because carbon-fluorine bonds are more hydrophobic than carbon-hydrogen bonds. These are just some of the reasons why the addition of fluorine to organic molecules has become such a hot topic in recent years.

## Chapter 2. Initial Discovery

### 2.1 Attempts at the Fluorine Mediated Rearrangement

The initial attempts at this rearrangement stemmed conceptually from prior work with diallylsilanes and molecular iodine and our theorized fluorine rearrangement based on others' work in the field. For instance, the Gilmour group reported a catalytic difluorination of olefins in up to 80% yield.<sup>14</sup> One example of their difluorinations was a long terminal alkene chain with a p-methoxybenzoate group at the opposing end (**25**). Treatment of **25** with p-iodotoluene (0.2 eq.), selectfluor (1.5 eq), a mixture of HF TEA : HF pyr 1:4.5 ratio (0.4 M), DCE (0.4 M) at rt for 14 h to yield the difluorinated compound **26**. The other example being phenylpropene **27** treated with the same conditions stated above to yield the difluorinated **28**. The proposed mechanism involves the use of a catalytic amount of p-iodotoluene **29** and 1.5 eq. of selectfluor **30** to form the aryliodonium difluoride **31** *in situ*. This then reacts with the alkene in **32**, forming the transient cation **33**. Subsequently, an activation-displacement sequence gives intermediates **33** and **34**, leading ultimately to the difluorinated product **35** and regeneration of **29**.

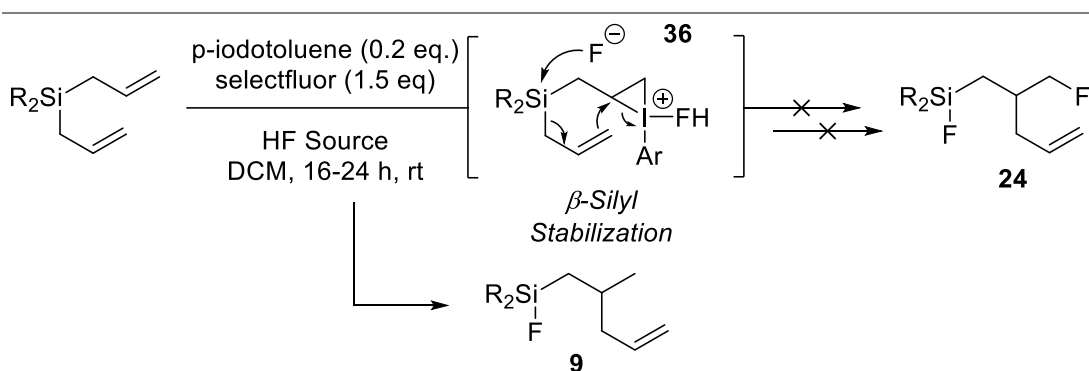
**Scheme 2.1.** Difluorination of alkenes **25** and **27** with the proposed mechanism.



Given the prior work done with diallylsilanes and the iodine mediated rearrangement along with the literature stated above a fluorine mediated rearrangement process was designed (Figure 2.1). The expected mechanism would be rather similar to the one proposed by the Gilmour group, but rather the intermediate **36** would undergo an intramolecular allylation followed by an activation displacement sequence driven by the formation of a Si-F bond resulting in the final product **14** (Table 2.1). We predicted that formation of a stable Si-F bond would be a potential driving force since it forms the strongest single bond known.<sup>19</sup> With both the diallyldimethylsilane and diallyldiphenylsilane being relatively cheap and available starting materials, we began by reproducing Gilmour's conditions with these diallylsilanes. The Gilmour group had previously shown that the success of these fluorinations can be very sensitive to the nature and amount of the HF

source, controlled by mixing HF-pyridine and HF-triethylamine. Our studies therefore screened many different combinations of these reagents as described in Table 2.1. For all of the trials listed, the formation of the fluorinated compound **24** never seemed to form, and mostly starting material remained. We did, however, see the formation of **9** which has already been documented as a result of a Bronsted-acid promoted rearrangement.<sup>10</sup>

**Table 2.1.** Attempted fluorine rearrangement products with p-iodotoluene, selectfluor, DCM, and an HF source.



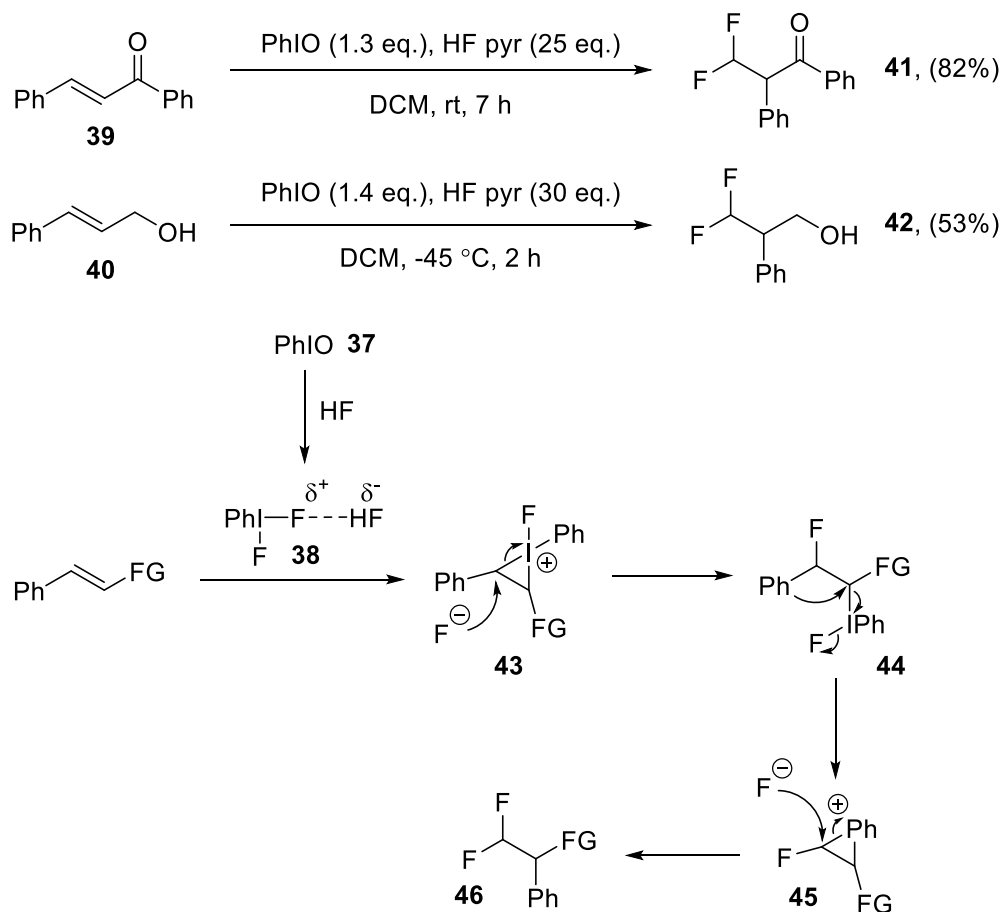
Entry	R	HF. pyr. (mL)	HF. TEA (mL)
1	Ph	0.25	0
2 <sup>a</sup>	Ph	0.25	0
3 <sup>b</sup>	Ph	0.50	0
4	Ph	0.50	0.10
5	Ph	0	0.25
6 <sup>a</sup>	Ph	0	0.25
7	Me	0	0.25
8 <sup>a</sup>	Me	0	0.25
9	Me	0.25	0
10 <sup>a</sup>	Me	0.25	0
11 <sup>a</sup>	Me	1	0
12 <sup>b</sup>	Me	0.50	0
13	Me	0.50	0.10

<sup>a</sup> Control reaction: No p-iodotoluene or selectfluor were added. <sup>b</sup> Addition of pyridine (6 equiv.).

Following those disappointing results, we wanted to screen different potential conditions for a fluorine-promoted diallylsilane rearrangement, and turned our focus to a report from the Kitamura

group who described an alkene difluorination with migration of an aryl group.<sup>20</sup> This system utilizes stoichiometric amounts of iodosobenzene (PhIO) (**37**) to make the aryliodonium difluoride **38** *in situ* from HF. They described different types of difluorinations, one being an  $\alpha$ -aryl- $\alpha,\beta$ -unsaturated ketone **39** and a cinnamyl alcohol **40** which yields **41** and **42**. The mechanism proposed by the Kitamura group involves PhIF<sub>2</sub> reacting with the arylalkene to produce **43** followed by nucleophilic attack of the fluoride ion to the bridged iodine intermediate forming **44**. This then undergoes removal of the PhI and migration of the phenyl group **45**, followed by an additional fluoride attack yielding **46**.

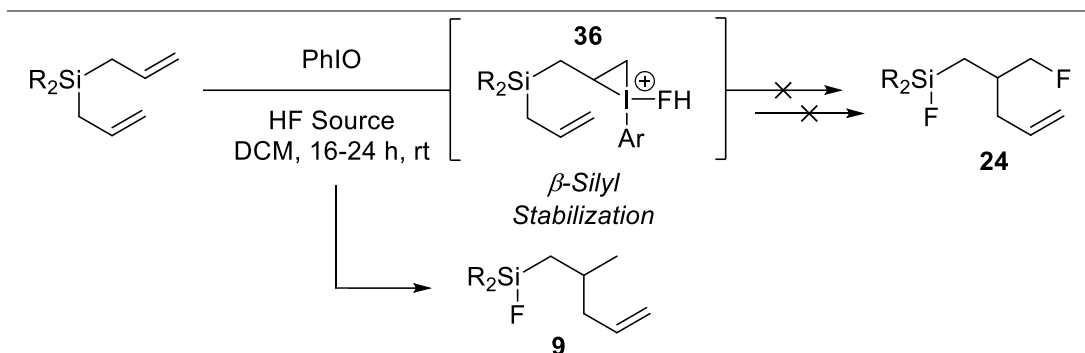
**Scheme 2.2.** Difluorination and aryl migration using PHIO.



With the p-iodotoluene and selectfluor route not yielding any of the desired rearrangement product we decided to attempt these conditions. Reactions using both diallyldimethyl- and diallyldiphenylsilanes with Kitamura's conditions were attempted, but unfortunately no

rearrangement product **24** was observed (Table 2.2). We did, however, see the formation of **9** again along with starting material.

**Table 2.2.** Attempted fluorine rearrangement products with PhIO, DCM, and an HF source.

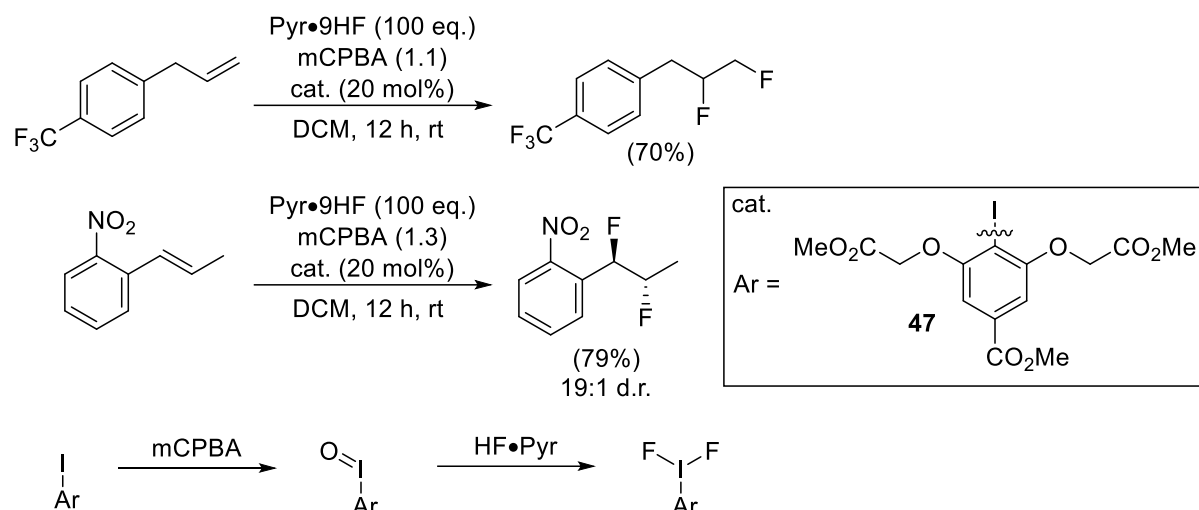


Entry	R	PhIO (equiv.)	HF. Pyr. (mL)	HF. TEA (mL)
<b>1</b>	Ph	1.1	0.27	0
<b>2<sup>a</sup></b>	Ph	1.1	0.27	0
<b>3<sup>b</sup></b>	Ph	2	0	0
<b>4</b>	Ph	1.1	0.20	0.05
<b>5</b>	Ph	1.3	0.16	0
<b>6</b>	Me	1.3	0.16	0
<b>7</b>	Me	1.1	0.20	0.05

<sup>a</sup> Addition of pyridine (6 equiv.). <sup>b</sup> BF<sub>3</sub>·Et<sub>2</sub>O was used as the fluorine source.

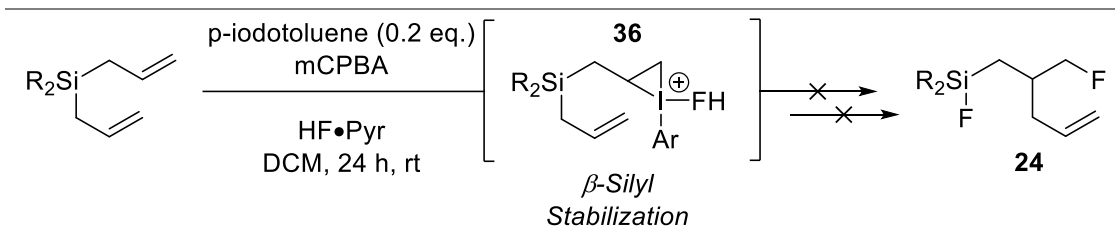
The Jacobsen group reported a similar iodine-catalyzed 1,2-difluorination of alkenes as well.<sup>15</sup> The difference here is that they didn't use PhIO, instead they used a catalytic amount of their iodoaromatic species **47** and mCPBA as an oxidant to form the aryliodonium difluoride (Scheme 2.3). This occurs through a stepwise oxidation to the iodosylarene and subsequent deoxyfluorination with an HF source. The Jacobsen group reports both terminal and substituted alkenes while using a derivative of aryliodine as a catalyst. The proposed mechanism reported is similar to what the Gilmour group reports.<sup>14</sup> Shown below are just two examples of some of the work they employed.

**Scheme 2.3.** Difluorination using mCPBA as catalyst oxidant.



With none of the above reactions yielding the desired product thus far, we decided to try one additional avenue to make these fluorinated compounds. Using the procedure adopted from the Jacobsen group we screened six different reaction conditions (Table 2.3). Sadly, the results were the same as before with mostly starting material remaining and no evidence for **24**.

**Table 2.3.** Attempted fluorine rearrangement products with p-iodotoluene, mCPBA, DCM, and HF pyr.



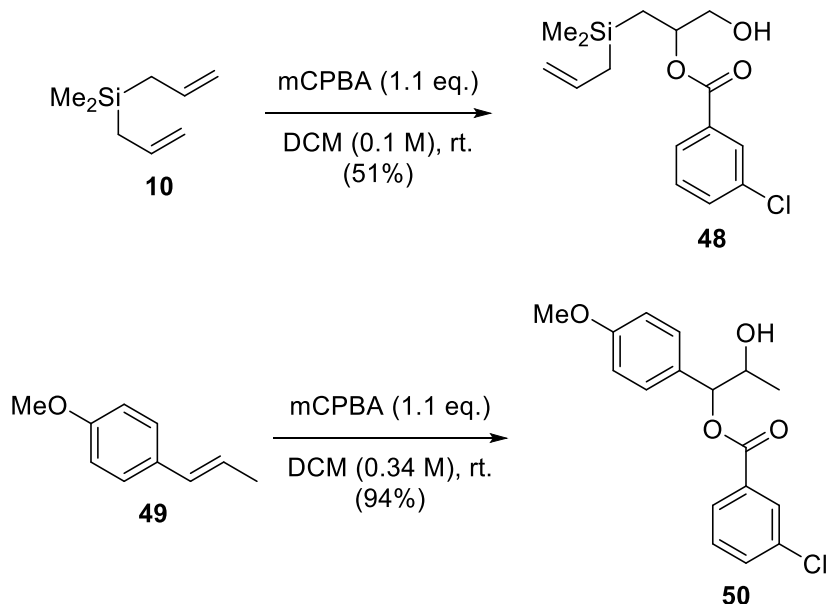
Entry	R	mCPBA (equiv.)	HF. Pyr. (mL)
1	Ph	1.1	0.25
2	Ph	1.1	0.50
3 <sup>a</sup>	Ph	1.1	0.50
4	Ph	1.3	0.60
5	Me	1.1	0.25
6	Me	1.3	0.60

<sup>a</sup> Addition of pyridine (6 equiv.).

## 2.2 Epoxidation of allylsilanes

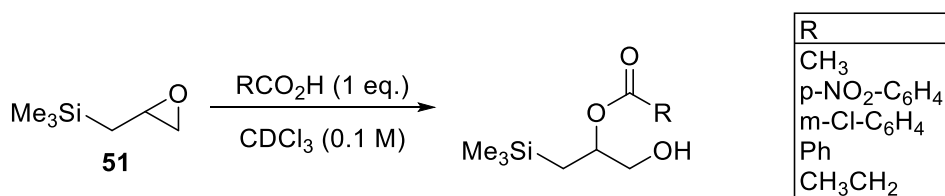
With our investigation into Jacobsen's conditions, the use of mCPBA as an oxidizer for aryliodonium formation led us to further investigate possible side reactions of diallylsilanes with mCPBA. For instance, one might expect the typical epoxidizing agent to form an epoxide at one or even both of the terminal alkenes. To test this, the reaction involving diallyldimethylsilane **10** and mCPBA was performed in DCM at room temperature. This resulted in the formation of a product where meta-chlorobenzoic acid, the mCPBA byproduct after epoxidation, opened the epoxide ring at the beta position giving the hydroxyester product **48** (Scheme 2.4). While this result was not desired, it did lead to a further understanding of how the groups on silicon can affect reactivity. With electron-donating groups such as dimethyl, we obtain the hydroxy ester which is similar to the result reported in the literature describing the formation of compound **50** from **49**.<sup>21</sup> The use of the diphenyl groups on silicon, however, did not give the same results. Instead, the mono-epoxide **52** was the major product. This is believed to happen due to the electron-withdrawing nature of the phenyl rings on silicon providing less stabilization of the beta-carbocation intermediate that would lead to the ester product.

**Scheme 2.4.** Epoxide openings from 3-chlorobenzoic acid of diallyldimethylsilane **10** and **49**.



The addition of metachlorobenzoic acid to silyl epoxides was also reported from the White group.<sup>22</sup> They reported that trimethyl epoxy silane **51** undergoes regiospecific ring opening from carboxylic acids to yield the hydroxyester shown below (Scheme 2.5). Their work demonstrates the favorability of acids to add into the beta position while in a chloroform solvent. Their rationale for this result is that this undergoes an intimate ion pair, with the preferred confirmation of the epoxide being antiperiplanar to silicon, which maximizes the expected  $\sigma_{C-Si} - \sigma^*_{C-O}$  interaction. They also report a crystal structure using triisopropylepoxysilane reacted with trinitrobenzoic acid to give the trinitrobenzoate derivative. This structure reports an elongated C-O bond distance at the beta position along with a dihedral angle of 180° for the Si-C-C-O bonds.

**Scheme 2.5.** Regioselective ring opening of trimethylepoxysilane with different acids.



It was found that the formation of the hydroxy ester could be suppressed by adding 10% Na<sub>2</sub>CO<sub>3</sub> in mCPBA for the diallyldimethylsilane. In this way, the monoepoxide could be formed but was difficult to isolate due to the volatility and lack of stability on silica. Alternatively, using in situ prepared oxone for the epoxidation was also investigated but had little success due to the inability to control the formation of the bis epoxide. It was determined that mCPBA was the best route for diallylsilanes. With the allyldiphenyl epoxysilane **52** isolated, we wanted to attempt an intramolecular epoxide allylation. In addition to contributing another potentially useful diallylsilane-based carbon-carbon bond forming process, this would also present an opportunity to convert the resulting primary alcohol to a fluorine further down the synthesis (e.g., by deoxyfluorination using the DAST).<sup>23</sup>

### 2.3 Attempts at an Intramolecular Epoxide Allylation

In an attempt to promote intramolecular epoxide allylation, several different Lewis Acids were screened (Table 2.4). Our hope was this would proceed through a  $\beta$ -silyl stabilized carbocation

intermediate **53** resulting in the rearranged product **54**. The first attempts with chloro Lewis acids all led to similar results which were the addition of chlorine to the beta position. All of these reactions led to essentially complete conversion of starting material into the chlorinated product **55** shown below.

**Table 2.4.** Attempts at intramolecular epoxide allylation with various Lewis Acids.

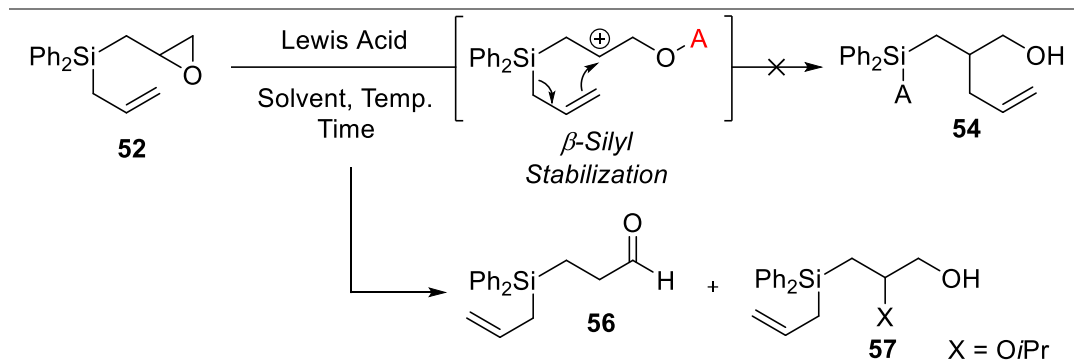
Entry	Lewis Acid	Solvent	Temp. (°C)	Time (h)	Conv. %
1	TiCl <sub>4</sub>	DCM	-78	1	44
2	TiCl <sub>4</sub>	DCM	-78	2	82 <sup>b</sup>
3	TiCl <sub>4</sub>	MeCN	-20	2	100
4	(Et) <sub>2</sub> AlCl	DCM	-78	1	100
5	(Et) <sub>2</sub> AlCl	DCM	25	0.5	100
6	(Et) <sub>2</sub> AlCl	DCM	25	1	100
7	Me <sub>3</sub> SiCl	DCM	-78	1	~50
8	Me <sub>3</sub> SiCl	DCM	25	1	100

<sup>a</sup>Conv % based on the amount of starting material reacted. <sup>b</sup> Isolated yield.

With a number of different conditions screened and a similar result being the formation of **55** we wanted to expand our search to other non-chlorine Lewis Acids (Table 2.5). To our surprise using  $\text{BF}_3 \cdot \text{Et}_2\text{O}$  (entries 1-3) resulted in aldehyde **56** via a Meinwald rearrangement and not the desired product.<sup>24</sup> Switching to  $\text{Ti}(\text{O-iPr})_4$  (entries 4-6) resulted in recovery of starting material even while heating to 60 °C for 4 hr. When using a different solvent, hexafluoroisopropanal (HFIP) (entry 7), we saw the addition of an isopropoxy group to the beta position **57**. The use of TBDMS triflate (entry 8) resulted in what looked to be polymerization. Other Lewis acids such as  $\text{Sn}(\text{OTf})_2$ ,  $\text{Sc}(\text{OTf})_3$ ,

$\text{Bi}(\text{OTf})_3$ , and  $\text{BiBr}_3$  were also screened but in no cases gave any of the intramolecular allylation product by  $^1\text{H}$  NMR analysis (entries 9-12). Rather these seemed to look like polymerization as well.

**Table 2.5.** Attempts at intramolecular epoxide allylation with non-chlorine Lewis Acids.



Entry	Lewis Acid	Solvent	Temp. (°C)	Time (h)	Conv. %
1	$\text{BF}_3 \bullet \text{Et}_2\text{O}$	DCM	0	1	100
2	$\text{BF}_3 \bullet \text{Et}_2\text{O}$	DCM	-78	1	100
3	$\text{BF}_3 \bullet \text{Et}_2\text{O}$	DCM	-78	2	100
4	$\text{Ti(O-iPr)}_4$	DCM	0	1	0
5	$\text{Ti(O-iPr)}_4$	DCM	25	16	0
6	$\text{Ti(O-iPr)}_4$	PhMe	60	4	0
7	$\text{Ti(O-iPr)}_4$	HFIP	25	4	100
8	TBDMS Triflate	DCM	25	16	100
9	$\text{Sn}(\text{OTf})_2$	DCM	25	16	100
10	$\text{Sc}(\text{OTf})_3$	DCM	25	16	100
11	$\text{Bi}(\text{OTf})_3$	DCM	25	16	100
12	$\text{BiBr}_3$	DCM	25	16	100

<sup>a</sup>Conv % based on the amount of starting material reacted.

We also investigated the use of DAST and Deoxo-Fluor to promote the intramolecular epoxide allylation. It was thought that these reagents would cause epoxide opening and allylation followed by deoxyfluorination of the rearranged alcohol to yield **24**. Once again, no intramolecular allylation was observed. Instead, the reactions led to the addition of fluorine to the beta position which was then followed by a deoxyfluorination leading to compound **58**.

**Table 2.6.** Attempts at fluorine product **24** with deoxyfluorination Lewis Acids.

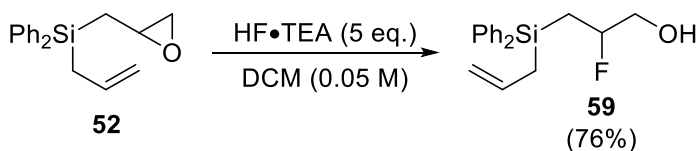
Entry	Lewis Acid	Solvent	Temp. (°C)	Time (h)	Conv. %
1	DAST	DCM	0 to 25	16	100
2	DAST	DCM	25	16	100
3	Deoxo-Fluor	PhMe	0 to 25	16	100

<sup>a</sup>Conv % based on the amount of starting material reacted.

#### 2.4. Initial Discovery of Fluorohydrin

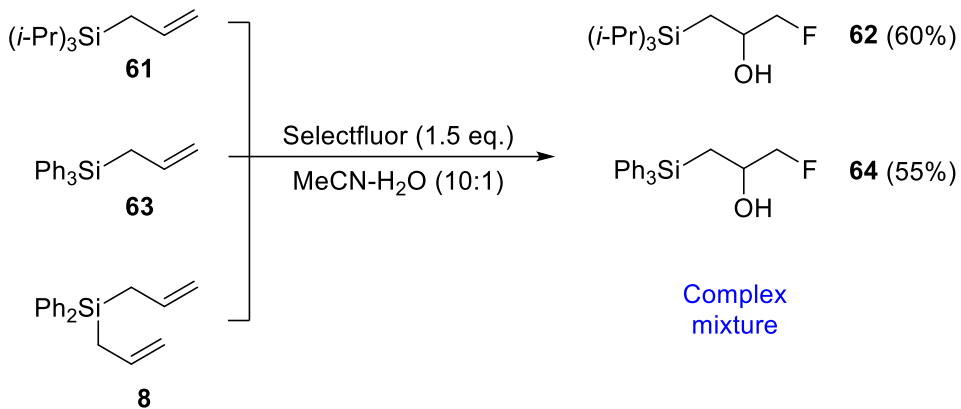
With the failure of Lewis acids to promote the intramolecular epoxide allylation, the use of a Brønsted acid was investigated. In this case, HF•pyr and HF•TEA were both employed for this reaction which was expected to lead to fluorosilane product **24**, again driven by formation of a strong Si-F bond. Instead, fluorohydrin **59** was isolated in 76% yield upon treatment of diallyldiphenylsilane with HF•TEA in DCM at room temperature for 16 hours (Scheme 2.6). Under the same conditions, HF•pyr led to a more complex mixture as indicated by NMR analysis, whereas the conversion using HF•TEA was rather clean with little to no side products. The formation of the fluorohydrin took place in mild conditions being that it proceeded at room temperature with five equivalents of HF•TEA. This was appealing because the reagent HF•TEA is a milder version, being significantly less acidic and therefore easier to handle. Additionally, epoxide openings with HF•TEA generally require more forcing conditions (see Chapter 3).

**Scheme 2.6.** The initial discovery of allyldiphenyl fluorohydrin from HF•TEA.



Interestingly the synthesis of fluorohydrins from allylsilanes has been reported by the Wang group but with the opposite regioselectivity.<sup>25</sup> The group reports the ability of selectfluor in acetonitrile and water to promote the fluorination and subsequent attack of the nucleophile (water in this case) of allylsilanes (Scheme 2.7). They report that allyltriisopropylsilane **61** and allyltriphenylsilane **63** undergo this transformation into fluorohydrins **62** and **64**, respectively with good yields. The use of diallyldiphenylsilane **8** was highly reactive and stated to not give the desired fluorinated product under the standard conditions.<sup>25</sup> With our group presenting the opposite regioselectivity of these fluorohydrins this piqued our interest in this new and unknown chemistry.

**Scheme 2.7.** Opposite regioselectivity of fluorohydrins from selectfluor with allylsilanes.



### Chapter 3. Fluorohydrin Synthesis

#### 3.1 Introduction to Fluorohydrins

Fluorohydrins have become a subject of recent interest in organofluorine chemistry and are involved in the preparation of monofluorinated analogs of biologically active natural products.<sup>26,16</sup> Moreover, fluorohydrins which contain a fluorine atom adjacent to an alcohol are conformationally constrained where fluorine prefers to lie *gauche* to oxygen.<sup>17</sup> Originally, this was attributed to a C-F · · · H-O hydrogen bond due to the electronegativity of fluorine. However, it has been proven that fluorine hardly ever accepts hydrogen bonds.<sup>27</sup> Recent DFT calculations and NBO analysis suggest that the  $\sigma_{\text{C-H}} \rightarrow \sigma^*_{\text{C-F}}$  hyperconjugation is the dominant force that gives rise to the fluorohydrin *gauche* effect (Figure 3.1).<sup>28</sup> A similar phenomenon is the anomeric effect which is considered a

donor→acceptor interaction.<sup>29</sup> The fluorine *gauche* effect has been described with a variety of substrates including fluorine, oxygen, nitrogen, and most recently sulfur.<sup>30</sup> This topic has been gaining traction lately because of the ability to control rotation about C(sp<sup>3</sup>)-C(sp<sup>3</sup>) bonds which is important for the design of functional molecules.<sup>30</sup>

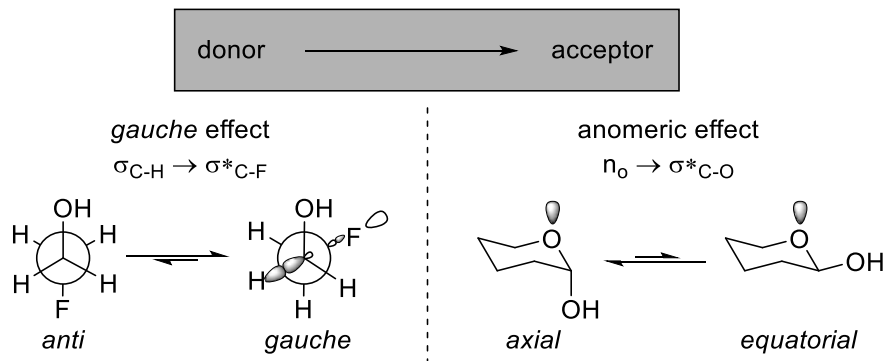
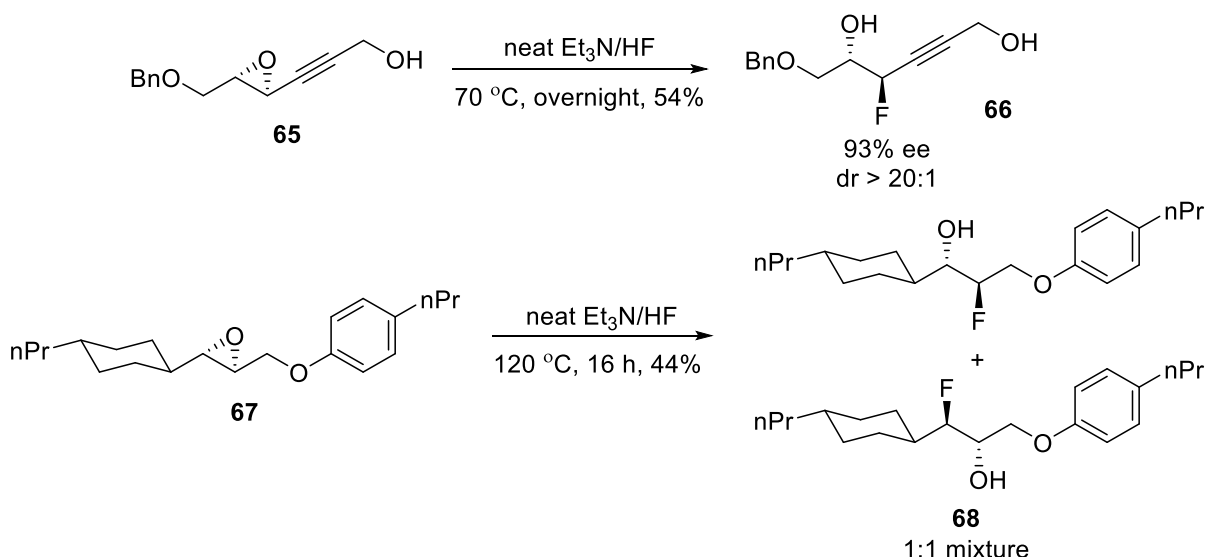


**Figure 3.1.** The *gauche* and anomeric effect due to hyperconjugation from donor-acceptor interactions.

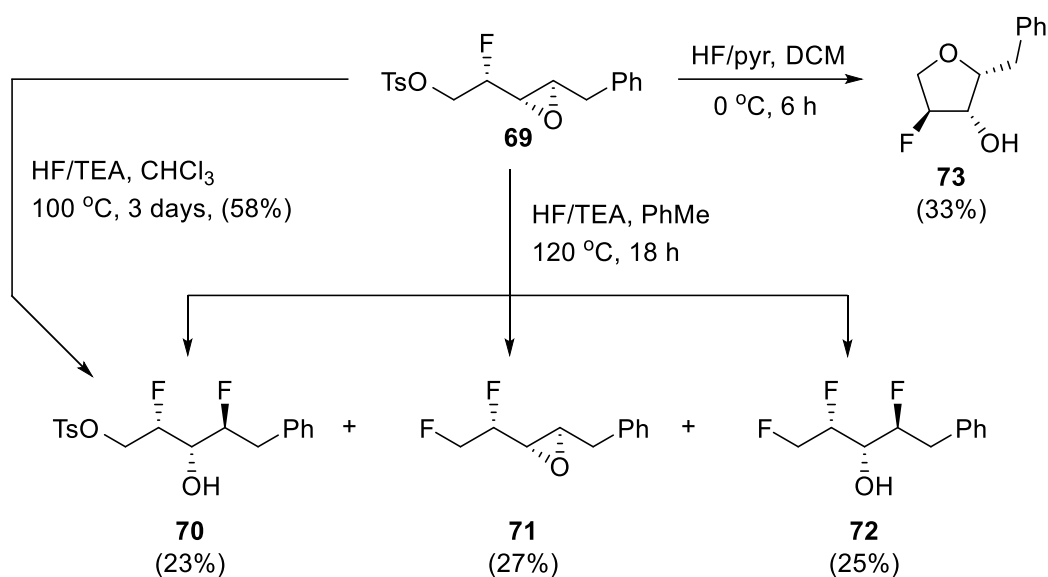
There are several ways to synthesize fluorohydrins but this thesis will focus on the nucleophilic ring opening of epoxides with HF sources. The opening of epoxides with HF•TEA usually requires neat HF•TEA or high temperatures. This is due to the reduced acidity and, as a consequence, does not protonate the epoxide as readily.<sup>31</sup> In most cases this results in an S<sub>N</sub>2 process, whereas in most cases HF•pyr being more acidic results in the protonation of the epoxide followed by a carbocation which results in an S<sub>N</sub>1 mechanism. Having the advantage of retaining stereochemistry is one of the benefits of using HF•TEA as opposed to HF•pyr. Chen and coworkers, along with Al-Maharik and coworkers, report two examples of nucleophilic fluoride opening of an epoxide under relatively forcing conditions (Scheme 3.1).<sup>32,33</sup> In the first example, the epoxide **65** is treated with only HF•TEA and allowed to stir overnight at 70 °C resulting in **66** in a 54% yield with both high ee and dr ratios. In the second example, epoxide **67** is also treated with neat HF•TEA and allowed to stir at 120 °C for 16 hours. This led to a 1:1 mixture of regioisomers **68** with a yield of 44% and complete stereointegrity.

**Scheme 3.1.** Epoxide openings of **65** and **67** under harsh conditions to yield fluorohydrins **66** and **68**.



The O'Hagan group reports HF•TEA opening of epoxides as well. They report the expected fluorohydrin **70** in 23% yield along with two by-products formed by the replacement of TsO with F **71** and **72** (Scheme 3.2).<sup>34</sup> The optimal conversion and selectivity were achieved by changing the solvent to CHCl<sub>3</sub> instead of PhMe which resulted in **70** in 58% yield. The overall conversion time of this reaction took longer with a reduction in temperature from 120 °C to 100 °C and proceeded in 3 days' time. Additionally, the use of HF•pyr on epoxide **69** results in the rearrangement product **73** through a benzenium ion intermediate.

**Scheme 3.2.** Reaction of epoxide **69** with HF•TEA resulting in by-products and optimization.

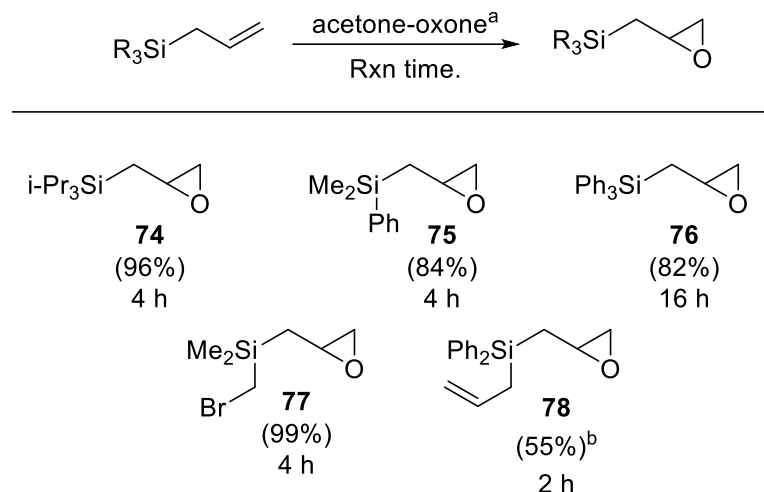


### 3.2 Optimization and Scope

As part of an ongoing program investigating new reactions of allylsilanes, we observed that epoxysilanes, prepared by epoxidation of the corresponding allylsilane, are cleanly converted to the corresponding fluorohydrin upon treatment with triethylamine trihydrofluoride under mild conditions. With the discovery of the formation of fluorohydrins from epoxysilanes with HF•TEA, we wanted to expand the number of compounds that were accessible under these conditions. Originally the epoxidation method being used was mCPBA with 10% Na<sub>2</sub>CO<sub>3</sub>. However, it was found to be difficult to separate mCPBA-derived benzoic acid from the epoxide with column chromatography on silica. Additionally, the use of mCPBA with 10% Na<sub>2</sub>CO<sub>3</sub> with allyltriisopropylsilane **61** and diallyldiisopropylsilane **4** resulted in the hydroxyester compound as shown in Chapter 2.2. This is most likely due to the electron-rich isopropyl groups on silicon which lead to the stabilized carbocation thus promoting the *m*-chlorobenzoic acid to attack. Considering these results, we decided to explore a different epoxidation method using oxone and acetone to form dimethyldioxirane *in situ*.<sup>35</sup> This epoxidation method avoided benzoic acid contamination and hydroxyester formation, and gave sufficiently pure epoxides that could be taken directly into the epoxide openings with HF•TEA.<sup>36</sup>

The oxone epoxidation did require some tuning depending on the groups on silicon. The procedure involved adding allylsilane, tetrabutyl ammonium hydrogen sulphate (TBAHS), aqueous  $K_2CO_3$ , and a 2:1 ratio of  $CH_3CN:DMM$  into a round bottom. Following this, oxone in EDTA and  $K_2CO_3$  in water were slowly added via syringe pump separately over the time shown in Scheme 3.3. The triisopropyl, dimethylphenyl, and (bromomethyl)dimethyl allylsilanes all proceeded with complete conversion of starting material in four hours. Allyltriphenylsilane required slow addition over 16 hours to afford a good yield (82%) of the epoxide **76**. For diallyldiphenylsilane it was typically difficult to selectively generate monoepoxide while using the oxone conditions. This epoxidation method led to significant amounts of the bisepoxide. Instead, mCPBA was used as the method to attain this epoxysilane **78** in 55%. Another exception was diallyldimethylsilane. Similar to allyltrimethylsilane, with the high volatility of these compounds precluded the use of higher boiling acetonitrile and dimethoxymethane solvents needed for the oxone epoxidation. Even the use of mCPBA in low-boiling DCM became troublesome to isolate and resulted in major losses while under reduced pressure. However difficult to isolate, we did develop a method that will be discussed later.

**Scheme 3.3.**<sup>a</sup> Oxone epoxidation of different allylsilanes with corresponding yields and reaction run times.



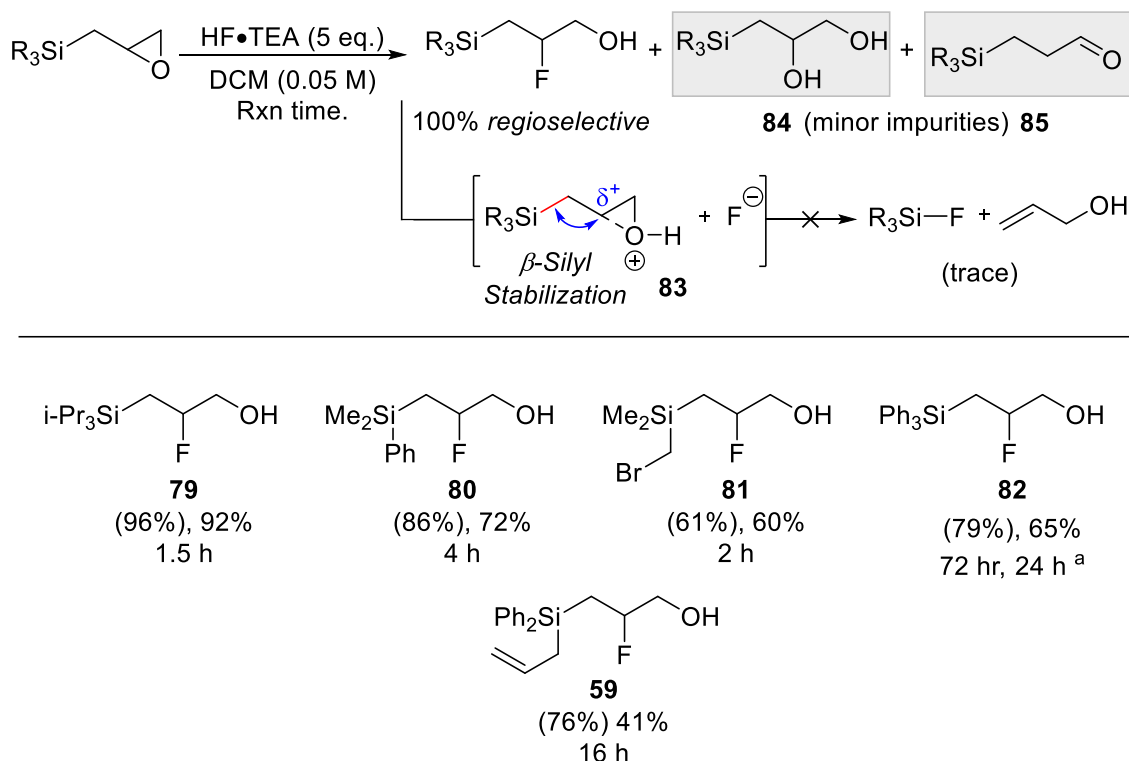
<sup>a</sup> Reagents and conditions: TBAHS (0.04 eq.), K<sub>2</sub>CO<sub>3</sub> (0.1 M aq., 0.2 eq.), CH<sub>3</sub>CN:DMM (2:1) (0.125 M), oxone (3 eq. in 0.125M 4 x 10<sup>-4</sup> M EDTA), K<sub>2</sub>CO<sub>3</sub> (13.3 eq. in 0.125 M H<sub>2</sub>O). <sup>b</sup> mCPBA (1.2 eq.), DCM (0.067 M)

With the epoxysilanes isolated pure, they were ready to be taken into the ring opening with HF•TEA. These reactions proceeded with the addition of five equivalents of HF•TEA in 0.05 M CH<sub>2</sub>Cl<sub>2</sub> at room temperature for the given times (Scheme 3.4). Initially, we were concerned about the competing formation of allyl alcohol and corresponding fluorosilane, driven by the formation of a stable Si-F bond.<sup>19</sup> However, through <sup>1</sup>H NMR analysis of the crude mixtures, we found that very small amounts, if any, of allyl alcohol were being formed. Other minor by-products observed were small amounts of the diol **84** and aldehyde **85**, the latter presumably being formed via a Meinwald-type rearrangement.<sup>24</sup> However, over the screening process, we did determine that the addition of 10 equivalents of HF•TEA as opposed to 5, and/or increasing the concentration of DCM to 0.1 M for the dimethylphenyl epoxysilane **80** resulted in significantly more allyl alcohol along with the aldehyde product **85**. All of the epoxysilanes tested except the triphenyl **76** proceeded to full conversion within 24 hours at rt. The only exception being the triphenyl epoxysilane **76** which was notably slower, taking three days to completely convert to the fluorohydrin **82** with the conditions

listed. We rationalize this reduced rate being due to the electron-withdrawing nature of the phenyl rings, thereby reducing the  $\beta$ -silyl effect in stabilizing the proposed cationic intermediate **83**, and slowing the reaction. Unlike the dimethylphenylsilyl fluorohydrin **80**, when increasing the equivalents of HF•TEA to 10 and increasing the concentration of DCM to 0.1 M, no formation of allyl alcohol and no decrease in yield was observed for the triphenylsilyl fluorohydrin **82**.

Some noteworthy aspects of this transformation are the ability of this to proceed at room temperature with complete regioselectivity and only some minor impurities. Other reports of fluorohydrin synthesis from HF•TEA opening of epoxides require high heat and no solvent to achieve high conversion.<sup>33</sup> We attribute this rate acceleration, along with control of regioselectivity, to the beta-silyl effect. Similar rate enhancements are observed for reactions involving cationic intermediates with a silicon group in the  $\beta$ -position.<sup>8,36</sup> It is worth mentioning the triisopropyl fluorohydrin **79**, even though it is recovered in excellent yield, decomposes rather quickly (within 48 hours) into the aldehyde product **85** with a small amount of allyl alcohol. We believe this is due to the strong electron-donating nature of the isopropyl groups weakening the C-F bond as a result of hyperconjugation from the silicon. All other silanes, especially ones containing electron-withdrawing groups are relatively stable once isolated.

**Scheme 3.4.** Fluorohydrin synthesis from epoxysilanes with an explanation of regioselectivity and structures of byproducts.



The isolated yield is given in parentheses, followed by the overall yield from allylsilanes. <sup>a</sup> HF•TEA (10 eq.), DCM (0.1 M).

A brief solvent study was done on the triphenylsilyl fluorohydrin synthesis to test reaction rates. For this DCM, THF, and MeCN were chosen, and all reactions were run under the same conditions (rt, 24 hours). We see that for entry 1, using DCM gives the best conversion of 50% (Table 3.1). When MeCN is employed (Entry 2) a considerable decrease in the opening of the epoxide is observed and mostly starting material is recovered. For entry 3, using THF we observe no formation of the fluorohydrin even after 24 hours.

**Table 3.1.** Conversion of triphenyl epoxysilane **76** to triphenylsilyl fluorohydrin **82** using different solvents.

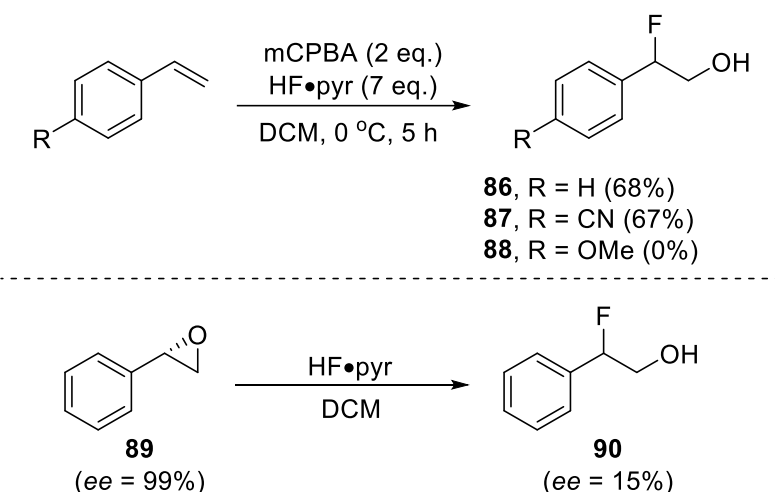
 <chem>Ph3SiCH2C1(O)CC1&gt;[HF•TEA (5 eq.)] Solvent (0.1 M) 24 h&gt;&gt;  <chem>Ph3SiCH2CFCH2OH</chem> </chem>		
Entry	Solvent	Conv. % to final prod.
<b>1</b>	DCM	50
<b>2</b>	MeCN	18
<b>3</b>	THF	0

Conversion % based on  $^1\text{H}$  NMR analysis.

### 3.3 One-pot Synthesis of Fluorohydrins

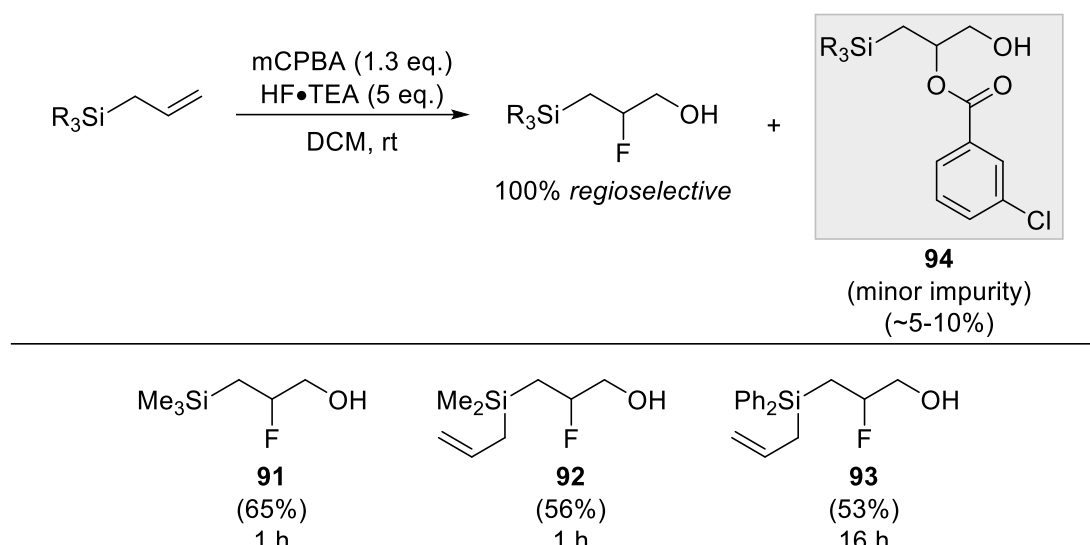
With the inability to utilize allylTMS and diallyldimethylsilane in the synthesis of fluorohydrins by first epoxidation due to volatility issues, a new method was sought out to generate the corresponding fluorohydrins for these compounds. The Sedgwick group reported a metal-free one-pot hydrofluorination of olefins using mCPBA and HF•Pyr (Scheme 3.5).<sup>37</sup> During the optimization of their reaction conditions, they report the use of HF•TEA yielding no reaction. With HF•pyr they report that several electron-withdrawing substituents were afforded in good yields, below are two examples of such transformations. The first substrate is styrene, and the second has a nitrile group in the para position. Both reactions resulted in a 68% for **86** and a 67% yield for **87**, respectively. Alternatively, the use of electron-donating groups **88** impeded the reaction, which they suggest is due to diminished electrophilicity of the benzylic carbon (the intermediate epoxide being the main species identified in the crude mixture).<sup>37</sup> In an effort to explore the mechanism of their transformation, (R)-styrene oxide **89** was subjected to nucleophilic ring opening with HF•pyr to afford **90**. This reaction underwent identical conditions to the one-pot procedure, and a major loss of optical purity was observed (>99% to 15% ee).

**Scheme 3.5.** One-pot synthesis of fluorohydrins from the Sedgwick group.



With those one-pot conditions in mind, we set out to try this on allylTMS with the hopes of forming the TMS fluorohydrin and avoiding having to isolate a volatile epoxide intermediate. To our satisfaction, with the conditions tuned to our substrate the TMS fluorohydrin **91** was afforded and isolated in 65% yield (Scheme 3.6). The addition of 1.3 equivalents of mCPBA and five equivalents of HF•TEA over 1 hour resulted in our desired product with complete regioselective control. However, the formation of an undesirable side product **94** was observed. This resulted from the intermediate epoxide opening from 3-chlorobenzoic acid, as seen in Chapter 2.2. Unfortunately, we were not able to separate these two compounds via column chromatography due to their similar polarities. Even so, this hydroxy ester only accounts for 5-10% of the isolated yield. With the minor impurity in mind, the good yield, and the practicality of these one-pot reactions, we wanted to expand this to both the diallyldimethyl- and diallyldiphenylsilane. With the same conditions, the allyldimethyl fluorohydrin **92** can be isolated in 56% yield in just 1 hour. The allyldiphenyl fluorohydrin **93** requires a longer reaction time (16 hours) but increases the yield from 41% to 53% using the one-pot as opposed to the two-step method. The only downside of this reaction is that a small amount of the hydroxy ester **94** is formed for all of the silanes.

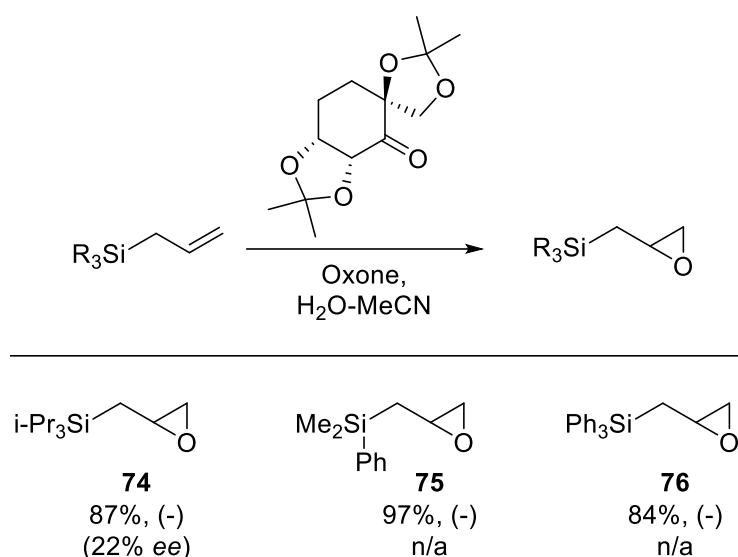
**Scheme 3.6.** One-pot synthesis of fluorohydrins from allylsilanes.



### 3.4 Probing the Mechanism

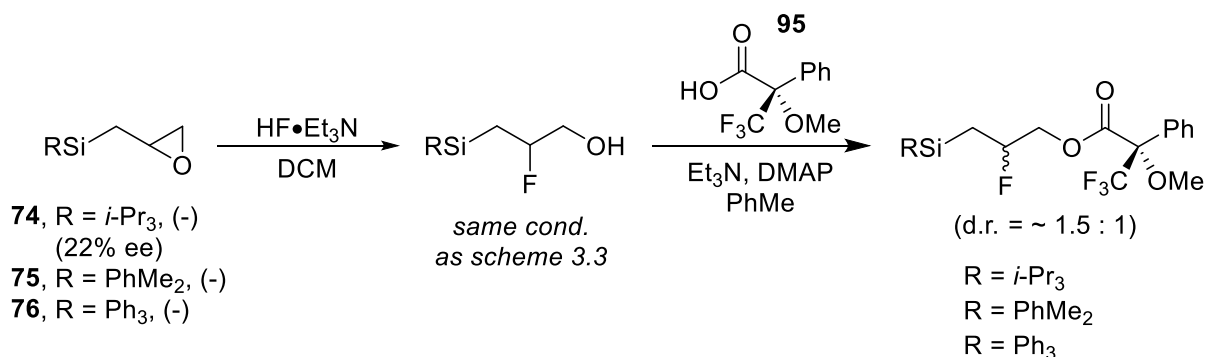
In an attempt to determine if the mechanism of this transformation was more S<sub>N</sub>1 or S<sub>N</sub>2-like, three different enantioenriched epoxides were prepared. Epoxysilanes **74-76** were produced in enantioenriched form by Shi epoxidation (Scheme 3.7).<sup>38</sup> Similar to the racemic sequence, when using allyltriphenylsilane the Shi epoxidation was much slower than the other differently substituted silanes.<sup>36</sup> Nonetheless, using a slightly more concentrated reaction mixture with extended times led to good yields of the triphenylsilyl epoxide **76**. Using the measured optical activity for triisopropyl silyl epoxide **74**, a comparison was made with what was reported previously in literature.<sup>38</sup> Epoxide **74** was obtained as a 62:38 mixture of enantiomers (22% ee), which was consistent with previously obtained values for the same transformation reported by the Shi group. Since **75** and **76** don't have optical activity data, we assume both the dimethylphenyl and triphenylsilanes have similarly enriched epoxides.

**Scheme 3.7.** Shi epoxidation of allylsilanes to give epoxysilanes.



With our enantioenriched silyl epoxides **74-76** in hand, the epoxides were treated with HF•TEA and DCM under the same conditions listed in scheme 3.4 (Scheme 3.8). Following this, an esterification with (*S*)-methoxy- $\alpha$ -(trifluoromethyl)phenylacetic acid (**95**) allowed for an assessment of fluorohydrin enantiopurity by  $^1\text{H}$  NMR analysis (Figure 3.2). By using this Mosher ester analysis, the enantiopurity of all three silyl fluorohydrins was determined to be  $\sim 1.5:1$ , indicating the enantiopurity of the starting epoxide was retained, and epoxide opening occurred via an  $\text{S}_{\text{N}}2$ -type mechanism.

**Scheme 3.8.** Enantioenriched epoxysilanes and their corresponding fluorohydrin with an assessment of fluorohydrin enantiopurity by conversion to the Mosher ester derivative.



Mosher esterification reactions proceed over 16 hours.

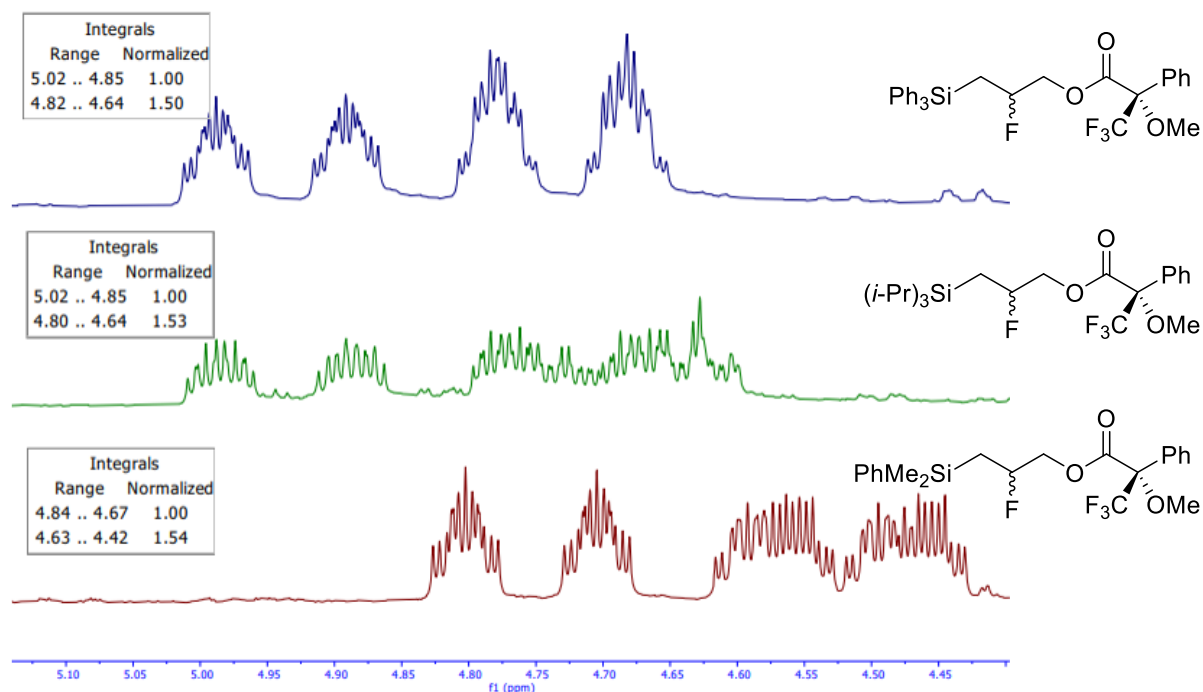
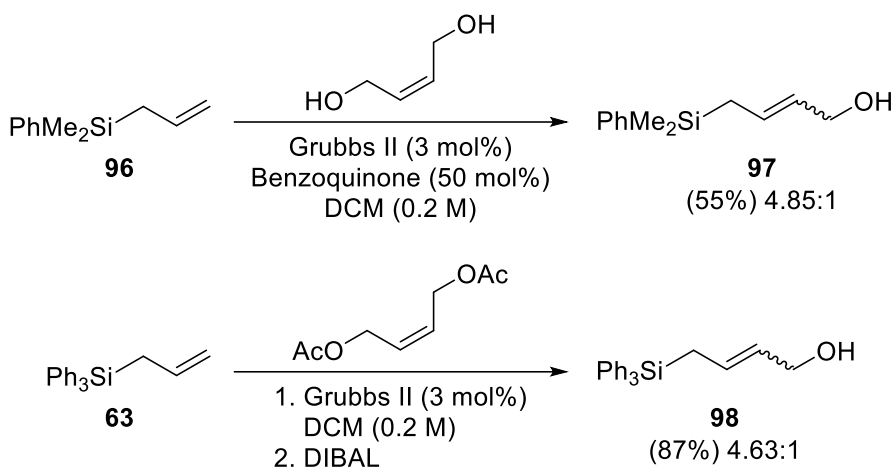


**Figure 3.2.** Mosher ester  $^1\text{H}$  NMR analysis of enantioenriched 3-silylfluorohydrins. Integration values for the  $\alpha$ -fluoro hydrogen in all cases was  $\sim 1.5:1$ , consistent with the ee measured for the triisopropylsilyl epoxide (22%).

The exploration of substituted allylsilanes was the next step in expanding the scope of these reactions. Having an additional group added onto the  $\gamma$ -position of an allyl silane would allow us to demonstrate the  $S_N2$ -like nature by forming diastereomers. In an effort to afford such compounds, allyldimethylphenylsilane **96** along with 3 equiv of cis-1,4-butenediol were combined using Grubbs metathesis conditions (scheme 3.9).<sup>39</sup> With the addition of benzoquinone to avoid isomerization, the transformation proceeded to give **97** in a moderate yield of 55%. The ratio of *trans:cis* in this mixture was determined to be 4.85:1 through  $^1\text{H}$  NMR analysis. The second compound of this nature we wanted to synthesize was the triphenylsilane version. The approach to this was slightly different, starting with the use of cis-2-butene-1,4-diyil diacetate and Grubbs II catalyst. Following this, DIBAL was used to reduce the ester down to the alcohol to give **98** in 87% yield. This ratio of the *trans:cis* mixture was determined to be 4.63:1 through  $^1\text{H}$  NMR analysis.

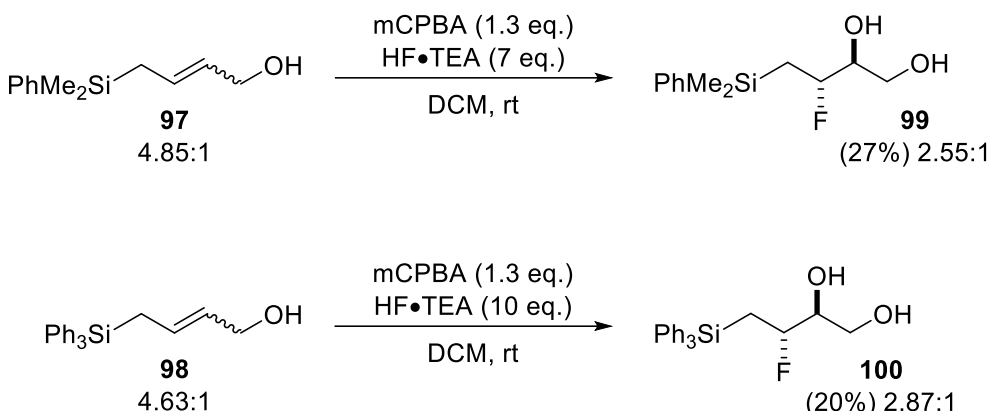
**Scheme 3.9.** Grubbs metathesis with allylsilanes to yield substituted 4-(silyl)but-2-en-1-ol of **97** and **98** in 55% and 87% yield, respectively.



Trans:cis ratio.

With these compounds isolated and the *trans:cis* ratio determined, we subjected these to our new one-pot conditions. The dimethylphenyl compound **97** underwent this transition to afford **99** with a poor yield of 27%. However though  $^{19}\text{F}$  NMR analysis the diastereomeric ratio was determined to be 2.55:1 (Scheme 3.10). This suggests inversion of the stereocenter in the  $\beta$ -position resulting from an  $\text{S}_{\text{N}}2$ -like mechanism. The triphenyl compound **98** unfortunately also resulted in a poor yield of 20% to give **100** with a diastereomeric ratio of 2.87:1. The ratio of starting material does not match the fluorohydrin suggesting the mechanism isn't perfectly  $\text{S}_{\text{N}}2$ . Both fluorohydriins shown below had no formation of but-3-ene-1,2-diol as a result of the elimination of fluorine based on the crude  $^1\text{H}$  NMR. Instead, the low yield could be attributed to having a disubstituted alkene. Analysis of the  $^{19}\text{F}$  NMR we do see a large singlet  $\sim -170$  ppm indicating a Si-F signal suggesting the elimination of fluorine. In this case that would require the formation of but-3-ene-1,2-diol which could have been water-soluble explaining the absence in the  $^1\text{H}$  NMR.

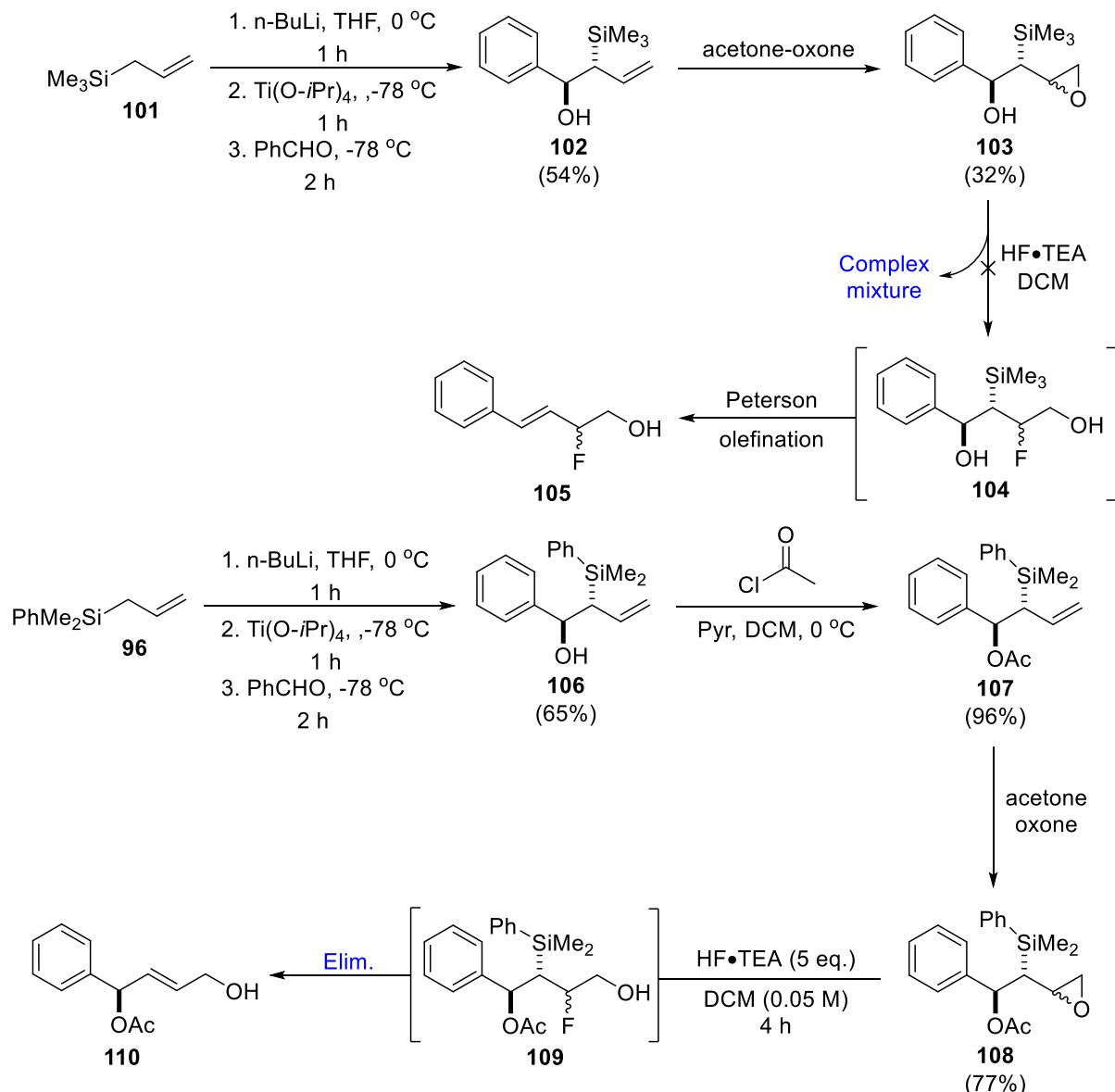
**Scheme 3.10.** One-pot reactions with 4-(silyl)but-2-en-1-ol to yield **99** and **100** with slight retention of stereochemistry.



To further explore the results shown above, a protected allylsilane was synthesized similarly to **98** but with dimethylphenylsilane. An additional substituted allylsilane was attained through the Landais group's method for forming  $\alpha$ -substituted allylsilanes.<sup>4</sup> In an effort to display the versatility of this reaction, having  $\alpha$ -substituted allylsilanes was an attractive next step. We initially started out with readily available allylTMS **101** to make this transformation. The first step in this sequence was to add nBuLi in THF at 0 °C to the desired silane to deprotonate the  $\alpha$ -proton with respect to silicon and form the carbanion (Scheme 3.11). Following this, a transmetalation with Ti(O-iPr)<sub>4</sub> at -78 °C and then the addition of benzaldehyde at -78 °C to give the  $\beta$ -hydroxysilane **102** in a 55% yield. This was then taken into an oxone epoxidation. However, the resulting epoxide (**103**) compound seemed to be rather sensitive and slightly decomposed on silica when purifying. Nonetheless, we subjected the epoxide obtained to our standard fluorination methods. It was thought that the fluorohydrin product **104** could undergo a Peterson olefination to afford **105**.<sup>40</sup> Unfortunately, the addition of HF•TEA to compound **103** resulted in a complex mixture, and no formation of the desired fluorohydrin was observed. Throughout our study, we noticed that having an electron-withdrawing group on silicon greatly enhances the stability of the fluorohydrin. With that in mind, allyldimethylphenylsilane **96** was chosen to enhance the stability of the fluorohydrin. The same methodology was applied to the dimethylphenyl system to give the  $\beta$ -hydroxysilane **106** in 65%

yield. Following this, esterification of the hydroxy group with acetyl chloride (**107**) was done to further stabilize this system after fluorination conditions. Under our standard oxone epoxidation conditions, epoxide **108** was cleanly obtained and ready to undergo nucleophilic ring opening from HF•TEA. Full conversion of starting material occurred, however we only observed **110** from the crude mixture resulting from the immediate elimination of fluorine-silicon moiety **109**. This reaction was attempted at room temperature and 0 °C both resulting in the same elimination product **110**.

**Scheme 3.11.** Formation of  $\alpha$ -substituted allylsilanes with subsequent epoxidation followed by HF•TEA.



## Chapter 4. Functionalization of Fluorohydrins

### 4.1 Transformations and Tamao Oxidation

Thus far, we have described a novel methodology for the synthesis of numerous fluorohydrins. In continuation of this work, we wanted to explore potential functionalizations of these fluorohydrins to elevate their utility in synthesis. A key objective in future functionalizations would be the preservation of fluorine in our substrates due to the unique properties that fluorine endows in chemical systems. Additionally, while silicon is an important element to many functional materials,<sup>41</sup> its conversion to a hydroxy group via a Tamao-Fleming oxidation<sup>42</sup> would lead to a more versatile alcohol functional group. However, a Tamao oxidation of the fluorohydrin directly would lead to a symmetrical diol, which would be less synthetically useful compared to an end-group differentiated diol. Therefore, initial functionalization of the existing alcohol of the fluorohydrin prior to Tamao was pursued thus allowing us to access these asymmetric diols.

To start, we decided to use the triphenyl fluorohydrin **82** and functionalize the primary alcohol side (Table 4.1). The first transformation investigated was the oxidation of the primary alcohol using Dess-Martin conditions to afford the corresponding aldehyde. The crude aldehyde was then reacted with our Wittig reagent **111** without further purification due to the slight decomposition of the aldehyde on silica. This afforded the unsaturated ester **112** which then allowed us to screen conditions for the Tamao oxidation. First, we tried a reaction with mCPBA, KHF<sub>2</sub>, and DMF (Entry 1) as described by Fleming which resulted in the recovery of starting material.<sup>43</sup> Often for a Tamao oxidation to succeed, the silicon must be activated by an electron-donating group. To achieve this with a triphenylsilane, most reported conditions required refluxing in the presence of TBAF or BF<sub>3</sub>-2AcOH.<sup>44,45</sup> Unfortunately, when implementing these conditions with **112** (Entry 2 and 3) we see only the elimination of fluorine and formation of the conjugated system **115**. We worried that the forcing conditions required for oxidation of a triphenylsilane would be plagued by this undesired elimination. Instead, the dimethylphenylsilane group has been shown to undergo activation toward oxidation more readily by converting the aryl silane into a halosilane in less harsh

conditions.<sup>43</sup> A similar unsaturated ester **113** bearing a dimethylphenylsilyl group was formed in the same manner as stated above. We then subjected this to  $\text{BF}_3\text{-2AcOH}$  (Entry 4) in hopes of completing the first step of the Tamao oxidation which would result in an activated silane to then be oxidized with peroxide yielding the desired alcohol product **114**. Sadly, once again we only observe the elimination product **115**.

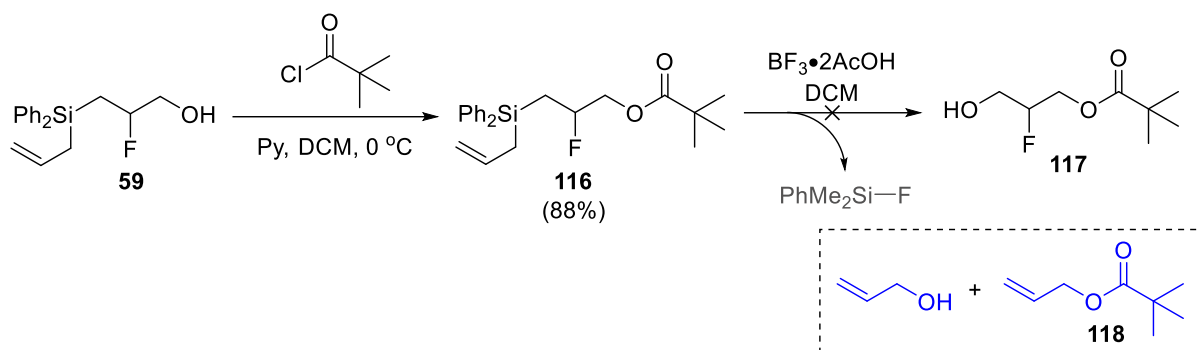
**Table 4.1.** Oxidation and Wittig product followed by Tamao-Fleming conditions with triphenyl and dimethylphenyl silyl.

The reaction scheme illustrates the synthesis of allylsilanes **112** and **113** from fluorohydrins **82** and **80**, respectively. **82** ( $R_3 = \text{Ph}_3$ ) and **80** ( $R_3 = \text{PhMe}_2$ ) react with 1) Dess-Martin periodinane in DCM at 0 °C for 1 h, and 2) Wittig reagent **111** ( $\text{Ph}_3\text{P}=\text{CHCO}_2\text{Et}$ ) to yield **112** ( $R_3 = \text{Ph}_3$ , 62%) and **113** ( $R_3 = \text{PhMe}_2$ , 54%). These intermediate allylsilanes are then subjected to "conditions" (see Table 4.1), which are shown to be PhMe<sub>2</sub>Si—F. The reaction leads to the formation of alcohol **114** and the elimination product **115**. The structure of **115** is shown in a dashed box.

Entry	Conditions	Time
1	$R_3 = \text{Ph}_3$ : mCPBA, KHF <sub>2</sub> , DMF	3 h
2	$R_3 = \text{Ph}_3$ : TBAF, DCM, $\Delta$	3 h
3	$R_3 = \text{Ph}_3$ : $\text{BF}_3\text{-2AcOH}$ , DCM, $\Delta$	5 h
4	$R_3 = \text{PhMe}_2$ : $\text{BF}_3\text{-2AcOH}$ , DCM, rt	5 min

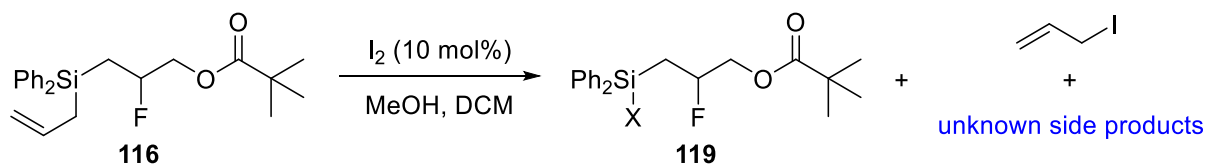
With our goal to still perform a Tamao oxidation to remove silicon, we investigated other substituents on silicon that might be more easily activated. It has been shown that allylsilanes can act as a masked hydroxy group. That is they are hydrolyzed upon treatment with  $\text{BF}_3\text{-2AcOH}$ .<sup>46</sup> Fortunately, our fluorohydrin **59** allowed us to explore this avenue for the substitution of silicon with an electron-withdrawing group toward a successful Tamao oxidation. First, we protected with the alcohol as a pivaloyl ester to differentiate this side (**116**). We decided to do this and not the oxidation followed by the Wittig to reduce the favorability of elimination to form a conjugated system. Unfortunately, when treating this protected silane **116** with  $\text{BF}_3\text{-2AcOH}$  to exchange the allyl group for a hydroxyl for a subsequent Tamao oxidation, we only observe the elimination product **118** and the deprotected allyl alcohol.

**Scheme 4.1.** Protection of fluorohydrin **59** and Tamao conditions for transformation of masked hydroxy group.



With  $\text{BF}_3\text{-2AcOH}$  not bearing fruit, we concluded these results are indicative of the favorable formation of a Si-F bond and thus high affinity for fluorine to act as a leaving group given its position  $\beta$  to silicon. If this initial formation of a stable Si-F bond was problematic, we decided to venture away from fluoride sources. Our next approach to conquering this challenge was the use of catalytic iodine with an alcohol to make a new silyl ether bond which would activate silicon aiding in the final step for the Tamao oxidation. A catalytic amount of iodine could be used due to the formation of hydroiodic acid following the formation of the silyl ether bond.<sup>47</sup> After performing this experiment, we could not isolate the expected silyl ether, however we did observe via  $^1\text{H}$  NMR the removal of the allyl group and formation of allyl iodide as expected. Unexpectedly the presence of new unknown proton signals all appear between the range of 3.0 – 5.0 ppm (Figure 4.1).

**Scheme 4.2.** Allyldiphenyl silane **116** reacting of I<sub>2</sub> and MeOH resulting in unknown side products.



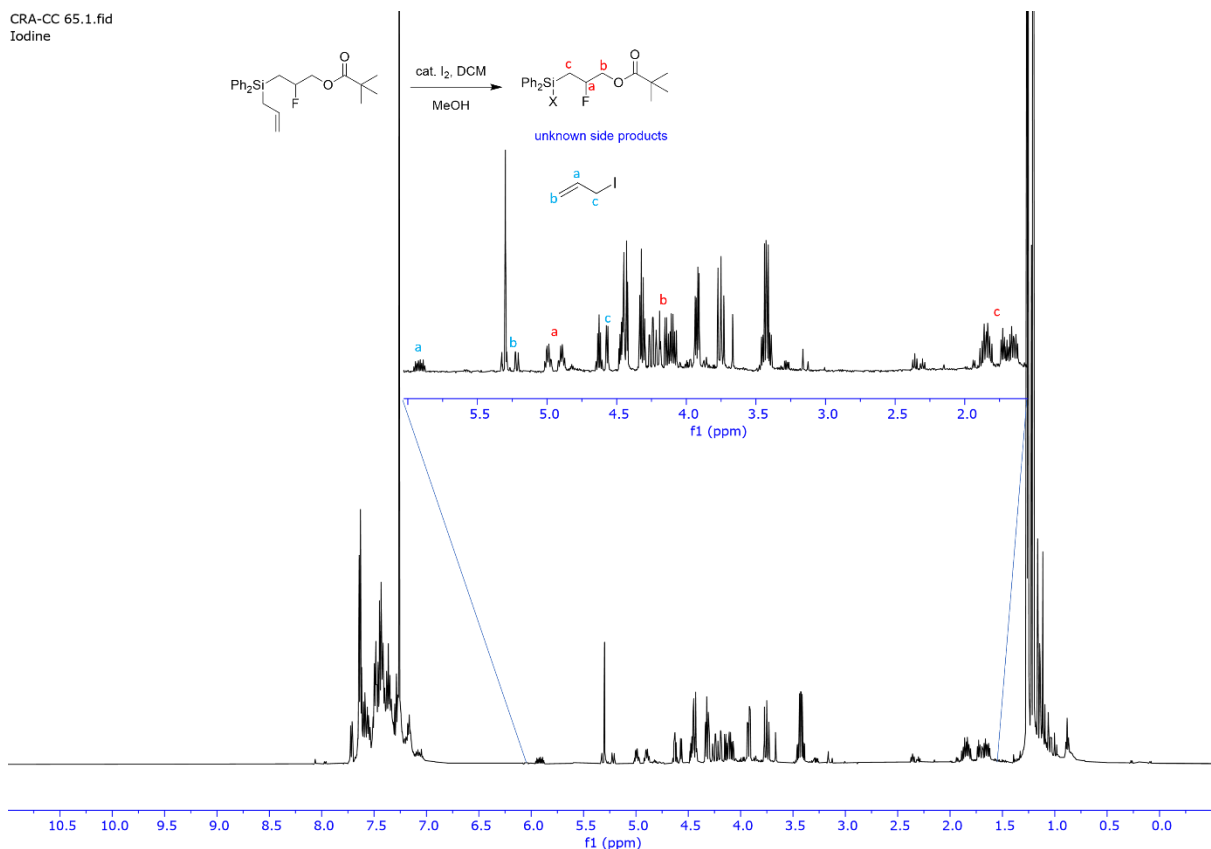


**Figure 4.1.**  $^1\text{H}$  NMR of  $I_2$ , MeOH with allyldiphenyl silane **116** resulting in unknown side products.

Looking at the COSY NMR of the allyl substitution reaction with catalytic iodine, we could identify the fluorohydrin along with allyl iodine, but we see that the splitting and downfield shifts of the unknown peaks do not line up with the expected silyl ether (Figure 4.2). The formation of two distinct entities each coupling with one neighbor but not coupling with each other was identified. Currently, the source of these signals remains unknown. However, we can conclude that a reaction did occur at the allyl group that was once attached to silicon. With the possibility of the new group on silicon (**X**) **119** being a heteroatom, we decided to subject this product mixture to standard Tamao conditions (Scheme 4.3).<sup>46</sup> This however resulted in the retrieval of starting material with no sign of our target molecule **117** once again.

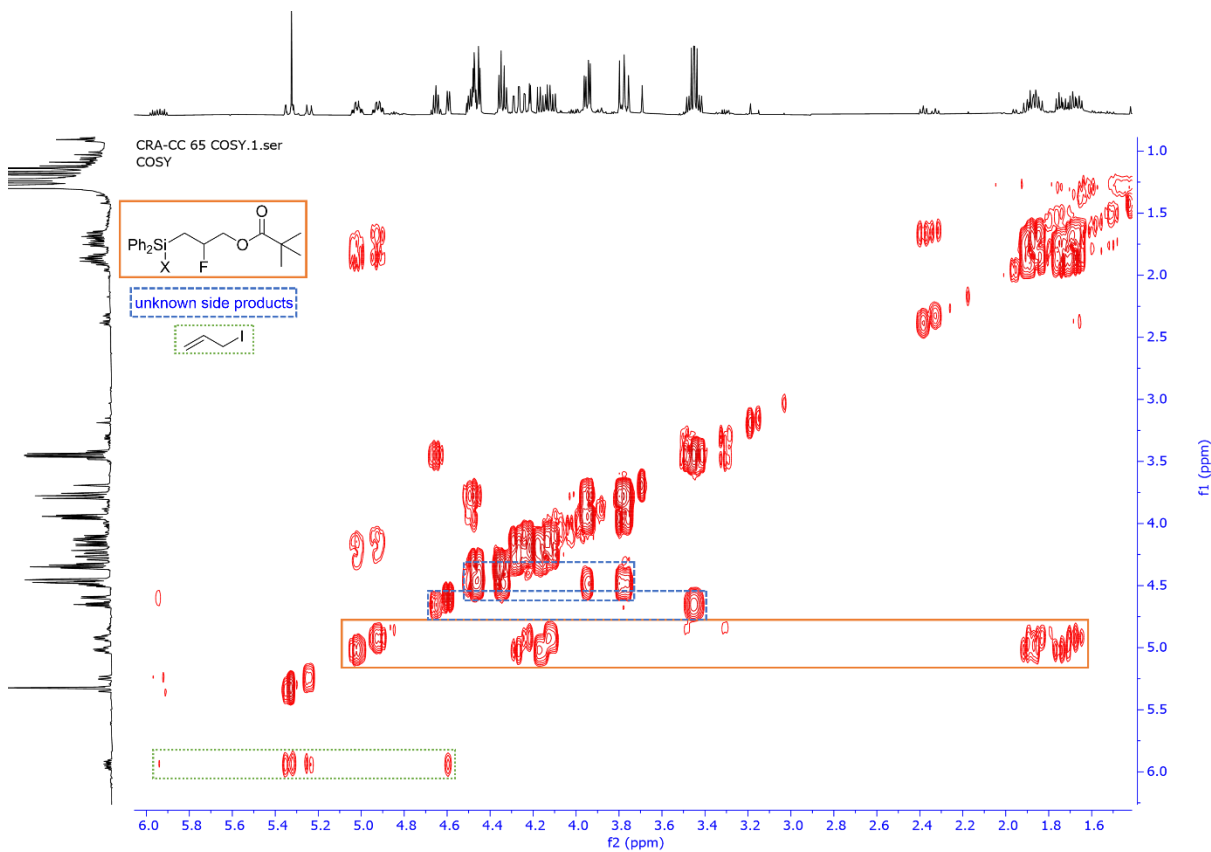
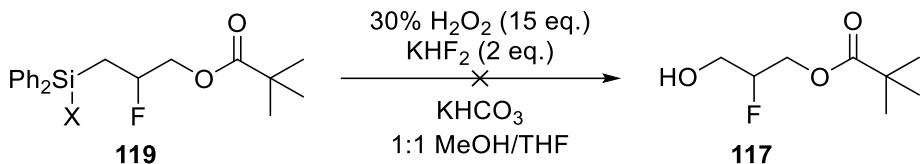


**Figure 4.2.** COSY NMR of I<sub>2</sub>, MeOH with allyldiphenyl silane **116** resulting in unknown side products.

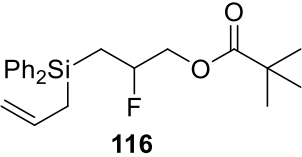
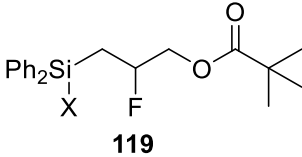
**Scheme 4.3.** Treatment of silane **119** with Tamao conditions, unfortunately recovering starting material.



Considering the lingering questions remaining from results from the prior iodine reactions, we wanted to attempt to understand what was happening during these reactions. A control reaction (Table 4.2, Entry 1) was performed using 0.1 equiv. of iodine with no alcohol present and resulted in retrieval of starting material. This supports the formation of hydroiodic acid in the presence of an alcohol. When using one equiv. of iodine (Entry 2) and again no alcohol, we observe a complex mixture via <sup>1</sup>H NMR. With full conversion of the starting material, the presence of the distinct proton signal adjacent to fluorine is not observed so degradation was assumed. To our surprise, with a catalytic amount of iodine and CyOH in place of MeOH resulted in only starting material (Entry 3).

With the lack of informative results from this sequence of experiments, we turned our attention to other conditions for a successful Tamao oxidation.

**Table 4.2.** Reaction conditions for screening unveiling the masked hydroxy group using iodine.

 <b>116</b>	$I_2$ (0.1 - 1 eq.) DCM <i>see Table</i>	 <b>119</b>	
Entry	$I_2$ (eq.)	CyOH (eq.)	% Conv.
<b>1</b>	0.1	0	0
<b>2</b>	1.0	0	100
<b>3</b>	0.1	2	0

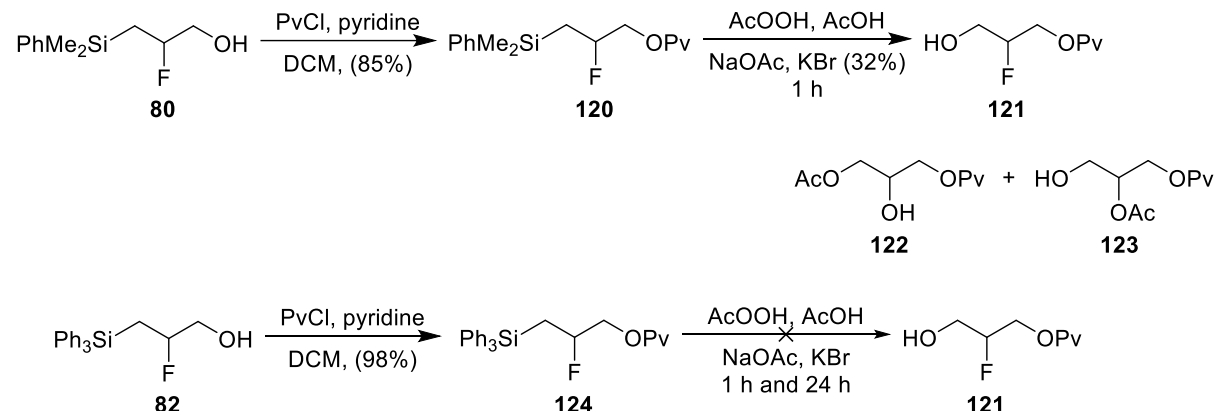
<sup>a</sup>Conv % based on the amount of starting material reacted.

With our options for a Tamao oxidation becoming limited, we decided to try a one-pot procedure. To date there are two different one-pot Tamao procedures described using the dimethylphenyl silyl group. The first uses  $Hg(OAc)_2$ ,  $AcOOH$ , and  $AcOH$  while the second uses  $KBr$ ,  $AcOOH$ ,  $AcOH$ , and  $NaOAc$ .<sup>42</sup> Also, both of these have been shown to undergo the Tamao oxidation with leaving groups, such as an alcohol beta to silicon. Even though our system is different, this piqued our interest because we still have fluorine beta to silicon. Even though our system is different, this piqued our interest because we still have fluorine beta to silicon. Even though our system is different, this piqued our interest because we still have fluorine beta to silicon. The latter was chosen so we could avoid the use of mercury for toxicity reasons.

The dimethylphenyl fluorohydrin **80** was first protected with pivaloyl chloride to afford **120** which was then ready for oxidation using the one-pot method (Scheme 4.4). Using methods adopted from Ibrahim group we subjected **120** to the conditions shown below.<sup>48</sup> Gratifyingly, this gave the differentiated 2-fluoro-1,3-propanediol **121**, albeit in low yield (32%). The low yield could be explained by the presence of **122** and **123** in the crude  $^1H$  NMR resulting from elimination followed by epoxidation and then ring opening. Additionally, we hoped that applying this same chemistry to the triphenylsilyl system **82** would allow us to increase the yield. Unfortunately, even when increasing the run time from 1 hour to 24 hours we see no sign of oxidation of the silicon and retrieved starting material (**124**). Nonetheless, compounds of type **121** have proven to be useful

tools to study enzymatic reactions involving glycerol,<sup>36,49</sup> as well as a starting point to access fluorinated carbohydrate analogues of medicinal value.<sup>50</sup> Our method provides a new entry to these important compounds.

**Scheme 4.4.** Protection of fluorohydrin **80** followed by One-pot Tamao conditions to synthesize **121**.



#### 4.2 Conformational Analysis of the Fluorine-Silicon Interaction

One consequence of adding fluorine to an organic molecule is changes to its conformation. For instance, the fluorine *gauche* effect describes a phenomenon where neighboring groups prefer to be *gauche* to fluorine (dihedral angle  $\sim 60^\circ$ ), driven by electrostatic and hyperconjugative effects. The fluorine *gauche* effect has been studied extensively over the last couple of decades with a large number of discoveries demonstrating conformational constraints for fluorine-containing molecules.<sup>29</sup> Examples include fluorine-fluorine, oxygen, nitrogen, and most recently the sulfur *gauche* effects.<sup>30</sup> However, there is only one computational report by the Rablen group that talks about a neighboring silicon fluorine interaction,<sup>51</sup> like that present in our fluorohydrin products. Rablen's report describes computational studies on 1-fluoro-2-silylethane (FSE). They state that when performing three different calculations, one calculated a preference for the *gauche* conformation over the *anti* conformer by 0.73 kcal mol<sup>-1</sup>. The other two higher levels of theory used in this study suggested that the *anti* conformation should be preferred. However, they report the preference for *anti* over *gauche* to only be 0.4-0.5 kcal mol<sup>-1</sup>. This result is quite surprising, because as mentioned the fluorine *gauche* effect is thought to be a consequence of hyperconjugation. The difference between C-Si and C-H hyperconjugative electron donation in FSE is expected to be quite

substantial<sup>51</sup> and would be expected to favor the *anti* conformation. They also examined 1,2-difluoroethane (DFE) which exhibits a strong preference for the *gauche* conformation that the authors explain by the traditional hyperconjugation. In FSE, electrostatic interactions between the C-Si and C-F bonds should contribute to a stabilized *gauche* conformer. Unlike DFE, the coulombic interactions should be attractive for FSE. In this way, hyperconjugation and electrostatics are conflicted and conformational preference for the *anti* or *gauche* conformer is small. This group also looked at the size of the dihedral angle in the *gauche* conformations of FSE and DFE. This angle should be less than the idealized 60° if electrostatic attraction is present, and greater than 60° if there is repulsion.<sup>51</sup> For DFE the dihedral angle is found to be 72° displaying substantial repulsion between the two C-F bonds. In *gauche* FSE the dihedral angle is 53° suggesting electrostatic attraction between silicon and fluorine.

A small computational study was performed by Tomás Neveselý from the Gilmour group, a colleague of Dr. O’Neil, of our TMS fluorohydrin **91**. From a hyperconjugation perspective, one would expect the system to favor the *anti* conformation. This is supported by the calculations, with the lowest energy state being anti. However, the preference of *anti* over *gauche* is only 0.6 kcal mol<sup>-1</sup> (Figure 4.3). The angle presented at the next lowest energy *gauche* conformation is ~50° suggesting an attraction between fluorine and silicon. In this same molecule, we also observe a fluorohydrin *gauche* effect between fluorine and the alcohol in the lowest energy conformations (Figure 4.4). Assuming some preference for the fluorine and silicon to be in the *anti* conformation, this would help us rationalize some of the results we’ve been gathering. With this conformation the electron density from σ<sub>C-Si</sub> - σ\*<sub>C-F</sub> would weaken the C-F bond rendering it a better leaving group and facilitating the eliminations we observed when attempting Tamao oxidations.

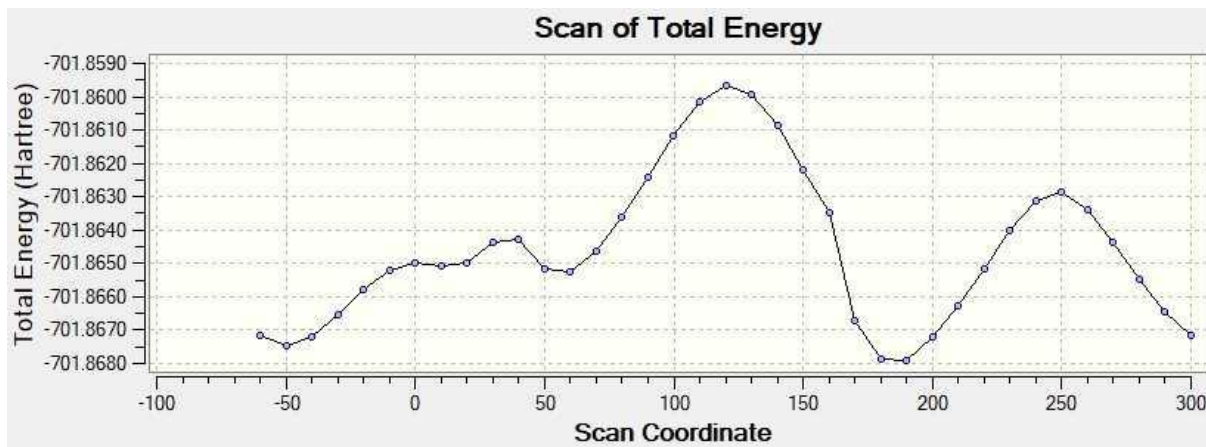


**Figure 4.3.** Computational study regarding rotation about the Si-C-C-F bond for TMS fluorohydrin **91**.

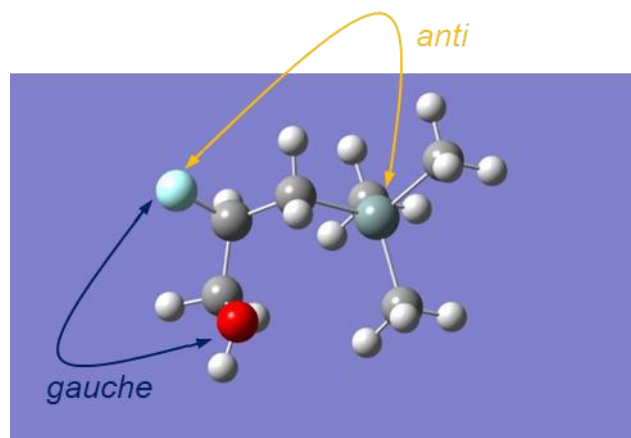


**Figure 4.4.** Image of TMS fluorohydrin **91** in lowest energy *anti* conformation.

These computational results are consistent with the stereoelectric theory (donor – acceptor interactions). However, the low conformational preference for *anti* was interesting and could point to additional conformational effects in these types of molecules. Fortunately, the triphenylsilyl fluorohydrin **82** was a solid and we figured attaining a crystal structure would allow us to investigate conformational aspects of these molecules even further. This could also help answer explain reactivity patterns, for instance why we observed the elimination of fluorine so readily. Several different crystallization methods were attempted. These included layering and vapor diffusion at both room temperature and 0 °C. Ultimately it was found that slow vapor diffusion at 0 °C could afford x-ray quality crystals. The crystals were then analysed, and the structure solved by Werner Kaminsky (Univ. of Washington) as shown in Figure 4.5. The crystal structure data shows two independent structures both of which are triple-disordered. This triple-disorder refers to the

uncertainty in the x,y,z planes as to where the crystal is in the unit cell. To our surprise, both structures have fluorine and silicon *gauche* to each other (Figure 4.5). This could be explained sterically if you consider the larger CH<sub>2</sub>OH group might prefer to reside *anti* from the triphenylsilyl group. Alternatively, the electron-poor silicon could prove to be electrostatically attractive toward the electronegative fluorine. This would also result in a smaller dipole moment further stabilizing this conformation. The dihedral angle between silicon and fluorine was observed to be 6° in the left crystal structure and 38° in the right. The ORTEP image of one shows the fluorine and alcohol *gauche* to one another with a dihedral angle of 18° (as shown in Figure 4.5 on the left), whereas in the other we observe the *anti* configuration (179°) for the fluorine and alcohol groups (right, structure). The dominant conformational bias in this system appears, therefore, to be a silicon-fluorine *gauche* effect.

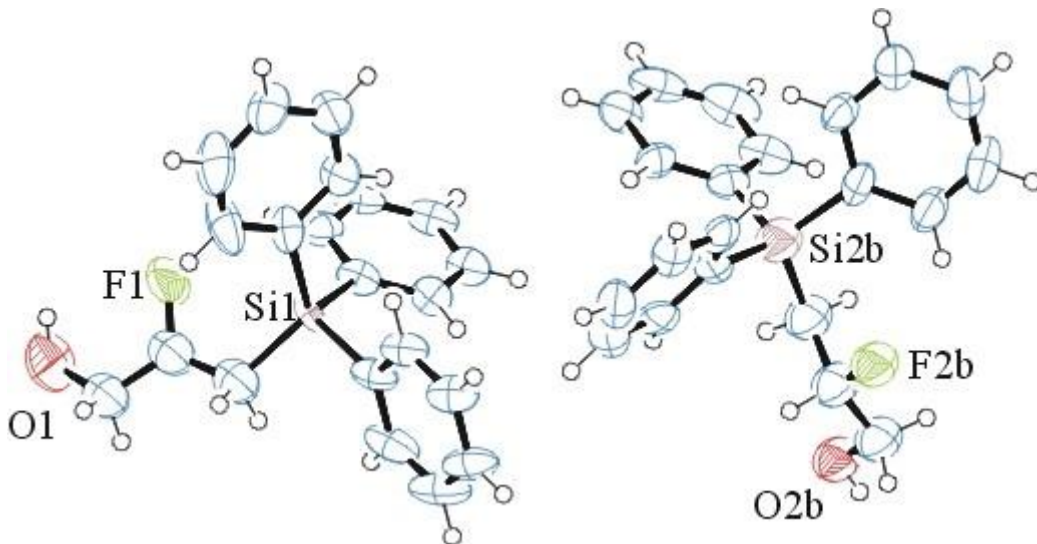


**Figure 4.5.** Crystal structure ORTEP image of triphenylsilyl fluorohydrin **82**.

With the conflicting results between the conformational analysis results for the TMS fluorohydrin **91** and triphenylsilyl fluorohydrin **82** we hoped to gather more information about these systems. Having only computational data for one and crystal data for the other also raises questions about how to compare these results. We therefore decided to try and grow a crystal structure of a dimethylphenylsilyl fluorohydrin **80** by first esterification with p-nitrobenzoic acid. The dimethylphenylsilyl fluorohydrin **80** was chosen over TMS fluorohydrin **91** due to hydroxyester

contamination of the TMS which was a consequence of needing to use the one-pot protocol for this volatile substrate. Unfortunately, following chromatography and isolation of the para-nitro benzoate product, we obtained an oil.

A well-accepted explanation for the fluorine *gauche* effect is the hyperconjugative donor-acceptor interactions between  $\sigma_{C-X} - \sigma^*_{C-F}$  where X is the donor (in most cases hydrogen). Even though this hyperconjugative model for the fluorine *gauche* explains the conformation of many fluorinated organic molecules, there have been reports where electrostatic interactions can override fluorine *gauche* effects. One example is from the Emenike group which concluded that electrostatic CH- $\pi$  interactions can override fluorine *gauche* effects.<sup>52</sup> They report making three model systems that should display uniform conformational preferences based on fluorine *gauche* effects since they all possess the same fluoroethyl chains (Figure 4.6). However, these fluoroethyl groups are in different environments, and model **125** fluoroethyl protons can form an intramolecular CH- $\pi$  interaction with the adjacent aromatic ring. They confirm through molecular modeling that the CH- $\pi$  interaction is theoretically more effective when nitrogen and fluorine are oriented *anti* rather than in the *gauche* conformation. On the opposite end, models **126** and **127** are incapable of forming intramolecular CH- $\pi$  interaction. Their DFT computational results suggested that these compounds prefer the *gauche* conformers. The lowest energy *anti* conformer of **125** is 0.39 kcal mol<sup>-1</sup> more stable than its lowest energy *gauche* conformer. Models **126** and **127** are more stable in their *gauche* conformer than *anti* conformer by 0.56 and 0.32 kcal mol<sup>-1</sup>, respectively.<sup>52</sup>

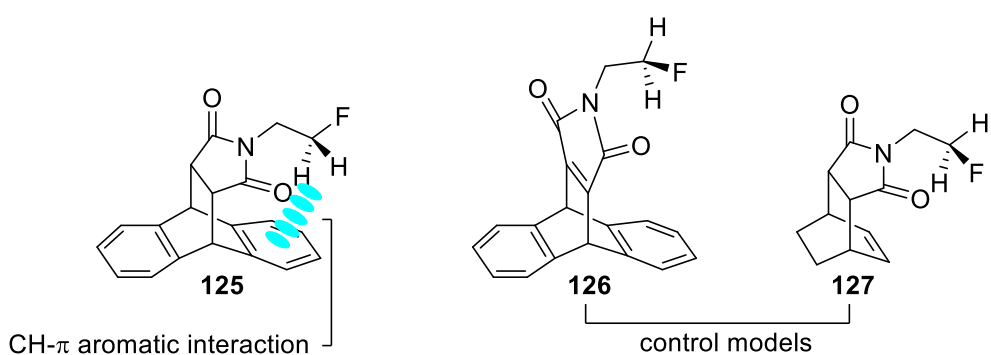


**Figure 4.6.** Model systems from the Emenike group.

To ascertain whether these predictions are valid in solution, they synthesized the model systems and compared their proton-fluorine vicinal coupling constants ( ${}^3J_{HF}$ ) to estimated theoretical values.<sup>52</sup> These experimental  ${}^3J_{HF}$  evaluated from  ${}^1H$  NMR represent weighted  ${}^3J_{HF}$  averages of the *gauche* and *anti* conformers (Eq. (1)), where  $F_g$  and  $F_a$  are the *gauche* and *anti* fractions, respectively. Equation (2) is a measure of conformational free energy, where  $K$  is the conformational equilibrium constant ( $0.5 F_g/F_a$ ). A  $K$  value greater than one corresponds to a negative  $\Delta G$  meaning fluorine *gauche* effects are present. A  $K$  value less than one displays the opposite, resulting in a positive  $\Delta G$  denoting an *anti* preference. According to their calculations, they report model **125** having a  $\Delta G = +0.17$  kcal mol<sup>-1</sup>, which indicated the presence of the *anti* conformation. In contrast, control models **126** and **127** show identical *gauche* effects with a  $\Delta G = -0.22$  kcal mol<sup>-1</sup>.

$$(1) \quad {}^3J_{HF(obs)} = {}^3J_{HF(g)} F_g + {}^3J_{HF(a)} F_a$$

$$(2) \quad \Delta G = -RT\ln K$$

Their group also looked at the  $CH_2F$  proton chemical shift for *anti*-preferring **125**, which was ~3.8 ppm. This is significantly shielded relative to the chemical shifts of the control models **126** and **127** observed at ~4.4 ppm. This is characteristic of an upfield chemical shift due to ring-current effects from the close proximity between methyl protons and the  $\pi$ -ring. To evaluate how this  $\pi$ -system might influence the fluorine *gauche* effect, a strongly electron-withdrawing nitro group was added to the aromatic ring for model **125**. They reported that the nitro group reduced the  $CH-\pi$  interaction energy  $\Delta G$  from +0.17 to -0.38 kcal mol<sup>-1</sup>. In other words, the electron-withdrawing nitro group was exclusively responsible for model **125**'s *gauche* preference. One could compare this system to ours despite being somewhat different. For electron-donating methyl groups on silicon as seen in the TMS fluorohydrin **91**, there is a slight preference for the *anti* conformation due to hyperconjugative effects. Replacement of these groups on silicon with electron-withdrawing phenyl groups as in the triphenylsilyl fluorohydrin **82**, results in a preferred *gauche* conformation.

Applying a similar NMR coupling constant technique to our fluorohydriins we can observe conformational constraints. Dolbier states in his book "Guide to Fluorine NMR for Organic Chemists"

that in rigid molecules the geometrical relationship of fluorine substitutes relative to vicinal hydrogens have distinct coupling constants (Figure 4.7 (A)).<sup>53</sup> The relationship being  $^3J_{HF}(anti)$  is 44 Hz whereas  $^3J_{HF}(gauche)$  is 10 Hz. For the case of fluoroethane, the H-F coupling constants comprise a weighted average of 26.4 Hz, simply the average of one *anti* and two *gauche* interactions. We see for our fluorohydrins the vicinal protons with respect to fluorine ( $\text{CH}_2\text{Si}$ ) have significantly different chemical shifts, 1.09 and 0.89 ppm for the trimethyl species **91**, compared to the more deshielded 2.03 and 1.76 ppm for the triphenyl species **82** (Figure 4.7 (B)). This is perhaps representative of the electron-donating nature of the three methyl groups on silicon further shielding the vicinal protons. We also observe a significant difference in coupling constants for the two methylene protons with both the TMS fluorohydrin **91** and triphenylsilyl fluorohydrin **82**. For TMS fluorohydrin **91** one of the protons (Ha) exhibits a  $^3J_{aF}(anti)$  = 35.3 Hz while the other (Hb) exhibits a  $^3J_{bF}(gauche)$  = 13.6 Hz. For triphenylsilyl fluorohydrin **82** one of the protons (Ha) exhibits a  $^3J_{aF}(anti)$  = 32.6 Hz while the other (Hb) exhibits a  $^3J_{bF}(gauche)$  = 13.5 Hz. Because we observe an *anti* and a *gauche* coupling constant for both species as opposed to two *gauche* or even an averaged coupling constant, this suggests that in solution this conformation is quite rigid. This could support a preference for the conformation exhibiting a fluorine-silicon *gauche* effect.

Furthermore, we wanted to see if NMR analysis could also be applied to understanding the conformation of the  $\text{CH}_2\text{OH}$  protons. Overlap of the  $\text{CH}_2\text{OH}$  protons in the fluorohydrins made this challenging. However, the pivaloyl protected triphenylsilyl fluorohydrin **124** provided adequate resolution of these signals.  $\beta$ -Fluoroesters have been shown to adopt the *gauche* conformation similar to fluorohydrins which allows us to make a direct comparison.<sup>54</sup> For these protons, both signals have  $^3J_{HF} = 22\text{-}25$  Hz suggesting averaging of coupling constants and little preference in solution for the *gauche* conformation at room temperature.

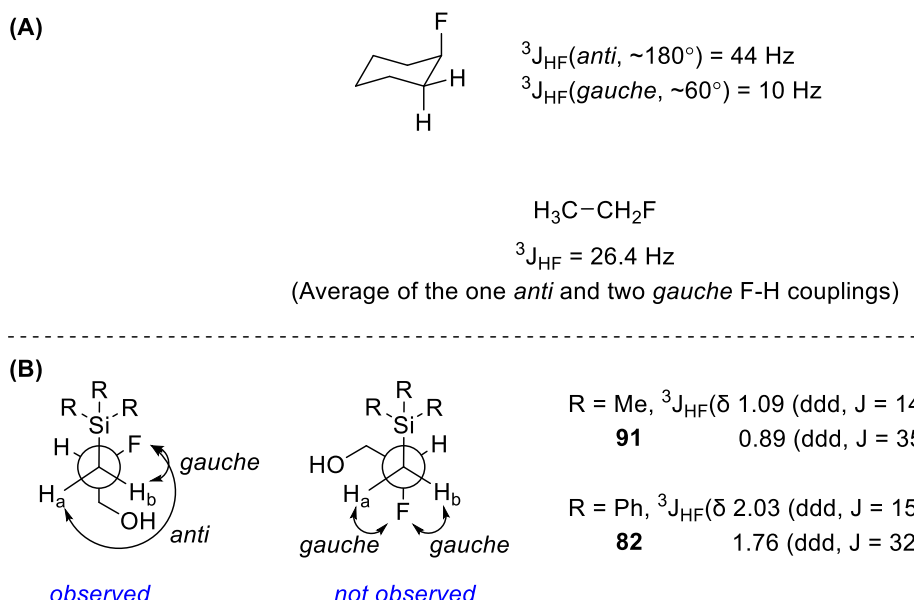


**Figure 4.7.** NMR coupling constant study using substrates **91** and **82**.

The second paper from the Thacker group approaches the fluorine *gauche* effect by considering electrostatic polarization instead of hyperconjugation.<sup>55</sup> This computational paper describes the electrostatics behind the 1,2-difluoroethane *gauche* effect using an Interacting quantum atoms (IQA) and relative energy gradient (REG) study. They report that in 1,2-difluoroethane, kinetic energy destabilizes the *gauche* conformation by  $-11.6 \text{ kJ mol}^{-1}$  compared to the *anti* conformation. The kinetic energy of the system represents the steric interactions between atoms in a system. They hypothesized this kinetic instability for the *gauche* conformation being due to their location closer to each other as opposed to the *anti* conformation. Hyperconjugation energy stabilizes the *gauche* conformation by  $2.1 \text{ kJ mol}^{-1}$  compared to the *anti* conformation. This was then followed by electrostatic energy stabilizing the *gauche* conformer by  $14.5 \text{ kJ mol}^{-1}$ . Despite the kinetic energy destabilizing the *gauche* conformation, the electrostatics have a greater preference for the *gauche* conformation, therefore dominating the system. They describe the largest IQA energies that stabilize the *gauche* effect over the *anti* to be 1,3 electrostatic interactions between C and F (C1-F7) (Figure 4.8). These 1,3 polarization terms show the largest change in energy for the whole dihedral angle and stabilizes when going from  $180^\circ$  to  $0^\circ$  by  $44.9 \text{ kJ mol}^{-1}$ . They also mention that since there are two equivalent 1,3 energy terms (C1-F7) and (C4-F8) the overall stability of the

*gauche* conformation is doubled. This is what they contribute to the overall *gauche* conformation of DFE.

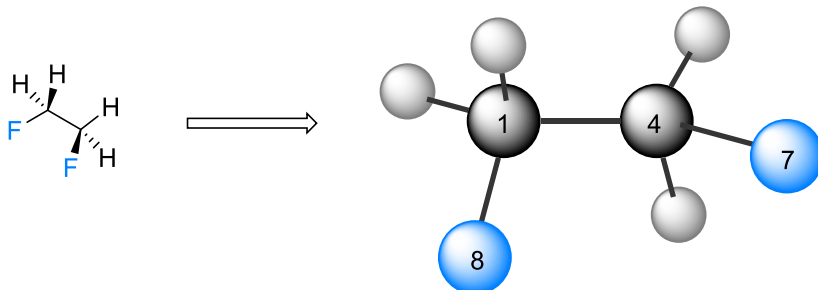
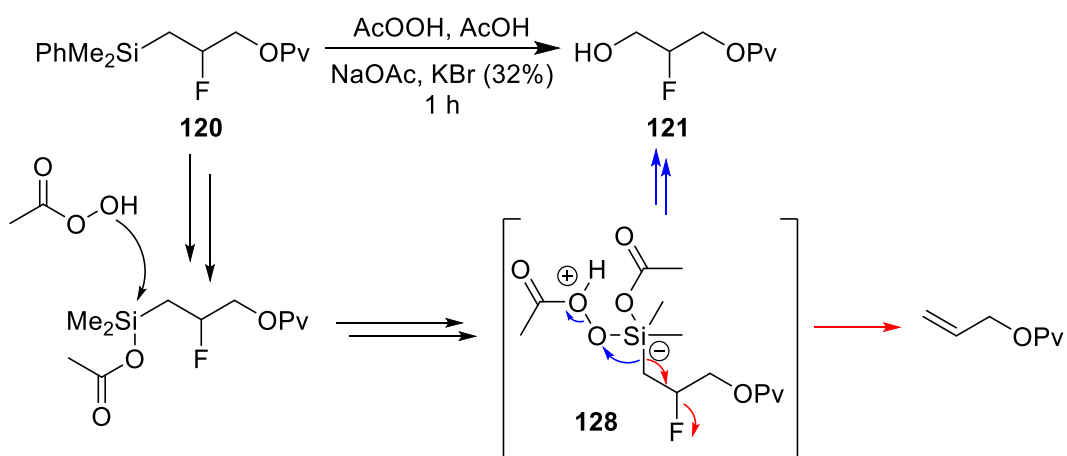


**Figure 4.8.** Global energy minima of DFE in the *gauche* conformation.

Based on the solved crystal structure and the NMR coupling constant study it seems evident that we are observing a fluorosilicon *gauche* effect. In this case, the fluorine silicon *gauche* effect would be the consequence of electrostatic interactions as opposed to hyperconjugation. These systems further support the importance of electrostatic interactions. This interaction could possibly help us understand why the Tamao oxidation yield was so low. If in solution the *gauche* interaction is observed due to electrostatics than during the Tamao the negatively charged silicon would facilitate an *anti* conformation increasing the likelihood of elimination **128** (Scheme 4.5).

**Scheme 4.5.** Possible explanation to elimination during the one-pot Tamao oxidations.



It would seem that performing further computational studies on the silicon fluorine moiety that we describe could be very useful for further understanding this effect. For instance, it is possible

that the system we present above allows for the tunability of this *gauche* effect depending on the substituents on silicon.

#### 4.3 Conclusions and Outlook

In conclusion, the exploration of a fluorine mediated rearrangement product led to the exciting discovery that various allylsilanes can be converted to the corresponding 3-silylfluorohydrins in good yields with excellent regioselectivity. This transformation is accomplished by epoxidation of said allylsilane followed epoxide opening with HF•TEA. Compared to other fluorohydrin syntheses by epoxide opening with HF•TEA, the formation of these silicon-substituted fluorohydrins occurs more readily (e.g. room temperature within one hour) and with higher regioselectivity that we attribute to a  $\beta$ -silyl effect. Reactions tended to be slower with phenyl-substituted silanes, which could be due to the electron-withdrawing nature of this group. However, extended reaction times allowed for these products to be successfully obtained in similarly high yield to other 3-silylfluorohydrins with differing substituents on silicon. Volatility of some intermediate epoxysilanes prompted us to investigate a one-pot epoxidation/epoxide opening reaction using a combination of mCPBA and HF•TEA. Yields for this one-pot procedure were generally in the same range as the overall yield from a two-step process involving epoxidation *in situ* generated oxone followed by treatment with HF•Et<sub>3</sub>N. However, the use of mCPBA generally gave small amounts of the 3-chlorobenzoate adduct resulting from 3-chlorobenzoic acid epoxide opening. For this reason, our preferred method for substrates with suitably low volatility remains the two-step sequence.

Conformational analysis of the TMS fluorohydrin **91** by DFT and the crystal structure of triphenylsilyl fluorohydrin **82** provides some evidence that electrostatics could be a main driving force for this fluorine-silicon *gauche* effect. Future work could involve computational studies on additional systems like this to better understand the origins of the fluorine *gauche* effect. With fluorohydrins synthesized from allylsilanes, I believe it is also reasonable to imagine an aziridine intermediate to form the fluoroamine. This system could potentially be a good handle for the incorporation into compounds later on. With this in mind, another future route of this work could

involve new or refined Tamao conditions to make these fluorine silicon moieties more appealing in synthesis.

## Chapter 5. Experimental

**General:** All reactions were carried out in Teflon vials in air unless otherwise noted. IR: Nicolet iS10 spectrometer, wavenumbers ( $\nu$ ) in  $\text{cm}^{-1}$ . All reagents were purchased and used as received unless otherwise mentioned. TLC analysis used 0.25 mm silica layer fluorescence  $\text{UV}_{254}$  plates. Flash chromatography: SilaCycle silica gel P60 (230-400 mesh). NMR: Spectra were recorded on a Varian Mercury 300, or Inova 500 spectrometer in the solvents indicated; chemical shifts ( $\delta$ ) are given in ppm, coupling constants ( $J$ ) in Hz. The solvent signals 2 were used as references (residual  $\text{CHCl}_3$  in  $\text{CDCl}_3$ :  $\delta_{\text{H}} \equiv 7.26$  ppm,  $\delta_{\text{C}} \equiv 77.0$  ppm; residual  $\text{C}_6\text{H}_6$  in  $\text{C}_6\text{D}_6$ :  $\delta_{\text{H}} \equiv 7.15$  ppm,  $\delta_{\text{C}} \equiv 128.0$  ppm).

### General Procedure (A1) Oxone Epoxidation.

To a mixture of allylsilane (1.0 mmol) and tert-butyl ammonium hydrogen sulfate (0.0136 g, 4 mol%) in MeCN-DMM (2:1) (8 mL), acetone (2.2 mL, 30 mmol), and aqueous  $\text{K}_2\text{CO}_3$  (0.1M) (0.2 mmol) was added. With vigorous stirring, oxone (3 mmol, in 8 mL of  $4 \times 10^{-4}$  M EDTA solution) and aqueous  $\text{K}_2\text{CO}_3$  (13.3 mmol, in 8 mL of  $\text{H}_2\text{O}$ ) were separately added via syringe pump over the indicated time. The reaction was extracted with hexanes (3 x 20 mL). The combined extractions were washed with brine and dried ( $\text{MgSO}_4$ ) before removing the solvent under reduced pressure. The crude material was then used directly into the next reaction without further purification.

### General Procedure (A2) $\text{HF}\bullet\text{Et}_3\text{N}$ Ring Opening.

A Teflon vial was charged with the epoxysilane (1 equiv) and DCM (0.05-0.1 M). The mixture was stirred and  $\text{HF}\bullet\text{Et}_3\text{N}$  (5 equiv) was added dropwise via syringe under air. The reaction vessel was sealed with a Teflon screw cap, and the solution was stirred over the indicated time at room temperature. The mixture was then poured into a beaker containing saturated aqueous  $\text{NaHCO}_3$  (75 mL) and allowed to stir until no evolution of  $\text{CO}_2$  was observed. The mixture was transferred to a separatory funnel and extracted with  $\text{CH}_2\text{Cl}_2$  (3 x 25 mL). The combined organic layers were dried ( $\text{MgSO}_4$ ) before removing the solvent under reduced pressure. The crude product was then purified by flash column chromatography on silica.

### General Procedure (B) One-Pot Fluorohydrin.

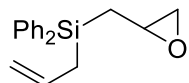
This procedure was adapted from that previously described by Sedgwick et al.:<sup>37</sup> A Teflon vial was charged with mCPBA (1.3 equiv) and DCM (0.0625-0.1 M) and stirred until the mCPBA had dissolved. With stirring,  $\text{HF}\bullet\text{Et}_3\text{N}$  (5-7 equiv) was then added followed immediately by the allylsilane (1 equiv) via syringe. The reaction vessel was sealed with a Teflon screw cap and the solution was stirred for

the indicated time at room temperature. The mixture was then poured into a beaker containing saturated aqueous NaHCO<sub>3</sub> (75 mL) and allowed to stir until no evolution of CO<sub>2</sub> was observed. The mixture was transferred to a separatory funnel and extracted with CH<sub>2</sub>Cl<sub>2</sub> (3 x 25 mL). The combined organic extracts were dried with MgSO<sub>4</sub> and filtered before removing the solvent under reduced pressure. The crude product was then purified by flash column chromatography on silica.

#### **General Shi Epoxidation Procedure**

To a mixture of the allylsilane (1.0 mmol) and *tert*-butyl ammonium hydrogen sulfate (0.0136 g, 4 mol%) in acetonitrile (15 mL), Shi catalyst (77.5 mg, 0.3 mmol) was added buffer (0.05 M Na<sub>2</sub>B4O<sub>7</sub> · 10 H<sub>2</sub>O in 4 x 10-4 M aqueous Na<sub>2</sub>(EDTA) (10 mL, 0.1 M). With vigorous stirring, a solution of oxone (1.38 mmol, in 6.5 mL of 4 x 10-4 M Na<sub>2</sub>(EDTA) solution) and aqueous K<sub>2</sub>CO<sub>3</sub> (5.8 mmol, in 6.5 mL of H<sub>2</sub>O) were separately added via syringe pump over the indicated time. Upon completion, the reaction mixture was extracted with hexanes (3 x 20 mL). The combined extracts were washed with brine, dried with MgSO<sub>4</sub>, and filtered before removing the solvent under reduced pressure. The crude product was used directly in the next reaction without further purification using procedure A2.

**(S)-3-(Triisopropylsilyl)propene oxide.** [α]<sub>D</sub><sup>25</sup> = -5.66 (*c* 1.45, CH<sub>2</sub>Cl<sub>2</sub>). NMR spectral data identical.<sup>38</sup>

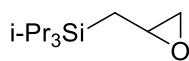


#### **allyl(oxiran-2-ylmethyl)diphenylsilane (52)**

The first part of general procedure A1. See the corresponding fluorohydrin for details.

**<sup>1</sup>H NMR** (500 MHz, CDCl<sub>3</sub>) δ 7.56 – 7.51 (m, 4H), 7.43 – 7.35 (m, 6H), 5.80 (ddt, *J* = 17.4, 10.1, 7.9 Hz, 1H), 4.98 – 4.88 (m, 2H), 3.03 (dddd, *J* = 7.8, 5.0, 3.9, 2.7 Hz, 1H), 2.67 (ddd, *J* = 4.9, 3.9, 0.9 Hz, 1H), 2.35 (dd, *J* = 5.0, 2.7 Hz, 1H), 2.19 (dt, *J* = 7.9, 1.2 Hz, 2H), 1.78 (dd, *J* = 14.4, 4.8 Hz, 1H), 1.18 (dd, *J* = 14.5, 8.3 Hz, 1H).

**<sup>13</sup>C NMR** (126 MHz, CDCl<sub>3</sub>) δ 134.87, 134.87, 134.43, 134.40, 133.43, 129.72, 128.00, 115.04, 49.90, 49.00, 20.90, 17.23.

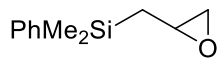


#### **triisopropyl(oxiran-2-ylmethyl)silane (74)**

The first part of general procedure A1. See the corresponding fluorohydrin for details.

**<sup>1</sup>H NMR** (500 MHz, CDCl<sub>3</sub>) δ 3.03 (dtd, *J* = 8.7, 4.1, 2.7 Hz, 1H), 2.81 (ddd, *J* = 4.9, 3.8, 1.1 Hz, 1H), 2.47 (dd, *J* = 5.0, 2.8 Hz, 1H), 1.29 (dd, *J* = 14.4, 4.3 Hz, 1H), 1.10 – 1.04 (m, 21H), 0.63 (dd, *J* = 14.3, 9.0 Hz, 1H).

**<sup>13</sup>C NMR** (126 MHz, CDCl<sub>3</sub>) δ 50.69, 49.70, 18.65, 14.20, 11.02.

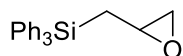


### **dimethyl(oxiran-2-ylmethyl)(phenyl)silane (75)**

The first part of general procedure A1. See the corresponding fluorohydrin for details.

**<sup>1</sup>H NMR** (500 MHz, CDCl<sub>3</sub>) δ 7.55 – 7.50 (m, 2H), 7.39 – 7.35 (m, 3H), 2.98 (dddd, *J* = 8.0, 5.2, 3.9, 2.7 Hz, 1H), 2.73 (ddd, *J* = 4.9, 3.9, 0.9 Hz, 1H), 2.37 (dd, *J* = 5.0, 2.8 Hz, 1H), 1.40 (ddd, *J* = 14.3, 4.9, 0.8 Hz, 1H), 0.85 (dd, *J* = 14.2, 8.2 Hz, 1H), 0.37 (s, 3H), 0.37 (s, 3H).

**<sup>13</sup>C NMR** (126 MHz, CDCl<sub>3</sub>) δ 138.15, 133.48, 129.25, 127.93, 50.31, 48.65, 20.43, -2.56, -2.62.

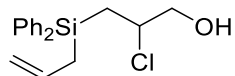


### **(oxiran-2-ylmethyl)triphenylsilane (76)**

The first part of general procedure A1. See the corresponding fluorohydrin for details.

**<sup>1</sup>H NMR** (500 MHz, CDCl<sub>3</sub>) δ 7.58 – 7.53 (m, 5H), 7.47 – 7.36 (m, 10H), 3.17 – 3.11 (m, 1H), 2.67 (t, *J* = 4.4 Hz, 1H), 2.35 (dd, *J* = 5.0, 2.7 Hz, 1H), 2.12 (dd, *J* = 14.5, 4.5 Hz, 1H), 1.41 (ddd, *J* = 14.5, 8.5, 0.9 Hz, 1H).

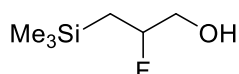
**<sup>13</sup>C NMR** (126 MHz, CDCl<sub>3</sub>) δ 135.59, 134.09, 129.82, 128.06, 50.09, 49.15, 18.42.



### **3-(allyldiphenylsilyl)-2-chloropropan-1-ol (55)**

Into a flame dried flask under nitrogen, allyl(oxiran-2-ylmethyl)diphenylsilane (74.5 mg, 0.266 mmol) along with DCM (13 mL, 0.02 M) were cool to -78 °C. Following this TiCl<sub>4</sub> (1 M in PhMe) (0.05 mL, 0.05 mmol) was added at -78 °C and allowed to stir for 2 hours. The reaction was quenched with aq. NaHCO<sub>3</sub> (30 mL) and extracted with DCM (3 x 20 mL). The combined organic extracts dried with MgSO<sub>4</sub> and filtered before removing the solvent under reduced pressure. The crude product was purified by flash column chromatography on silica (4:1 hexanes:ethyl acetate, R<sub>f</sub> ~ 0.15) to yield the compound as a colorless liquid (68.7 mg, 0.217 mmol, 81%).

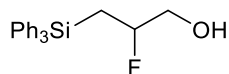
**<sup>1</sup>H NMR** (500 MHz, CDCl<sub>3</sub>) δ 7.59 – 7.51 (m, 4H), 7.45 – 7.37 (m, 6H), 5.86 – 5.74 (m, 1H), 5.00 – 4.90 (m, 2H), 4.19 (qd, *J* = 7.2, 3.5 Hz, 1H), 3.63 (dd, *J* = 12.1, 3.6 Hz, 1H), 3.51 (dd, *J* = 12.1, 7.1 Hz, 1H), 2.31 – 2.19 (m, 2H), 1.86 (ddd, *J* = 15.0, 7.9, 0.8 Hz, 1H), 1.77 (ddd, *J* = 14.9, 7.2, 1.0 Hz, 1H).  
**<sup>13</sup>C NMR** (126 MHz, CDCl<sub>3</sub>) δ 135.01, 134.95, 134.22, 133.91, 133.27, 129.90, 129.82, 128.13, 128.04, 115.32, 68.89, 63.30, 21.11, 19.77.



### 2-fluoro-3-(trimethylsilyl)propan-1-ol (91)

From allyltrimethylsilane (114 mg, 1.00 mmol) following procedure B was added HF•Et<sub>3</sub>N (0.27 mL, 5.0 mmol, 5 equiv), DCM (16 mL, 0.0625 M) and stirred for 1 hour. The crude product was purified by flash column chromatography on silica (4:1 hexanes:ethyl acetate, R<sub>f</sub> ~ 0.34) to yield the compound as a colorless liquid (98.5 mg, 0.655 mmol, 65%).

**<sup>1</sup>H NMR** (500 MHz, CDCl<sub>3</sub>) δ 4.79 (ddtd, *J* = 50.1, 8.9, 6.4, 2.7 Hz, 1H), 3.74 – 3.59 (m, 2H), 1.09 (ddd, *J* = 14.5, 13.6, 8.7 Hz, 1H), 0.89 (ddd, *J* = 35.2, 14.5, 6.3 Hz, 1H), 0.09 (d, *J* = 0.8 Hz, 8H).  
**<sup>13</sup>C NMR** (126 MHz, CDCl<sub>3</sub>) δ 93.74 (d, *J* = 166.2 Hz), 67.30 (d, *J* = 22.8 Hz), 19.82 (d, *J* = 22.6 Hz), - 1.00.  
**<sup>19</sup>F NMR** (470 MHz, CDCl<sub>3</sub>) δ -176.05 (dddd, *J* = 49.3, 34.6, 28.7, 20.4, 13.7 Hz).



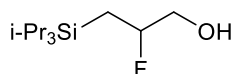
### 2-fluoro-3-(triphenylsilyl)propan-1-ol (82)

From allyltriphenylsilane (300 mg, 1.00 mmol) following procedure A1 was allowed to run for 16 hours. This was then taken directly into procedure A2 without purification. Epoxysilane (63.3 mg, 0.200 mmol), HF•Et<sub>3</sub>N (0.06 mL, 1 mmol, 5 equiv), DCM (2.5 mL, 0.08 M) stirred for 72 hours. The crude product was purified by flash column chromatography on silica (4:1 hexanes:ethyl acetate, R<sub>f</sub> ~ 0.2) to yield the compound as a white solid (53.5 mg, 0.16 mmol, 65%).

**<sup>1</sup>H NMR** (500 MHz, CDCl<sub>3</sub>) δ 7.56 – 7.53 (m, 5H), 7.44 – 7.36 (m, 10H), 4.92-4.76 (ddtd, *J* = 49.2, 8.4, 6.4, 2.9 Hz, 1H), 3.67 – 3.51 (m, 2H), 2.01 (ddd, *J* = 15.1, 13.6, 8.2 Hz, 1H), 1.74 (ddd, *J* = 32.6, 14.8, 6.4 Hz, 1H).  
**<sup>13</sup>C NMR** (126 MHz, CDCl<sub>3</sub>) δ 135.63, 134.01, 129.80, 128.06, 92.86 (d, *J* = 168.3 Hz), 66.89 (d, *J* = 22.6 Hz), 16.98 (d, *J* = 22.3 Hz).  
**<sup>19</sup>F NMR** (470 MHz, CDCl<sub>3</sub>) δ -173.21 – -173.55 (m).

**HRMS (ESI+)** Calculated for C<sub>21</sub>H<sub>21</sub>FNaOSi (M + Na): 359.123791. Found 359.124384

**IR** (neat) 3295, 3063, 2919, 2848, 1425, 1108, 1058, 703, 697 cm<sup>-1</sup>



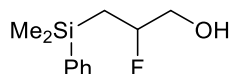
**2-fluoro-3-(triisopropylsilyl)propan-1-ol (79)**

From allyltriisopropylsilane (198 mg, 1.00 mmol) following procedure A1 was allowed to run for 4 hours. This was then taken directly into procedure A2 without purification. Epoxysilane (60 mg, 0.28 mmol), HF•Et<sub>3</sub>N (0.08 mL, 1.4 mmol, 5 equiv), DCM (5.6 mL, 0.05 M) stirred for 1.5 hours. The crude product was purified by flash column chromatography on silica (4:1 hexanes:ethyl acetate, R<sub>f</sub> ~ 0.4) to yield the compound as a colorless liquid (63.7 mg, 0.272 mmol, 92%).

**<sup>1</sup>H NMR** (500 MHz, CDCl<sub>3</sub>) δ 4.82 (ddddd, *J* = 49.7, 9.8, 7.2, 4.9, 2.7 Hz, 1H), 3.76 – 3.58 (m, 2H), 1.15 – 1.01 (m, 23H), 0.86 (ddd, *J* = 41.6, 14.9, 4.8 Hz, 1H).

**<sup>13</sup>C NMR** (126 MHz, CDCl<sub>3</sub>) δ 93.33 (d, *J* = 166.2 Hz), 67.84 (d, *J* = 23.5 Hz), 18.72, 18.69, 12.19 (d, *J* = 25.1 Hz), 11.25.

**<sup>19</sup>F NMR** (470 MHz, CDCl<sub>3</sub>) δ -175.25 – -175.63 (m).



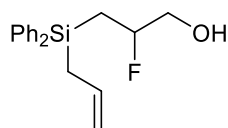
**3-(dimethyl(phenyl)silyl)-2-fluoropropan-1-ol (80)**

From allyldimethyl(phenyl)silane (176 mg, 1.00 mmol) following procedure A1 was allowed to run for 4 hours. This was then taken directly into procedure A2 without purification. Epoxysilane (192 mg, 1.00 mmol), HF•Et<sub>3</sub>N (0.27 mL, 5.0 mmol 5 equiv), DCM (20 mL, 0.05 M) stirred for 4 hours. The crude product was purified by flash column chromatography on silica (4:1 hexanes:ethyl acetate, R<sub>f</sub> ~ 0.2) to yield the compound as a colorless liquid (154 mg, 0.724 mmol, 72%).

**<sup>1</sup>H NMR** (500 MHz, CDCl<sub>3</sub>) δ 7.56 – 7.48 (m, 2H), 7.42 – 7.32 (m, 3H), 4.81-4.65 (ddtd, *J* = 50.0, 9.0, 6.4, 2.8 Hz, 1H), 3.67 – 3.51 (m, 2H), 1.81 (s, 1H), 1.32 (ddd, *J* = 14.6, 13.3, 8.7 Hz, 1H), 1.12 (ddd, *J* = 35.1, 14.6, 6.1 Hz, 1H), 0.38 (s, 3H), 0.36 (s, 3H).

**<sup>13</sup>C NMR** (126 MHz, CDCl<sub>3</sub>) δ 138.02, 133.50, 129.29, 127.97, 93.43 (d, *J* = 166.6 Hz), 67.14 (d, *J* = 22.8 Hz), 19.25 (d, *J* = 22.7 Hz), -2.14, -2.64.

**<sup>19</sup>F NMR** (470 MHz, CDCl<sub>3</sub>) δ -175.73 (ddddd, *J* = 49.0, 34.7, 28.0, 21.1, 13.3 Hz).



**3-(allyldiphenylsilyl)-2-fluoropropan-1-ol (59)**

From diallyldiphenylsilane (238 mg, 0.900 mmol) following procedure B was added HF•Et<sub>3</sub>N (0.27 mL, 4.5 mmol, 5 equiv), DCM (9 mL, 0.1 M) and stirred for 10 hours. The crude product was purified by flash column chromatography on silica (4:1 hexanes:ethyl acetate, R<sub>f</sub> ~ 0.17) to yield the compound as a colorless liquid (143 mg, 0.476 mmol, 53%).

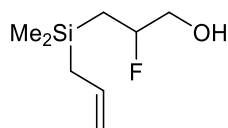
**<sup>1</sup>H NMR** (500 MHz, CDCl<sub>3</sub>) δ 7.54 (ddt, *J* = 12.4, 7.9, 1.5 Hz, 4H), 7.39 (dddd, *J* = 13.5, 8.0, 6.8, 4.7 Hz, 6H), 5.79 (dddd, *J* = 18.2, 15.8, 7.9, 1.2 Hz, 1H), 4.95 (dt, *J* = 16.9, 1.6 Hz, 1H), 4.91 (ddd, *J* = 10.0, 2.2, 1.0 Hz, 1H), 4.85-4.69 (ddtd, *J* = 49.2, 9.0, 6.0, 3.0 Hz, 1H), 3.66 – 3.52 (m, 2H), 2.20 (d, *J* = 7.9 Hz, 2H), 1.72 (ddd, *J* = 14.9, 12.5, 8.8 Hz, 1H), 1.44 (ddd, *J* = 35.5, 14.8, 5.9 Hz, 1H).

**<sup>13</sup>C NMR** (126 MHz, CDCl<sub>3</sub>) δ 134.94, 134.90, 134.43, 134.24, 133.46, 129.77, 129.72, 128.05, 127.98, 115.09, 92.93 (d, *J* = 167.2 Hz), 67.00 (d, *J* = 22.9 Hz), 21.05, 15.76 (d, *J* = 23.2 Hz).

**<sup>19</sup>F NMR** (470 MHz, CDCl<sub>3</sub>) δ -174.96 – -175.39 (m).

**HRMS (ESI+)** Calculated for C<sub>18</sub>H<sub>21</sub>FNaOSi (M + Na): 323.123791. Found 323.124277

**IR** (neat) 3324, 3070, 3047, 2927, 2869, 1629, 1427, 1106, 900, 844, 696 cm<sup>-1</sup>



**3-(allyldimethylsilyl)-2-fluoropropan-1-ol (92)**

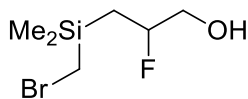
From diallyldimethylsilane (70 mg, 0.50 mmol) following procedure B was added HF•Et<sub>3</sub>N (0.13 mL, 2.5 mmol, 5 equiv), DCM (8 mL, 0.0625 M) and stirred for 1 hour. The crude product was purified by flash column chromatography on silica (4:1 hexanes:ethyl acetate, R<sub>f</sub> ~ 0.34) to yield the compound as a colorless liquid (50 mg, 0.28 mmol, 56%).

**<sup>1</sup>H NMR** (500 MHz, CDCl<sub>3</sub>) δ 5.77 (ddt, *J* = 16.6, 10.3, 8.1 Hz, 1H), 4.91 – 4.68 (m, 3H), 3.74 – 3.56 (m, 2H), 1.58 (dt, *J* = 8.1, 1.3 Hz, 2H), 1.09 (ddd, *J* = 14.6, 12.7, 9.1 Hz, 1H), 0.88 (ddd, *J* = 37.2, 14.6, 5.9 Hz, 1H), 0.08 (d, *J* = 0.9 Hz, 6H).

**<sup>13</sup>C NMR** (126 MHz, CDCl<sub>3</sub>) δ 134.40, 113.48, 93.49 (d, *J* = 165.9 Hz), 67.33 (d, *J* = 23.1 Hz), 23.56, 17.93 (d, *J* = 23.6 Hz), -3.01, -3.14.

**<sup>19</sup>F NMR** (470 MHz, CDCl<sub>3</sub>) δ -176.55 (ddddd, *J* = 49.5, 37.3, 28.5, 20.2, 12.6 Hz).

**HRMS (ESI+)** Calculated for C<sub>8</sub>H<sub>17</sub>FNaOSi (M + Na): 199.092491. Found 199.092151



### 3-((bromomethyl)dimethylsilyl)-2-fluoropropan-1-ol (81)

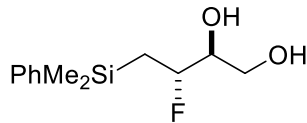
From allyl(bromomethyl)dimethylsilane (193 mg, 1.00 mmol) following procedure A1 was allowed to run for 4 hours. This was then taken directly into procedure A2 without purification. Epoxysilane (104 mg, 0.500 mmol), HF•Et<sub>3</sub>N (0.13 mL, 2.5 mmol, 5 equiv), DCM (10 mL, 0.05 M) stirred for 2 hours. The crude product was purified by flash column chromatography on silica (4:1 hexanes:ethyl acetate, R<sub>f</sub> ~ 0.4) to yield the compound as a colorless liquid (68.8 mg, 0.300 mmol, 60%).

<sup>1</sup>H NMR (500 MHz, CDCl<sub>3</sub>) δ 4.89–4.72 (ddddd, *J* = 49.5, 9.6, 6.7, 5.0, 2.7 Hz, 1H), 3.75 – 3.58 (m, 2H), 2.52 (d, *J* = 2.5 Hz, 2H), 1.22 (ddd, *J* = 14.8, 11.1, 9.8 Hz, 1H), 1.02 (ddd, *J* = 40.6, 14.9, 5.0 Hz, 1H), 0.22 (s, 6H).

<sup>13</sup>C NMR (126 MHz, CDCl<sub>3</sub>) δ 93.24 (d, *J* = 166.2 Hz), 67.36 (d, *J* = 24.4 Hz), 17.48 (d, *J* = 25.1 Hz), 17.08, -3.21, -3.23.

<sup>19</sup>F NMR (470 MHz, CDCl<sub>3</sub>) δ -177.82 (dtdd, *J* = 49.8, 40.3, 20.8, 11.2 Hz).

HRMS (ESI+) Calculated for C<sub>6</sub>H<sub>14</sub>BrFNaOS (M + Na): 250.987353. Found 250.988441



### 4-(dimethyl(phenyl)silyl)-3-fluorobutane-1,2-diol (99)

From 4-(dimethyl(phenyl)silyl)but-2-en-1-ol (128 mg, 0.620 mmol) following procedure B was added HF•Et<sub>3</sub>N (0.23 mL, 4.3 mmol, 7 equiv), DCM (6.2 mL, 0.1 M) and stirred for 4 hour. The crude product was purified by flash column chromatography on silica (1:1 hexanes:ethyl acetate, R<sub>f</sub> ~ 0.1) to yield the compound as a colorless liquid (40.8 mg, 0.168 mmol, 27%).

Mixture of diastereomers

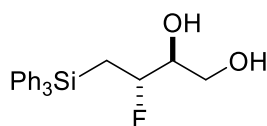
<sup>1</sup>H NMR (500 MHz, CDCl<sub>3</sub>) δ 7.57 – 7.50 (m, 4H), 7.37 (dtd, *J* = 5.1, 3.8, 1.4 Hz, 6H), 4.75 – 4.58 (m, 2H), 3.77 – 3.55 (m, 6H), 1.35 (tt, *J* = 16.3, 10.9 Hz, 2H), 1.25 – 1.10 (m, 2H), 0.39 – 0.36 (m, 12H).

Single diastereomer

<sup>13</sup>C NMR (126 MHz, CDCl<sub>3</sub>) δ 133.54, 129.81, 129.26, 127.95, 93.35 (d, *J* = 166.7 Hz), 75.27 (d, *J* = 20.5 Hz), 63.29 (d, *J* = 6.2 Hz), 19.29 (d, *J* = 25.7 Hz), -2.08, -2.59.

Mixture of diastereomers

<sup>19</sup>F NMR (470 MHz, CDCl<sub>3</sub>) δ -180.18 (tt, *J* = 46.1, 12.3 Hz), -183.53 (tdd, *J* = 46.2, 18.6, 10.3 Hz).



**3-fluoro-4-(triphenylsilyl)butane-1,2-diol (100)**

From 4-(triphenylsilyl)but-2-en-1-ol (224 mg, 0.678 mmol) following procedure B was added HF•Et<sub>3</sub>N (0.37 mL, 6.8 mmol, 10 equiv), DCM (6.8 mL, 0.1 M) and stirred for 16 hour. The crude product was purified by flash column chromatography on silica (1:1 hexanes:ethyl acetate, R<sub>f</sub> ~ 0.1) to yield the compound as a colorless liquid (49.7 mg, 0.136 mmol, 20%).

Mixture of diastereomers

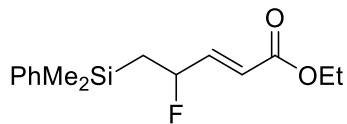
<sup>1</sup>H NMR (500 MHz, CDCl<sub>3</sub>) δ 7.58 – 7.52 (m, 10H), 7.46 – 7.34 (m, 19H), 4.85 – 4.67 (m, 2H), 3.77 – 3.55 (m, 6H), 2.12 – 1.96 (m, 2H), 1.91 – 1.73 (m, 2H).

Single diastereomer

<sup>13</sup>C NMR (126 MHz, CDCl<sub>3</sub>) δ 135.66, 134.09, 129.78, 128.03, 92.77 (d, *J* = 168.3 Hz), 74.81 (d, *J* = 20.0 Hz), 63.45 (d, *J* = 5.5 Hz), 17.05 (d, *J* = 24.9 Hz).

Mixture of diastereomers

<sup>19</sup>F NMR (470 MHz, CDCl<sub>3</sub>) δ -177.33 (t, *J* = 45.6 Hz), -181.42 – -181.85 (m).

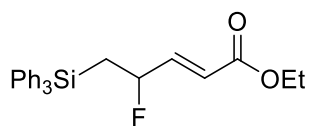


**ethyl (E)-5-(dimethyl(phenyl)silyl)-4-fluoropent-2-enoate (113)**

In an open air atmosphere 3-(dimethyl(phenyl)silyl)-2-fluoropropan-1-ol (188 mg, 0.885 mmol) in DCM (8.9 mL, 0.1 M) was cooled to 0 °C and Dess-Martin periodinane (300 mg, 0.708 mmol) was added. This was allowed to stir for 20 minutes then removed from ice and an additional Dess-Martin periodinane (300 mg, 0.708 mmol) was added. The mixture was allowed to warm to room temperature and stir for 40 minutes. This reaction was quenched with aq. Na<sub>2</sub>S<sub>2</sub>O<sub>3</sub> (30 mL) and extracted with DCM (3 x 20 mL). The combined organic extracts dried with MgSO<sub>4</sub> and filtered before removing the solvent under reduced pressure. The crude product was taken into the following Wittig reaction without further purification. Into a flame dried flask under nitrogen, the crude product, THF (8.9 mL, 0.1 M), and then ethyl (triphenylphosphoranylidene)acetate **111** (462 mg, 1.33 mmol) were allowed to stir at room temperature for 16 hours. This mixture was then transferred to a round bottom and the solvent was removed under reduced pressure. The crude

product was purified by flash column chromatography on silica (4:1 hexanes:ethyl acetate,  $R_f \sim 0.7$ ) to yield the compound as a colorless liquid (135 mg, 0.480 mmol, 54%).

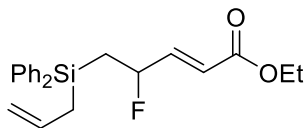
**<sup>1</sup>H NMR** (500 MHz, CDCl<sub>3</sub>) δ 7.53 – 7.50 (m, 2H), 7.39 – 7.35 (m, 3H), 6.83 (ddd,  $J = 18.6, 15.7, 4.6$  Hz, 1H), 5.95 (dt,  $J = 15.6, 1.7$  Hz, 1H), 5.17 (ddddd,  $J = 48.0, 8.7, 6.3, 4.6, 1.7$  Hz, 1H), 4.19 (q,  $J = 7.1$  Hz, 2H), 1.43 (td,  $J = 14.6, 8.7$  Hz, 1H), 1.33 – 1.21 (m, 4H), 0.38 (d,  $J = 0.8$  Hz, 3H), 0.37 (s, 3H).  
**<sup>13</sup>C NMR** (126 MHz, CDCl<sub>3</sub>) δ 166.05, 146.74 (d,  $J = 20.1$  Hz), 137.69, 133.55, 129.34, 127.98, 120.30 (d,  $J = 10.6$  Hz), 90.06 (d,  $J = 171.7$  Hz), 60.56, 23.74 (d,  $J = 24.1$  Hz), 14.21, -2.17, -2.49 (d,  $J = 1.5$  Hz).  
**<sup>19</sup>F NMR** (470 MHz, CDCl<sub>3</sub>) δ -168.43 (dddd,  $J = 48.7, 33.7, 18.7, 14.5$  Hz).



#### **ethyl (E)-4-fluoro-5-(triphenylsilyl)pent-2-enoate (112)**

In an open air atmosphere 2-fluoro-3-(triphenylsilyl)propan-1-ol (229 mg, 0.680 mmol) in DCM (6.8 mL, 0.1 M) was cooled to 0 °C and Dess-Martin periodinane (231 mg, 0.545 mmol) was added. This was allowed to stir for 20 minutes then removed from ice and an additional Dess-Martin periodinane (231 mg, 0.545 mmol) was added. The mixture was allowed to warm to room temperature and stir for 40 minutes. This reaction was quenched with aq. Na<sub>2</sub>S<sub>2</sub>O<sub>3</sub> (30 mL) and extracted with DCM (3 x 20 mL). The combined organic extracts dried with MgSO<sub>4</sub> and filtered before removing the solvent under reduced pressure. The crude product was taken into the following Wittig reaction without further purification. Into a flame dried flask under nitrogen, the crude product, THF (6.8 mL, 0.1 M), and then ethyl (triphenylphosphoranylidene)acetate **111** (355 mg, 1.02 mmol) were allowed to stir at room temperature for 16 hours. This mixture was then transferred to a round bottom and the solvent was removed under reduced pressure. The crude product was purified by flash column chromatography on silica (4:1 hexanes:ethyl acetate,  $R_f \sim 0.6$ ) to yield the compound as a colorless liquid (170 mg, 0.420 mmol, 62%).

**<sup>1</sup>H NMR** (500 MHz, CDCl<sub>3</sub>) δ 7.57 – 7.52 (m, 5H), 7.46 – 7.35 (m, 10H), 6.87 – 6.75 (m, 1H), 5.92 (ddd,  $J = 15.9, 2.1, 1.4$  Hz, 1H), 5.26 (ddddd,  $J = 47.6, 8.3, 6.3, 4.3, 1.8$  Hz, 1H), 4.16 (q,  $J = 7.1$  Hz, 2H), 2.11 (ddd,  $J = 14.8, 13.1, 8.8$  Hz, 1H), 1.85 (ddd,  $J = 34.5, 14.8, 6.1$  Hz, 1H), 1.26 (t,  $J = 7.1$  Hz, 3H).  
**<sup>13</sup>C NMR** (126 MHz, CDCl<sub>3</sub>) δ 165.92, 146.46 (d,  $J = 20.0$  Hz), 135.69, 133.75, 129.86, 128.08, 120.42 (d,  $J = 10.8$  Hz), 89.50 (d,  $J = 173.2$  Hz), 60.52, 21.49 (d,  $J = 24.1$  Hz), 14.21.  
**<sup>19</sup>F NMR** (470 MHz, CDCl<sub>3</sub>) δ -166.86 (dddd,  $J = 47.7, 33.3, 19.1, 13.1$  Hz).



**ethyl (E)-5-(allyldiphenylsilyl)-4-fluoropent-2-enoate**

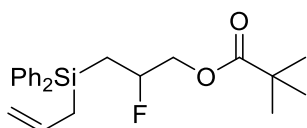
Into a flame dried flask under nitrogen, DCM (8.7 mL, 0.2 M) and oxalyl chloride 0.23 mL, 2.6 mmol) was cooled to -78 °C. DMSO (0.250 mL, 3.47 mmol) was added and allowed to stir for 15 minutes at -78 °C then 3-(allyldiphenylsilyl)-2-fluoropropan-1-ol (521.5 mg, 1.736 mmol) was added and stirred for 20 minutes. Following this TEA (1.22 mL, 8 mmol) was added and allowed to stir for 1 hour. The reaction was then quenched with water (30 mL) and extracted with DCM (3 x 20 mL). The combined organic extracts dried with MgSO<sub>4</sub> and filtered before removing the solvent under reduced pressure. A portion crude material was taken directly into the following reaction without further purification. Into a flame dried flask under nitrogen, the crude material (149 mg, 0.500 mmol) along with THF (5 mL, 0.1 M), then ethyl (triphenylphosphoranylidene)acetate **111** (261 mg, 0.750 mmol) was added and allowed to stir overnight. This mixture was then transferred to a round bottom and the solvent was removed under reduced pressure. The crude product was purified by flash column chromatography on silica (4:1 hexanes:ethyl acetate, R<sub>f</sub> ~ 0.5) to yield the compound as a colorless liquid (139 mg, 0.378 mmol, 76%).

**<sup>1</sup>H NMR** (500 MHz, CDCl<sub>3</sub>) δ 7.56 – 7.48 (m, 4H), 7.39 (dddd, *J* = 11.6, 8.3, 6.2, 4.3 Hz, 6H), 6.81 (ddd, *J* = 18.6, 15.6, 4.6 Hz, 1H), 5.92 (dt, *J* = 15.7, 1.7 Hz, 1H), 5.77 (ddt, *J* = 17.9, 9.9, 7.9 Hz, 1H), 5.18 (ddtd, *J* = 47.8, 9.0, 4.6, 1.6 Hz, 1H), 4.98 – 4.89 (m, 2H), 4.17 (q, *J* = 7.1 Hz, 2H), 2.22 – 2.19 (m, 2H), 1.81 (ddd, *J* = 14.7, 13.0, 9.0 Hz, 1H), 1.59 (ddd, *J* = 35.4, 14.7, 5.9 Hz, 1H), 1.27 (t, *J* = 7.2 Hz, 3H).

**<sup>13</sup>C NMR** (126 MHz, CDCl<sub>3</sub>) δ 165.94, 146.47 (d, *J* = 20.2 Hz), 134.97, 134.94, 134.05, 133.95, 133.27, 129.81, 129.79, 128.06, 128.01, 120.41 (d, *J* = 10.7 Hz), 115.22, 89.64 (d, *J* = 172.1 Hz), 60.56, 21.00 (d, *J* = 1.6 Hz), 20.18 (d, *J* = 24.5 Hz), 14.21.

**<sup>19</sup>F NMR** (470 MHz, CDCl<sub>3</sub>) δ -168.10 (dddd, *J* = 48.0, 35.4, 18.7, 12.8 Hz).

**IR** (neat) 3070, 2975, 2921, 1718, 1427, 1267, 1178, 1108, 975, 898, 698 cm<sup>-1</sup>



**3-(allyldiphenylsilyl)-2-fluoropropyl pivalate (116)**

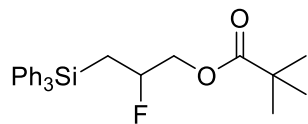
To a solution of 3-(allyldiphenylsilyl)-2-fluoropropan-1-ol (184 mg, 0.615 mmol) in DCM (3.1 mL, 0.2 M) at 0 °C was added pyridine (0.150 mL, 1.85 mmol) and pivaloyl chloride (0.180 mL, 1.48 mmol). The mixture was allowed to slowly warm to room temperature while stirring over 16 hours. The

reaction was quenched with aq. NaHCO<sub>3</sub> (30 mL) and extracted with DCM (3 x 20 mL). The combined organic extracts dried with MgSO<sub>4</sub> and filtered before removing the solvent under reduced pressure. The crude product was purified by flash column chromatography on silica (4:1 hexanes:ethyl acetate, R<sub>f</sub> ~ 0.7) to yield the compound the pivaloyl ester as a colorless liquid (209 mg, 0.550 mmol, 89%).

**<sup>1</sup>H NMR** (500 MHz, CDCl<sub>3</sub>) δ 7.56 – 7.49 (m, 4H), 7.44 – 7.35 (m, 6H), 5.78 (ddt, J = 16.9, 10.2, 8.0 Hz, 1H), 4.97 – 4.75 (m, 3H), 4.13 (ddd, J = 26.3, 12.3, 2.7 Hz, 1H), 4.04 (ddd, J = 21.4, 12.3, 6.5 Hz, 1H), 2.22 – 2.19 (m, 2H), 1.72 (ddd, J = 14.9, 11.3, 9.6 Hz, 1H), 1.44 (ddd, J = 38.0, 14.8, 5.2 Hz, 1H), 1.20 (s, 9H).

**<sup>13</sup>C NMR** (126 MHz, CDCl<sub>3</sub>) δ 178.15, 134.96, 134.89, 134.30, 134.09, 133.40, 129.77, 129.72, 128.04, 127.97, 115.12, 89.59 (d, J = 171.5 Hz), 67.28 (d, J = 23.1 Hz), 38.82, 27.16, 20.95 (d, J = 1.6 Hz), 16.13 (d, J = 24.2 Hz).

**<sup>19</sup>F NMR** (470 MHz, CDCl<sub>3</sub>) δ -173.70 (ddddd, J = 48.5, 38.0, 26.2, 21.5, 11.3 Hz).



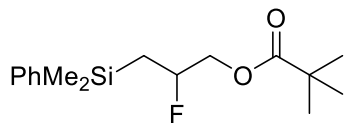
#### 2-fluoro-3-(triphenylsilyl)propyl pivalate (124)

To a solution of 2-fluoro-3-(triphenylsilyl)propan-1-ol (170 mg, 0.500 mmol) in DCM (2.5 mL, 0.2 M) at 0 °C was added pyridine (0.100 mL, 1.25 mmol) and pivaloyl chloride (0.12 mL, 1.0 mmol). The mixture was allowed to slowly warm to room temperature while stirring over 16 hours. The reaction was quenched with aq. NaHCO<sub>3</sub> (30 mL) and extracted with DCM (3 x 20 mL). The combined organic extracts dried with MgSO<sub>4</sub> and filtered before removing the solvent under reduced pressure. The crude product was purified by flash column chromatography on silica (4:1 hexanes:ethyl acetate, R<sub>f</sub> ~ 0.5) to yield the compound the pivaloyl ester as a colorless liquid (207 mg, 0.490 mmol, 98%).

**<sup>1</sup>H NMR** (500 MHz, CDCl<sub>3</sub>) δ 7.60 – 7.55 (m, 5H), 7.47 – 7.37 (m, 10H), 4.92 (ddtd, J = 48.5, 8.7, 5.8, 2.6 Hz, 1H), 4.17 (ddd, J = 25.7, 12.4, 2.3 Hz, 1H), 4.07 (ddd, J = 22.1, 12.4, 6.3 Hz, 1H), 2.04 (ddd, J = 15.0, 12.3, 8.8 Hz, 1H), 1.77 (ddd, J = 35.1, 15.0, 5.8 Hz, 1H), 1.22 (s, 9H).

**<sup>13</sup>C NMR** (126 MHz, CDCl<sub>3</sub>) δ 178.10, 135.67, 133.91, 129.84, 128.08, 89.47 (d, J = 172.7 Hz), 67.18 (d, J = 22.8 Hz), 38.84, 27.19, 17.42 (d, J = 23.6 Hz).

**<sup>19</sup>F NMR** (470 MHz, CDCl<sub>3</sub>) δ -171.63 (ddddd, J = 48.1, 44.7, 23.7, 12.0 Hz).



**3-(dimethyl(phenyl)silyl)-2-fluoropropyl pivalate (120)**

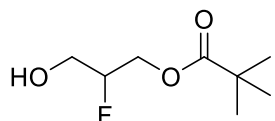
To a solution of 3-(dimethyl(phenyl)silyl)-2-fluoropropan-1-ol (212 mg, 0.956 mmol) in DCM (4.8 mL, 0.2 M) at 0 °C was added pyridine (0.23 mL, 2.9 mmol) and pivaloyl chloride (0.28 mL, 2.3 mmol).

The mixture was allowed to slowly warm to room temperature while stirring over 16 hours. The reaction was quenched with aq. NaHCO<sub>3</sub> (30 mL) and extracted with DCM (3 x 20 mL). The combined organic extracts dried with MgSO<sub>4</sub> and filtered before removing the solvent under reduced pressure. The crude product was purified by flash column chromatography on silica (4:1 hexanes:ethyl acetate, R<sub>f</sub> ~ 0.7) to yield the compound the pivaloyl ester as a colorless liquid (242 mg, 0.819 mmol, 85%).

**<sup>1</sup>H NMR** (500 MHz, CDCl<sub>3</sub>) δ 7.54 – 7.50 (m, 2H), 7.39 – 7.36 (m, 3H), 4.80 (ddddd, *J* = 49.1, 9.3, 6.9, 5.7, 2.5 Hz, 1H), 4.14 (ddd, *J* = 27.6, 12.4, 2.5 Hz, 1H), 4.03 (ddd, *J* = 20.7, 12.4, 6.8 Hz, 1H), 1.32 (ddd, *J* = 14.8, 12.4, 9.2 Hz, 1H), 1.21 (s, 9H), 1.14 (ddd, *J* = 36.5, 14.6, 5.7 Hz, 1H), 0.38 (d, *J* = 0.9 Hz, 3H), 0.36 (d, *J* = 0.9 Hz, 3H).

**<sup>13</sup>C NMR** (126 MHz, CDCl<sub>3</sub>) δ 178.24, 137.91, 133.51, 129.30, 127.97, 90.08 (d, *J* = 170.9 Hz), 67.44 (d, *J* = 22.9 Hz), 38.83, 27.15, 19.63 (d, *J* = 23.6 Hz), -2.18, -2.65.

**<sup>19</sup>F NMR** (470 MHz, CDCl<sub>3</sub>) δ -173.78 (ddddd, *J* = 48.7, 33.3, 27.7, 20.6, 12.4 Hz).



**2-fluoro-3-hydroxypropyl pivalate (121)**

The pivaloyl ester (80.9 mg, 0.273 mmol, 1 equiv), KBr (48.7 mg, 0.410 mmol, 1.5 equiv), and NaOAc (67.7 mg, 0.820 mmol) were dissolved in acetic acid (1.3 mL) and the mixture was cooled to 0 °C. Additional NaOAc (178.6 mg, 2.17 mmol) was added followed by peracetic acid (0.96 ml, 4.7 mmol) and the mixture stirred for 15 minutes before adding additional peracetic acid (2.2 mL, 9.8 mmol). The flask was removed from the ice bath and allowed to warm while stirring for 1 hour. The reaction was carefully quenched by slowly adding aq. Na<sub>2</sub>S<sub>2</sub>O<sub>3</sub> (6 mL). Additional aq. NaHCO<sub>3</sub> (40 mL) was added and solid NaHCO<sub>3</sub> was added until effervescence ceased. Upon completion, the reaction mixture was extracted with CH<sub>2</sub>Cl<sub>2</sub> (3 x 20 mL). The combined organic extracts dried with MgSO<sub>4</sub> and filtered before removing the solvent under reduced pressure. The crude product was purified by flash column chromatography on silica (4:1 hexanes:ethyl acetate, R<sub>f</sub> ~ 0.17) to yield the compound as a colorless liquid (15.4 mg, 0.0860 mmol, 32%).

**<sup>1</sup>H NMR** (500 MHz, CDCl<sub>3</sub>) δ 4.74 (dqd, J = 47.9, 4.9, 4.1 Hz, 1H), 4.37 – 4.25 (m, 2H), 3.79 (dd, J = 21.4, 4.8 Hz, 2H), 1.22 (s, 9H).

**<sup>13</sup>C NMR** (126 MHz, CDCl<sub>3</sub>) δ 178.52, 91.18 (d, J = 173.5 Hz), 62.54 (d, J = 24.0 Hz), 61.75 (d, J = 23.2 Hz), 38.89, 27.12.

**<sup>19</sup>F NMR** (470 MHz, CDCl<sub>3</sub>) δ -197.46 (dq, J = 48.3, 21.6 Hz).

## Crystal Data

Crystallographic analysis for compound **82**.

A colorless needle, measuring 0.375 x 0.100 x 0.080 mm<sup>3</sup> was mounted on a loop with oil. Data was collected at -173°C on a Bruker APEX II single crystal X-ray diffractometer, Mo-radiation, equipped with a Miracol X-ray optical collimator.

Crystal-to-detector distance was 40 mm and exposure time was 10 seconds per frame for all sets. The scan width was 0.5°. Data collection was 100% complete to 25° in 9. A total of xxx reflections were collected covering the indices, h = -xx to xx, k = -xx to xx, l = -xx to xx. 6584 reflections were symmetry independent and the R<sub>int</sub> = 0.0858 indicated that the data was of average quality (0.07). Indexing and unit cell refinement indicated a C-centered monoclinic lattice lattice. The space group was found to be C2 (No. 5).

The data was integrated and scaled using SAINT, SADABS within the APEX2 software package by Bruker.<sup>56</sup>

The data appeared twinned via 180 degrees about reciprocal (0 0 1) (CELL\_NOW<sup>57</sup>) and after multi-domain integration (SAINT, SADABS within the APEX2 software package by Bruker<sup>58</sup>) the data was merged utilizing twinabs.<sup>59</sup>

Solution by direct methods (SHELXT<sup>60</sup> or SIR97<sup>61</sup>) produced a complete heavy atom phasing model consistent with the proposed structure. The structure was completed by difference Fourier synthesis with SHELXL.<sup>62</sup> Scattering factors are from Waasmair and Kirfel<sup>63</sup>. Hydrogen atoms were placed in geometrically idealised positions and constrained to ride on their parent atoms with C---H distances in the range 0.95-1.00 Angstrom. Isotropic thermal parameters U<sub>eq</sub> were fixed such that they were 1.2U<sub>eq</sub> of their parent atom U<sub>eq</sub> for CH's and 1.5U<sub>eq</sub> of their parent atom U<sub>eq</sub> in case of methyl groups. All non-hydrogen atoms were refined anisotropically by full-matrix least-squares.

The asymmetric unit of this chiral space group contains two independent molecules. The functional groups of both are triple disordered. The disorder required application of restraints on the displacement parameters of the disordered moieties. The phenyl groups are optimized. The disordered group can be distinguished as a dominant cis conformation (as shown in Fig. 1 on the left) and two trans configurations as shown on the right.

The structure is of high quality and ready for publication. Table 1 summarizes the data collection details.

**Figure 5.1.** shows an ORTEP<sup>64</sup> of the asymmetric unit.

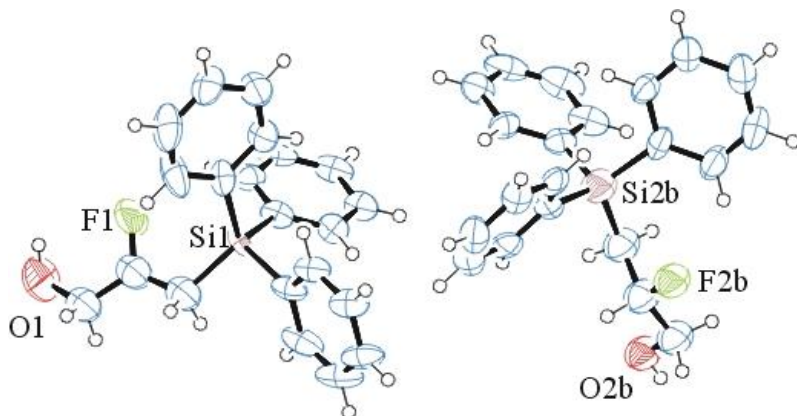


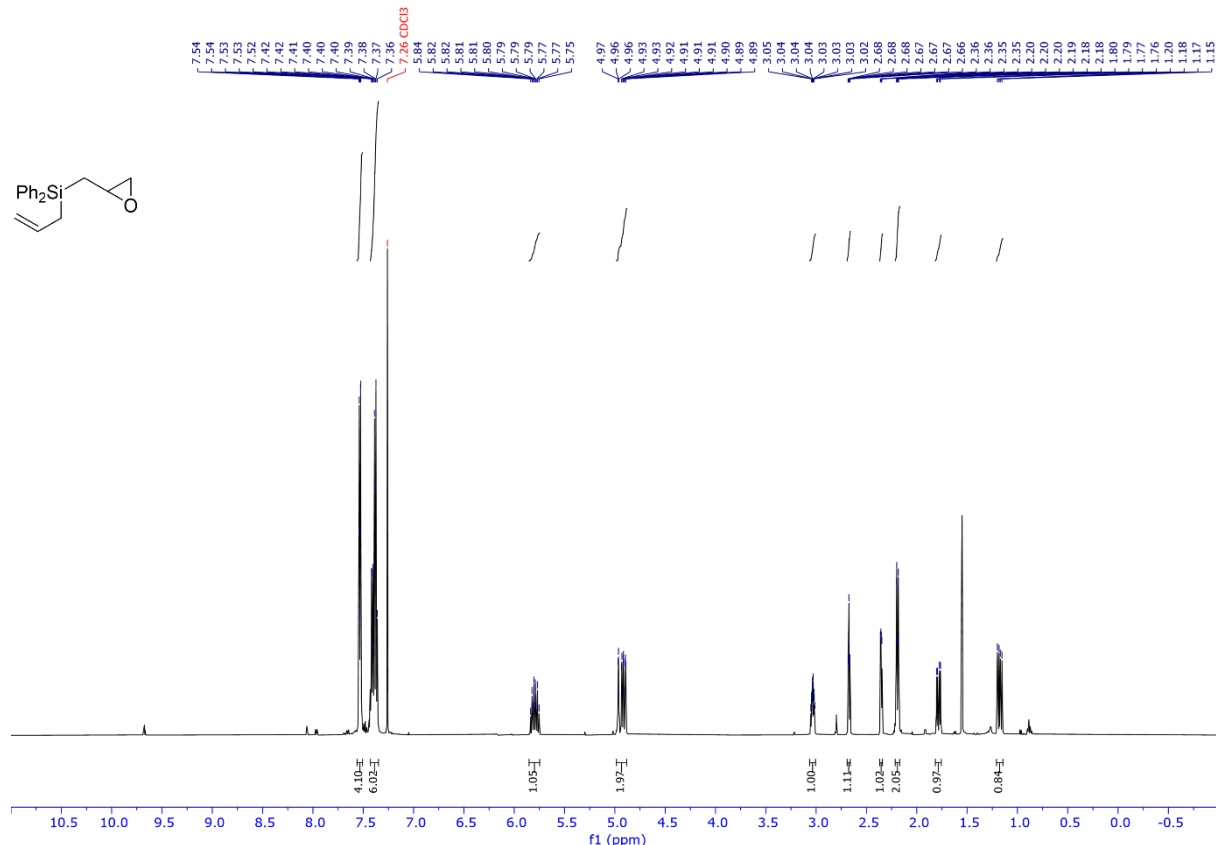
**Figure 5.1.** ORTEP of the structure with thermal ellipsoids at the 50% probability level. Disorder omitted for clarity.

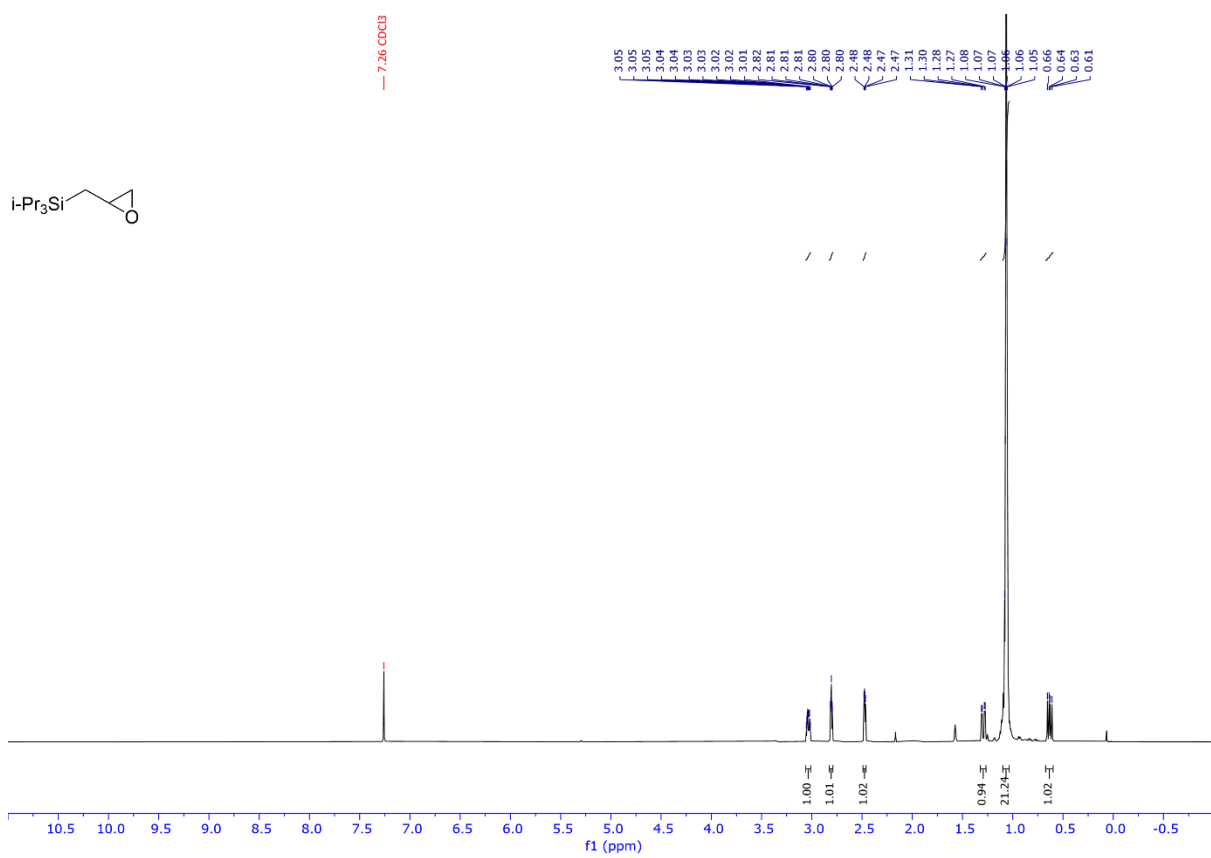
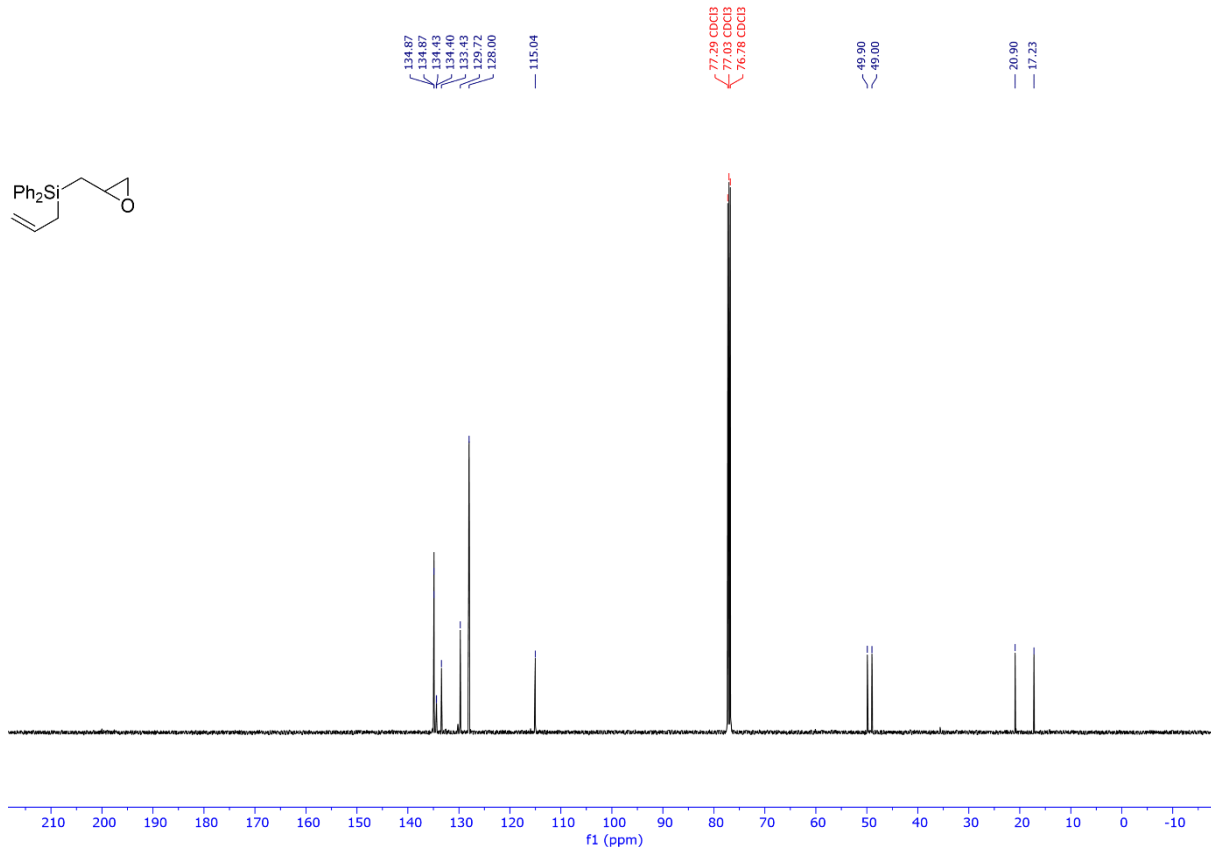
**Table 5.1.** Crystallographic data for compound **82**.

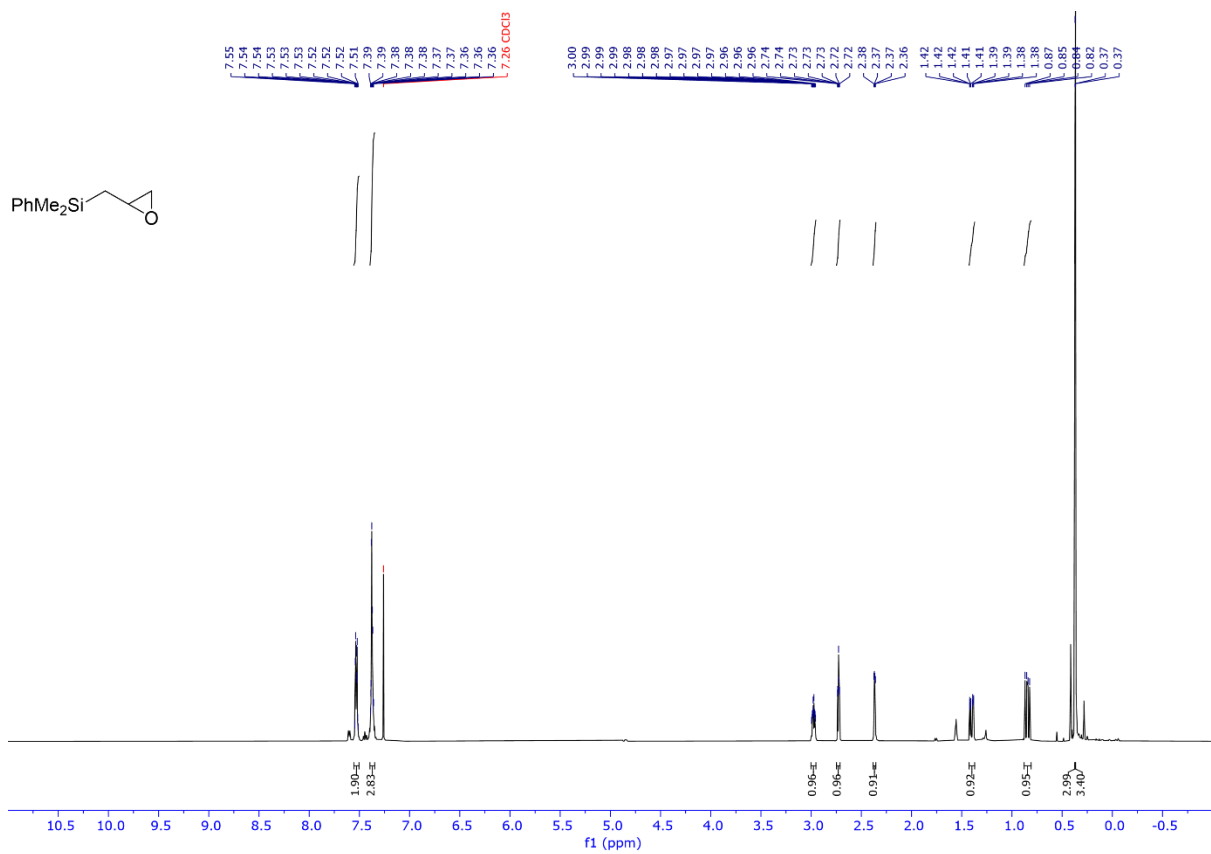
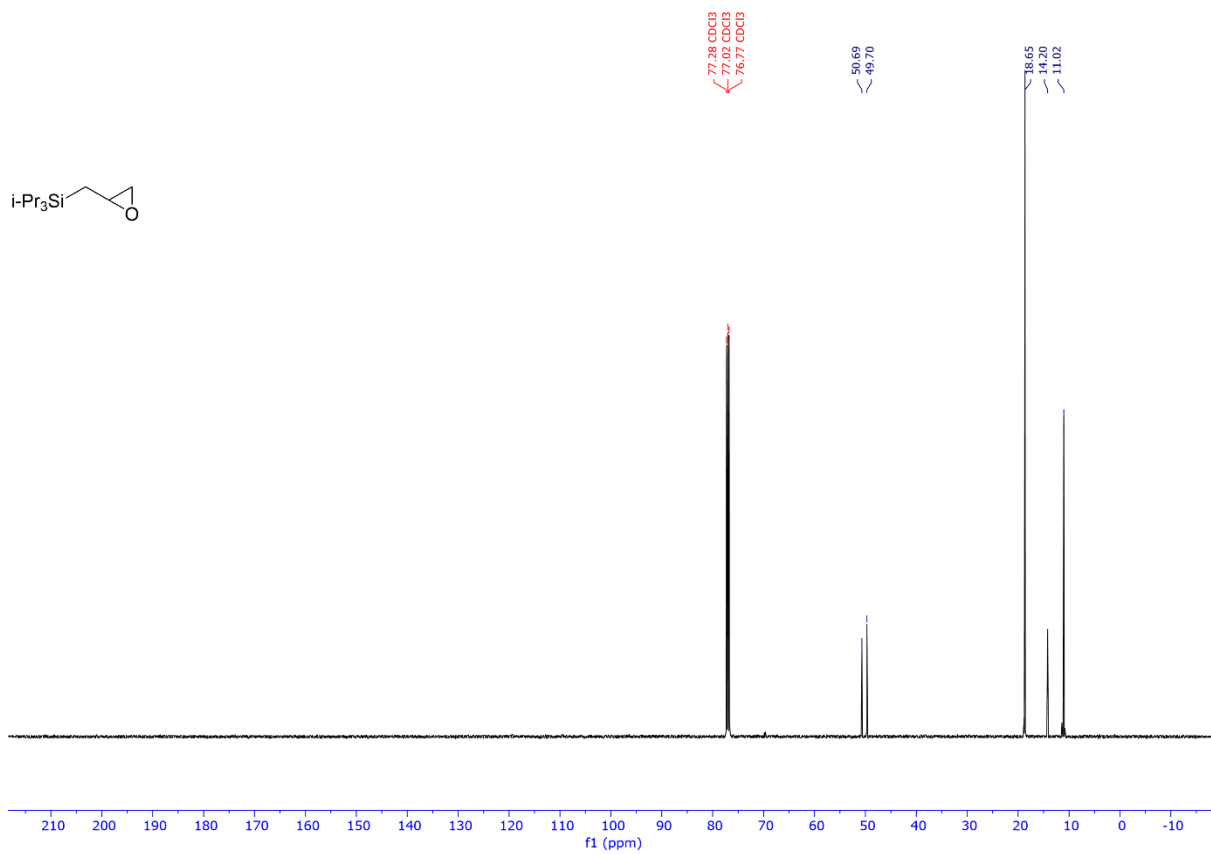
Empirical formula	C <sub>21</sub> H <sub>21</sub> F <sub>2</sub> O <sub>2</sub> Si		
Formula weight	336.47		
Temperature	100(2) K		
Wavelength	0.71073 Å		
Crystal system	Monoclinic		
Space group	C 2		
Unit cell dimensions	a = 32.472(4) Å	b = 7.0912(8) Å	c = 15.961(2) Å
	a = 90°.	b = 105.826(7)°.	g = 90°.
Volume	3536.0(7) Å <sup>3</sup>		
Z	8		

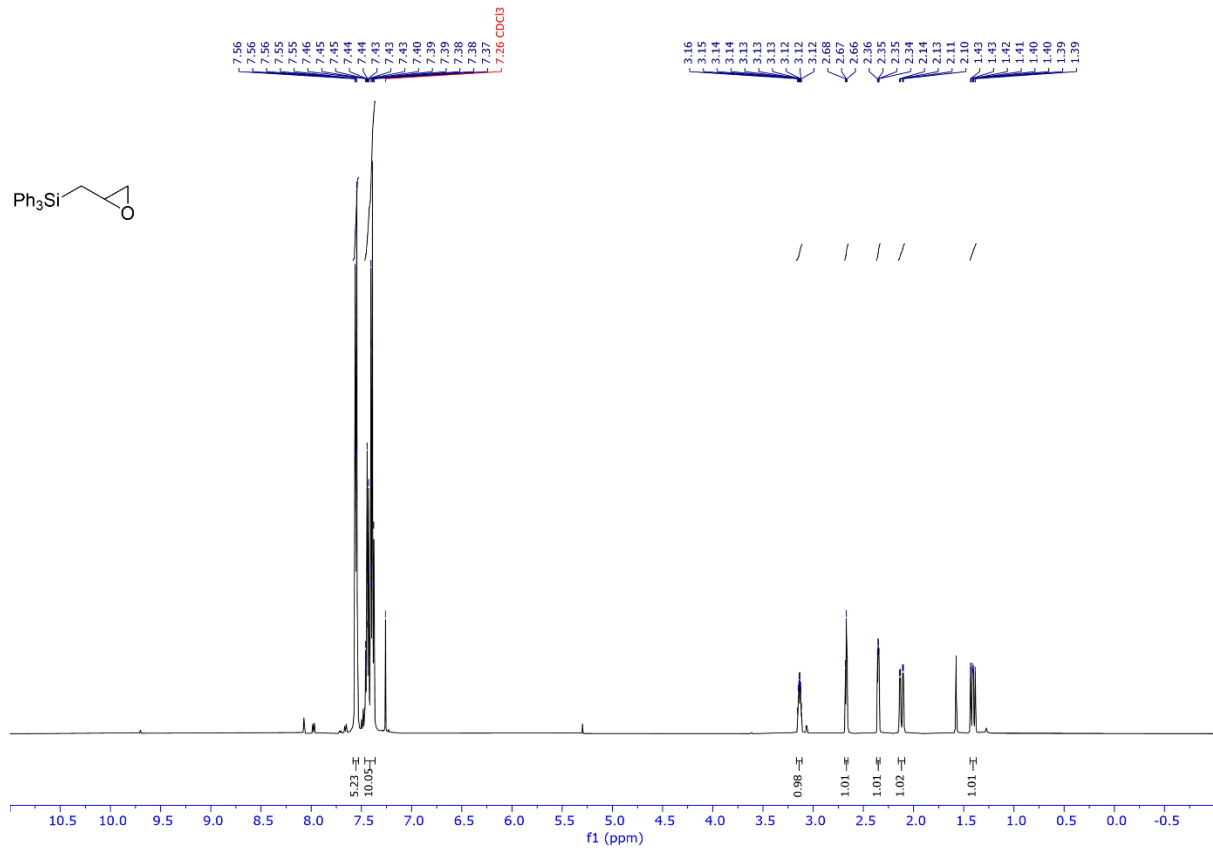
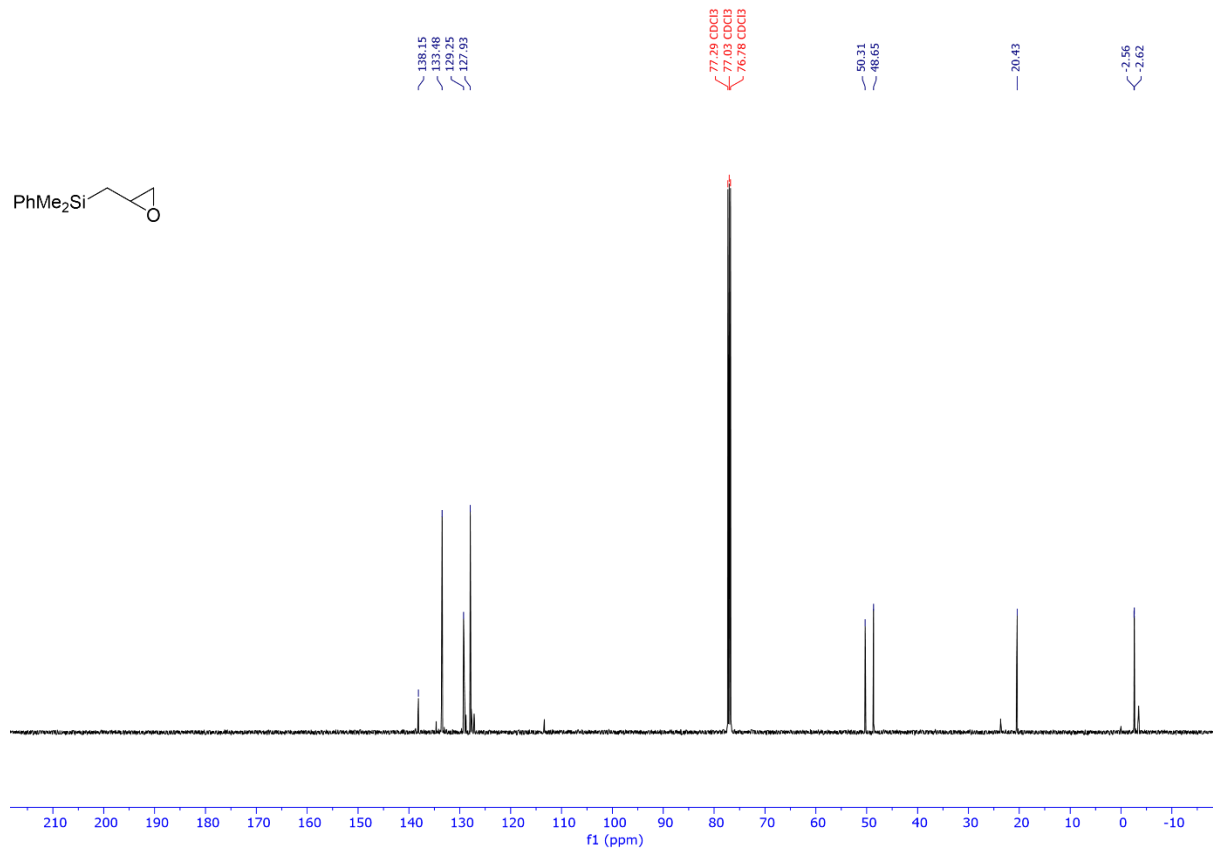
Density (calculated)	1.264 Mg/m <sup>3</sup>
Absorption coefficient	0.147 mm <sup>-1</sup>
F(000)	1424
Crystal size	0.375 x 0.100 x 0.080 mm <sup>3</sup>
Theta range for data collection	1.304 to 25.148°.
Index ranges	-38<=h<=37, -8<=k<=8, -18<=l<=19
Reflections collected	14857
Independent reflections	6584 [R(int) = 0.0858]
Completeness to theta = 25.148°	100.0 %
Refinement method	Full-matrix least-squares on F <sup>2</sup>
Data / restraints / parameters	6584 / 849 / 442
Goodness-of-fit on F <sup>2</sup>	1.038
Final R indices [I>2sigma(I)]	R1 = 0.0695, wR2 = 0.1668
R indices (all data)	R1 = 0.1020, wR2 = 0.1943
Absolute structure parameter	-0.21(9)
Largest diff. peak and hole	0.282 and -0.240 e.Å <sup>-3</sup>

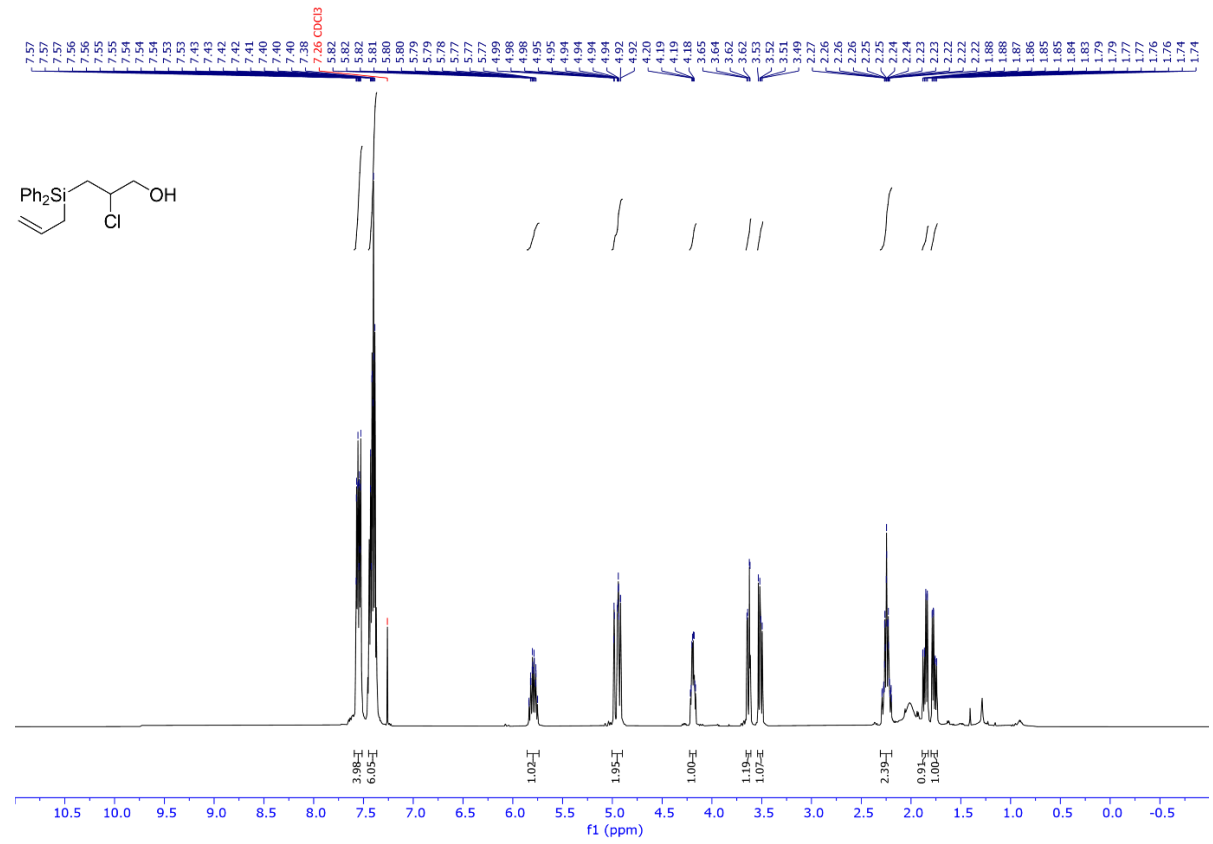
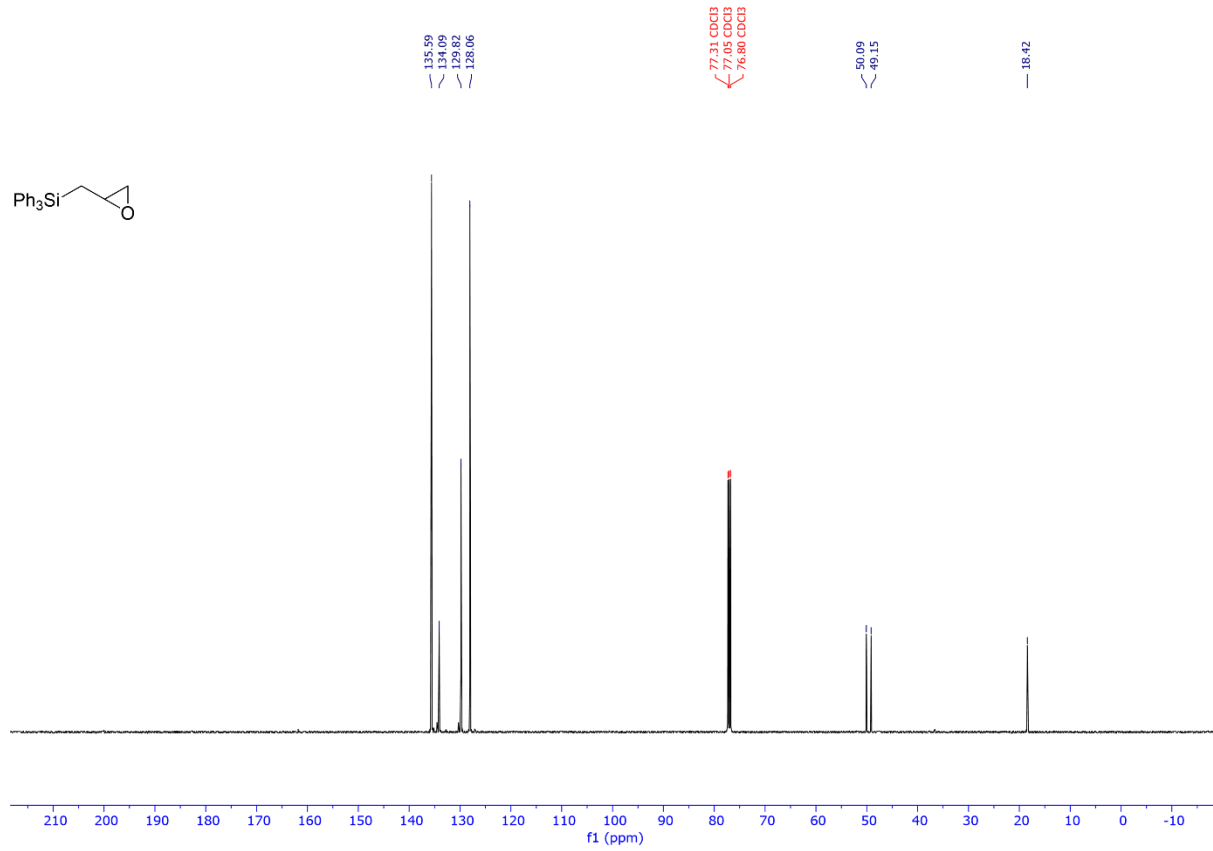
### Spectra

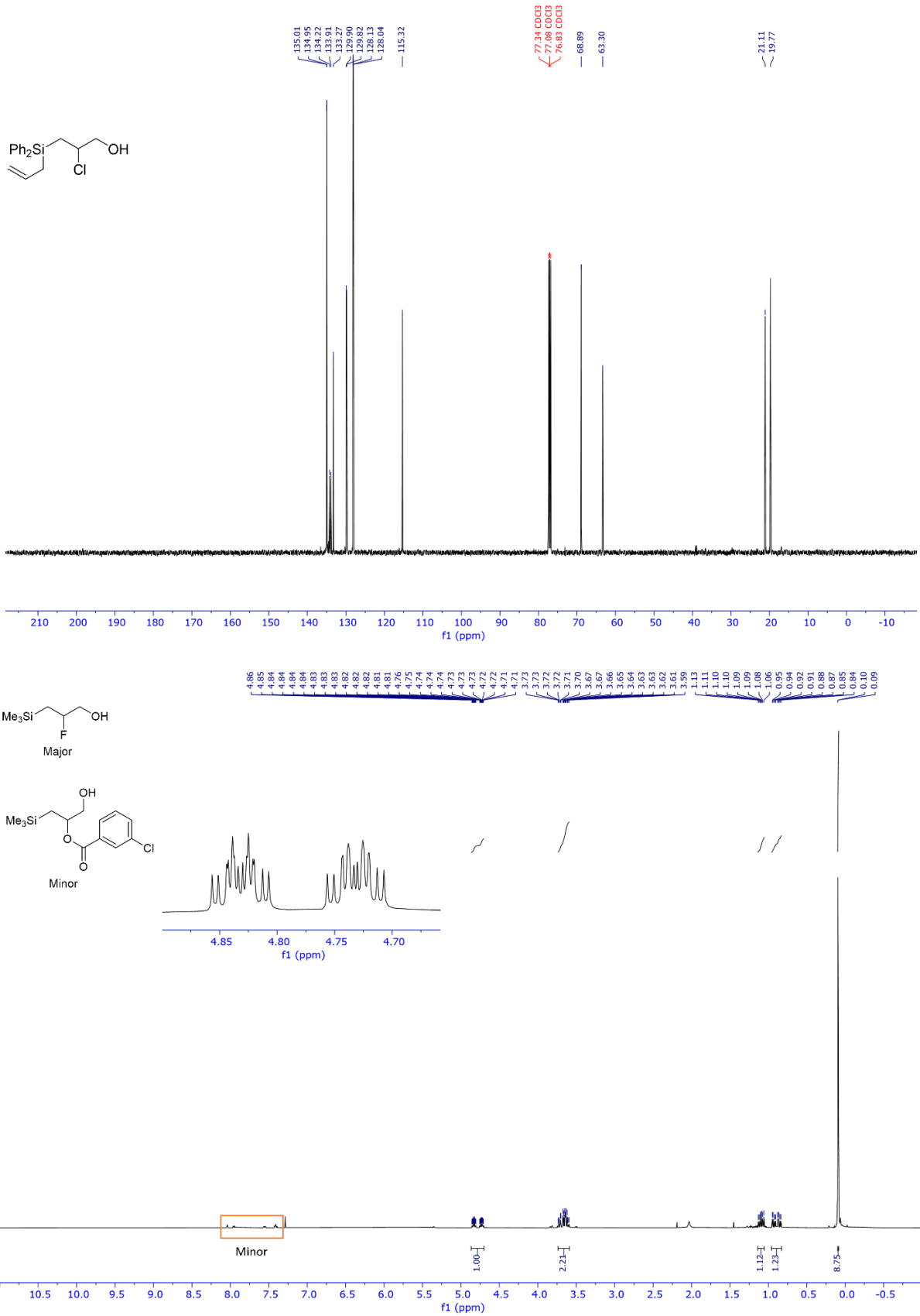


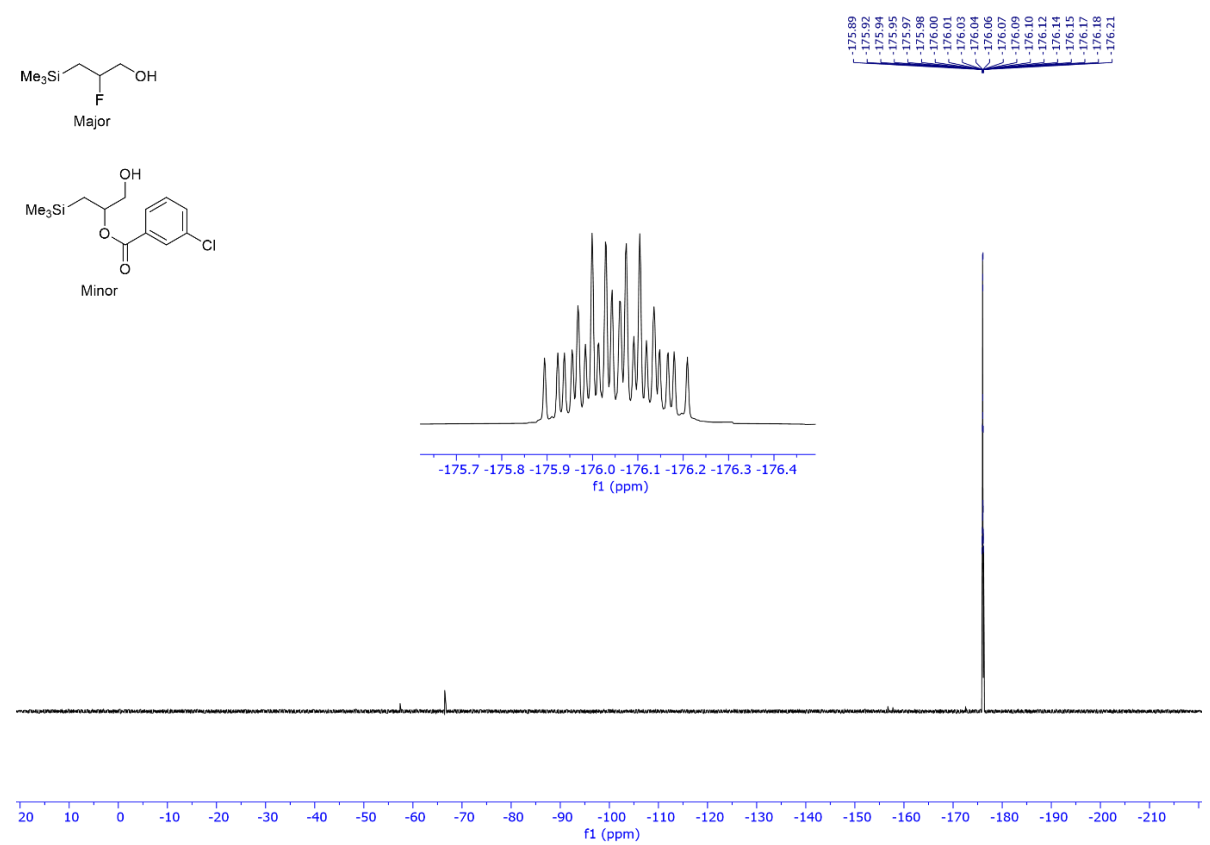
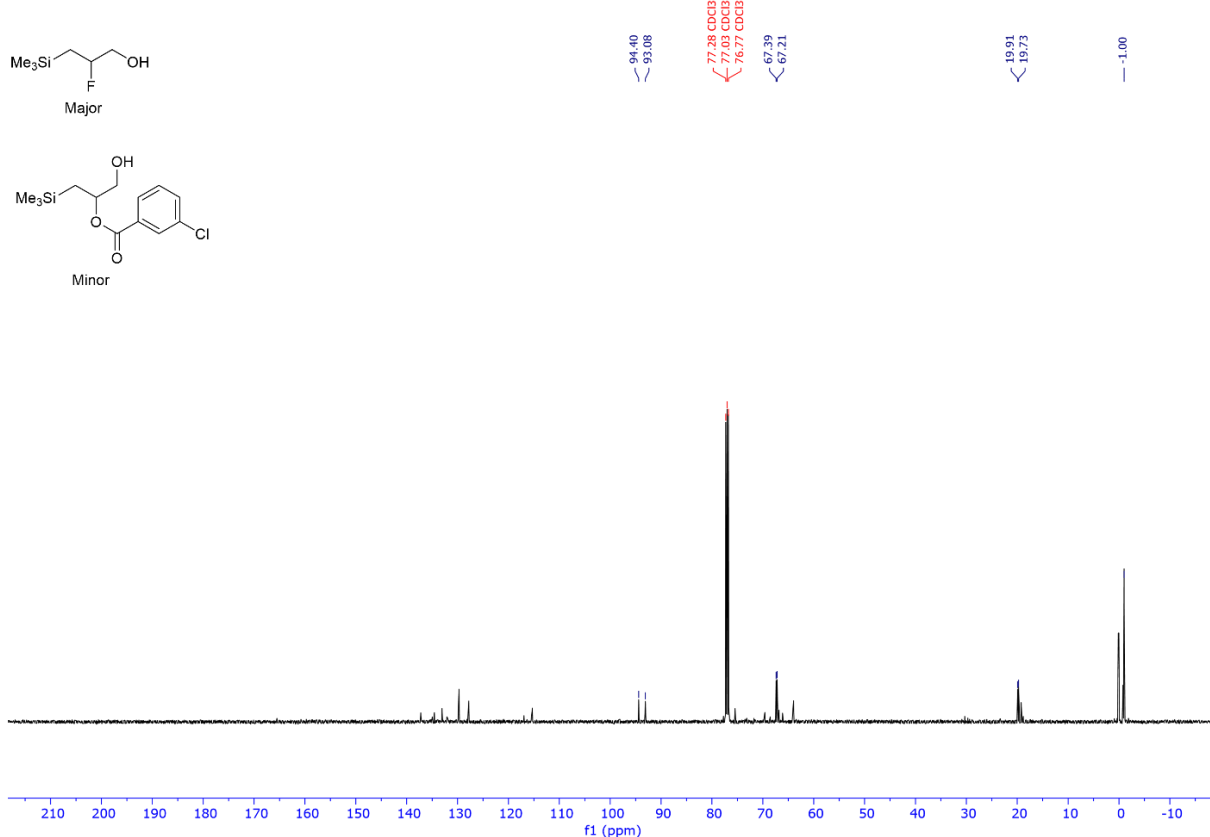


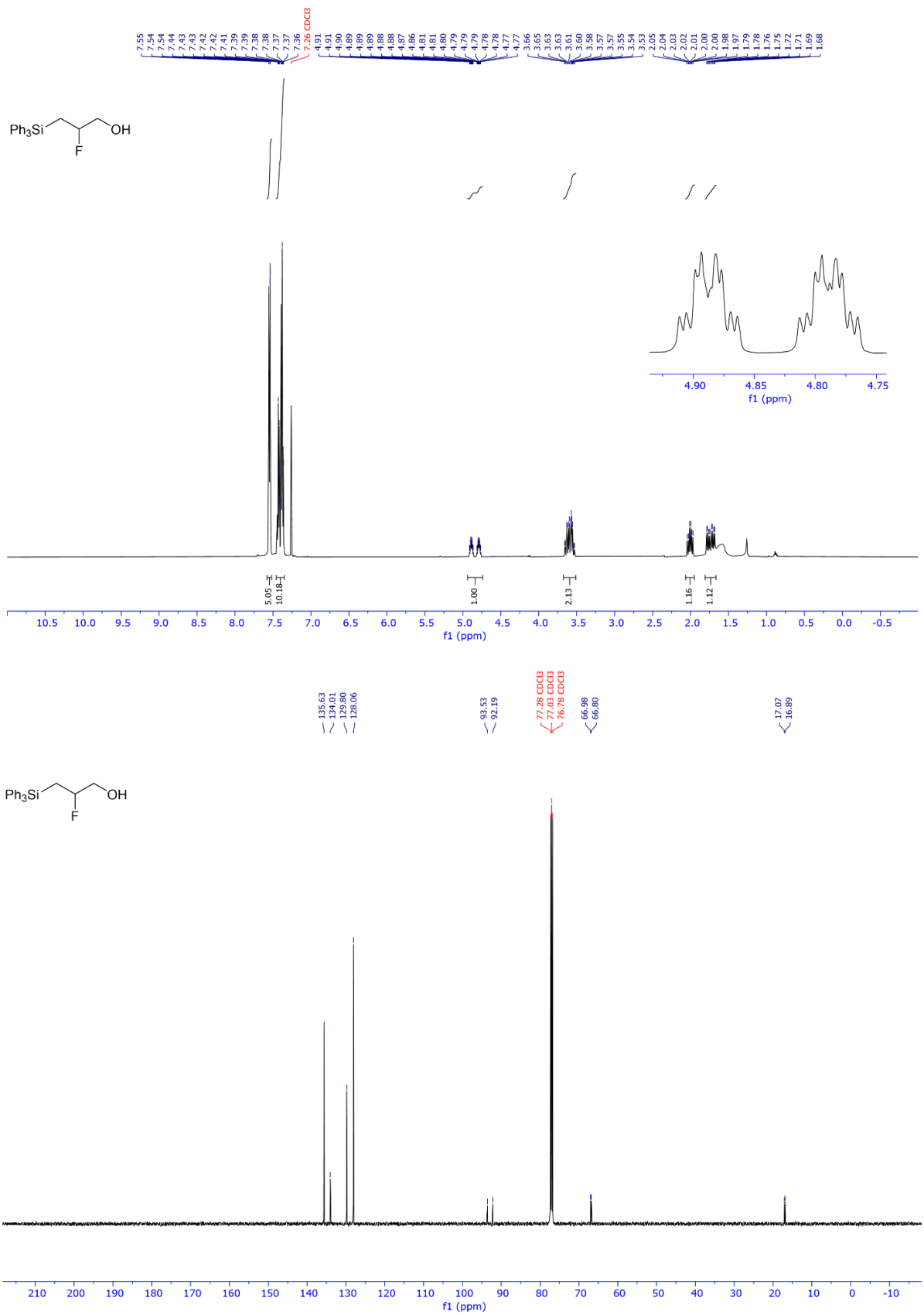


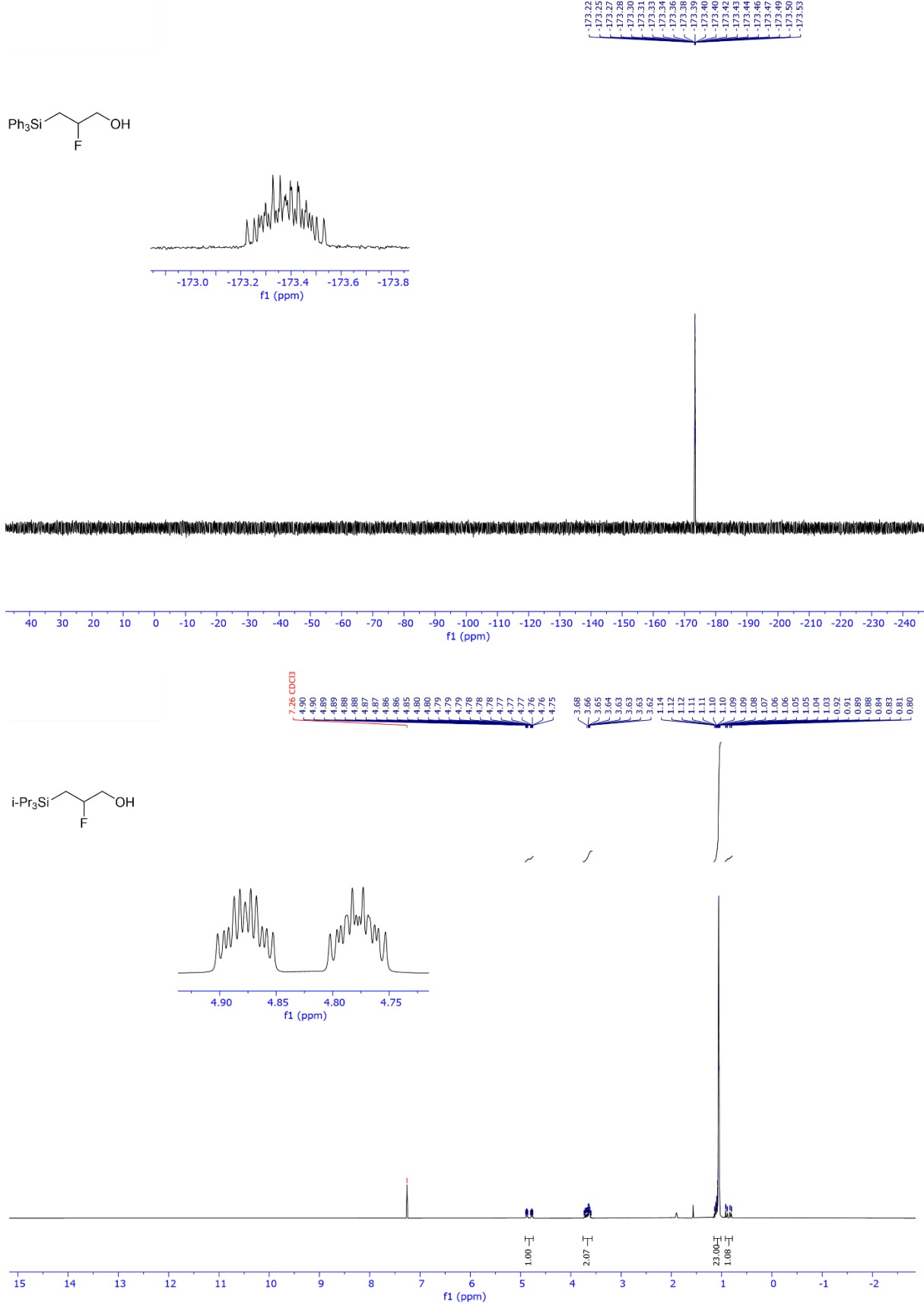


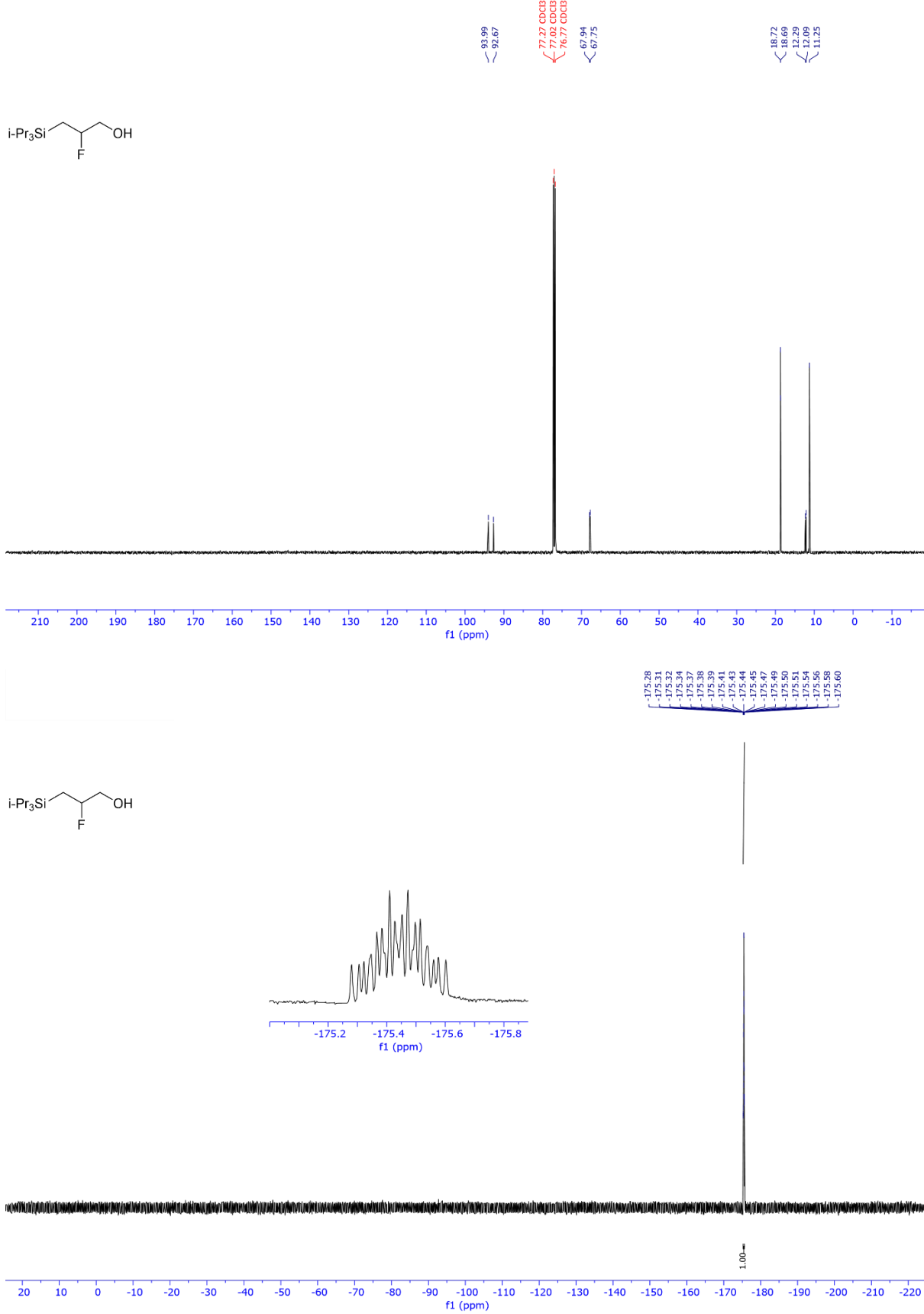


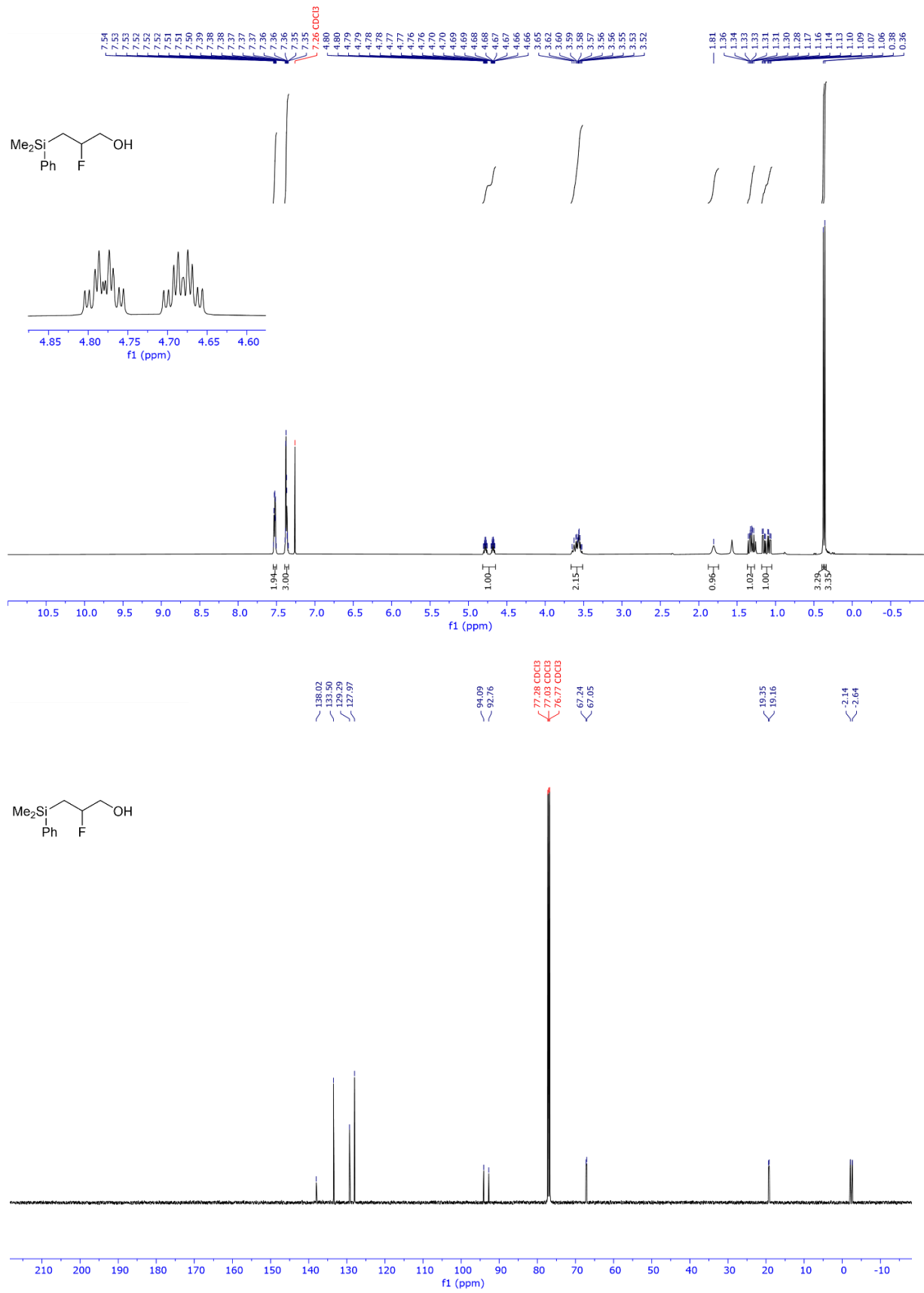


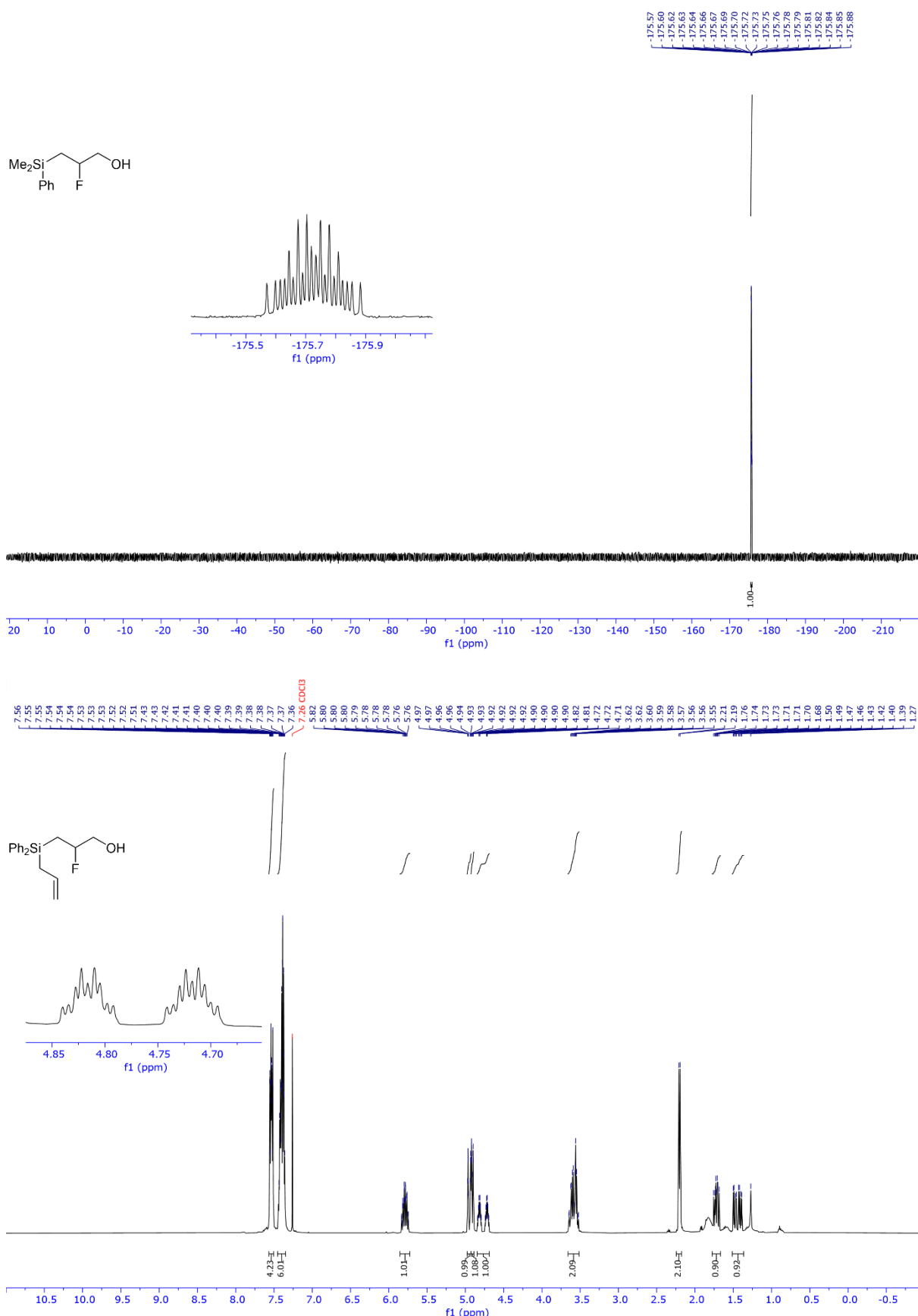


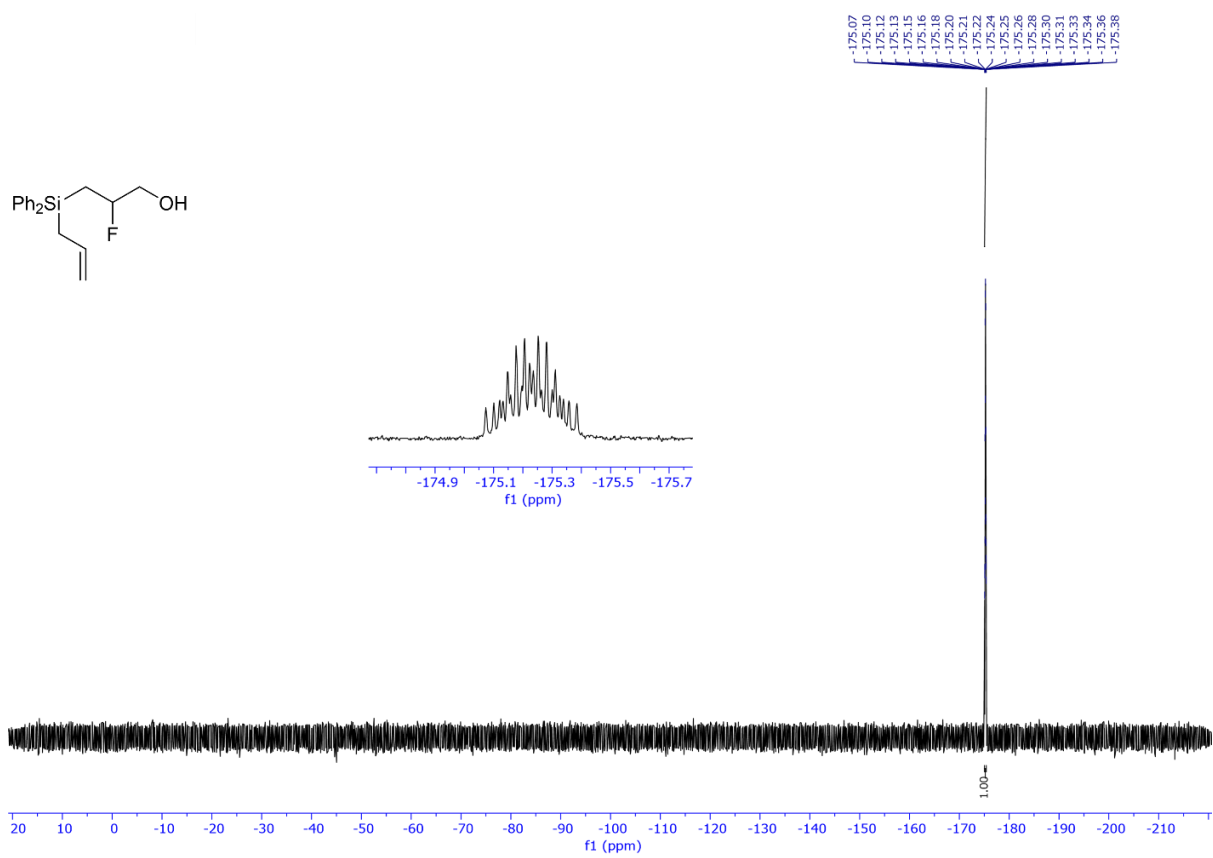
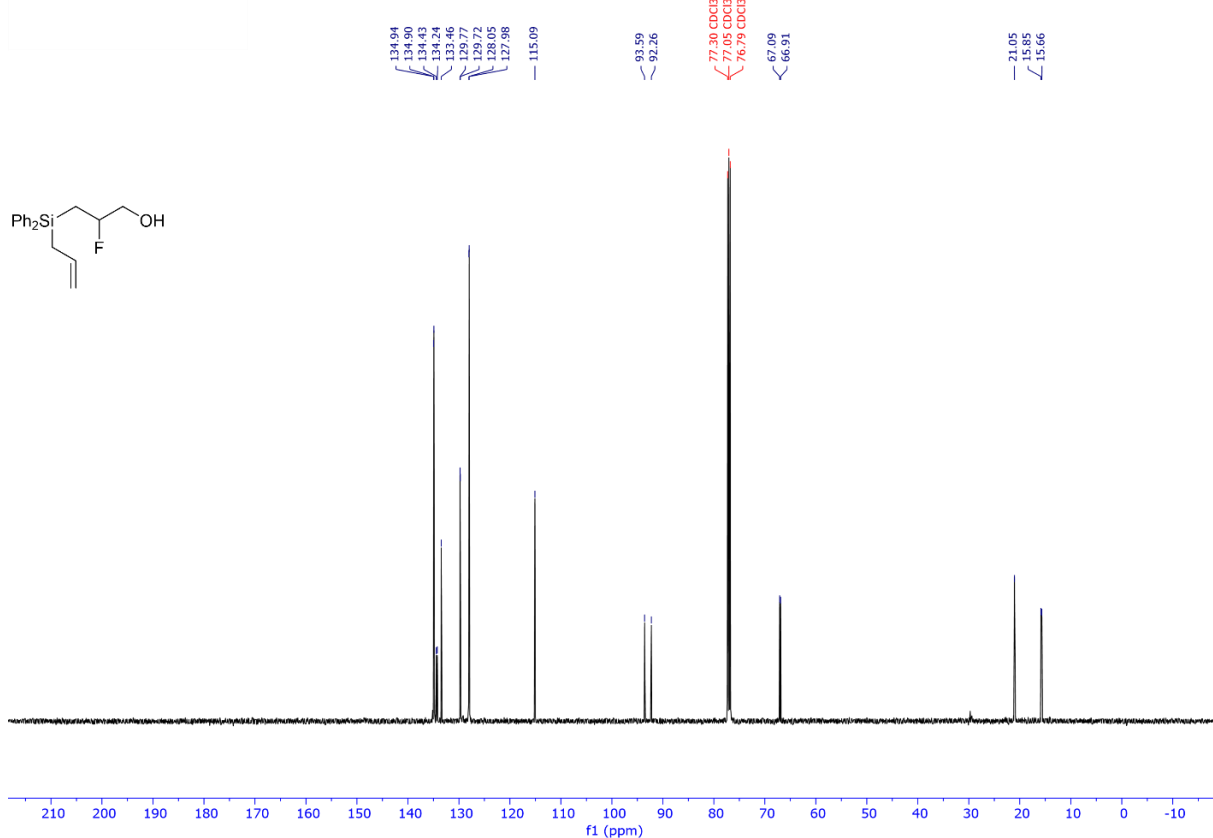


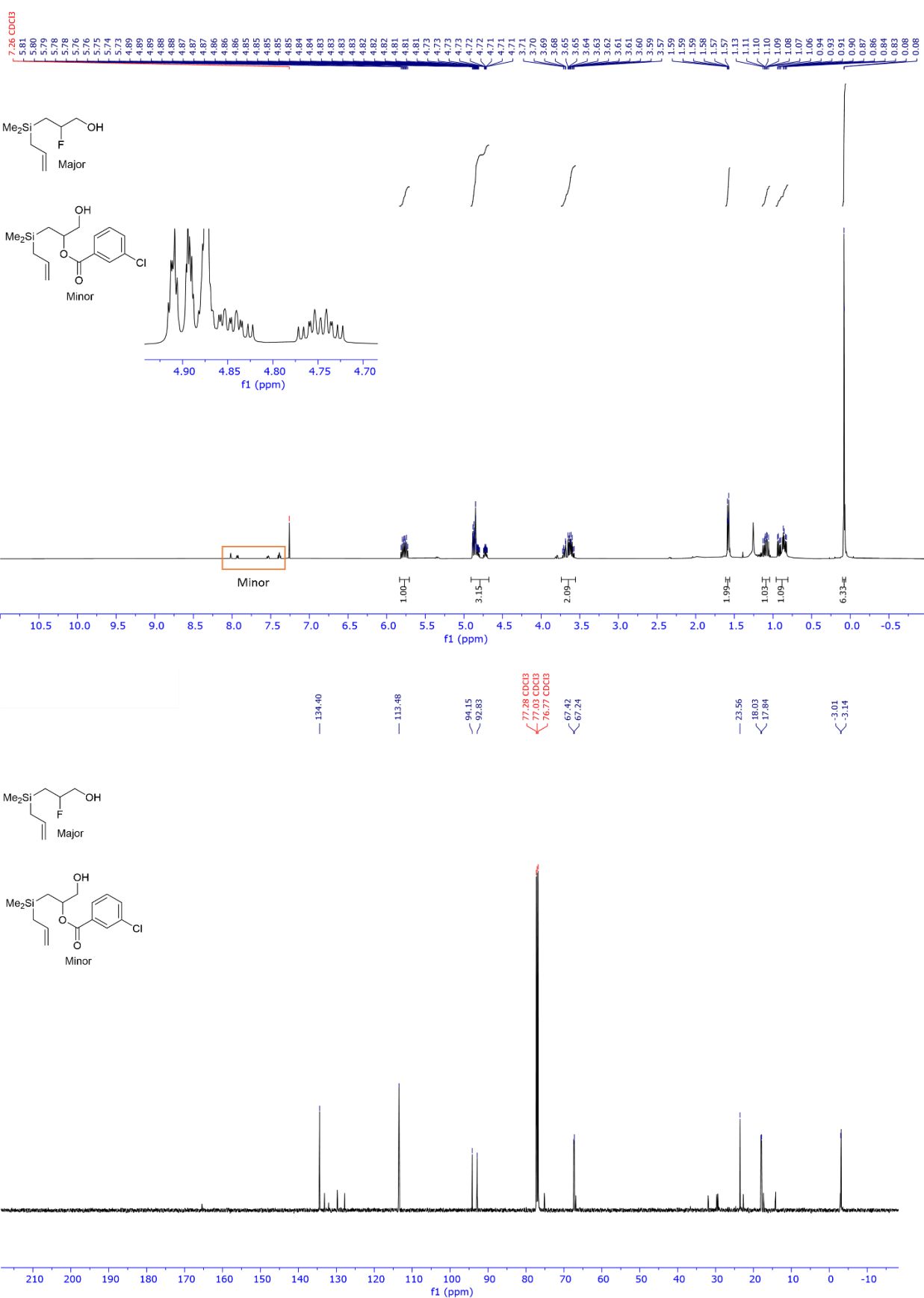


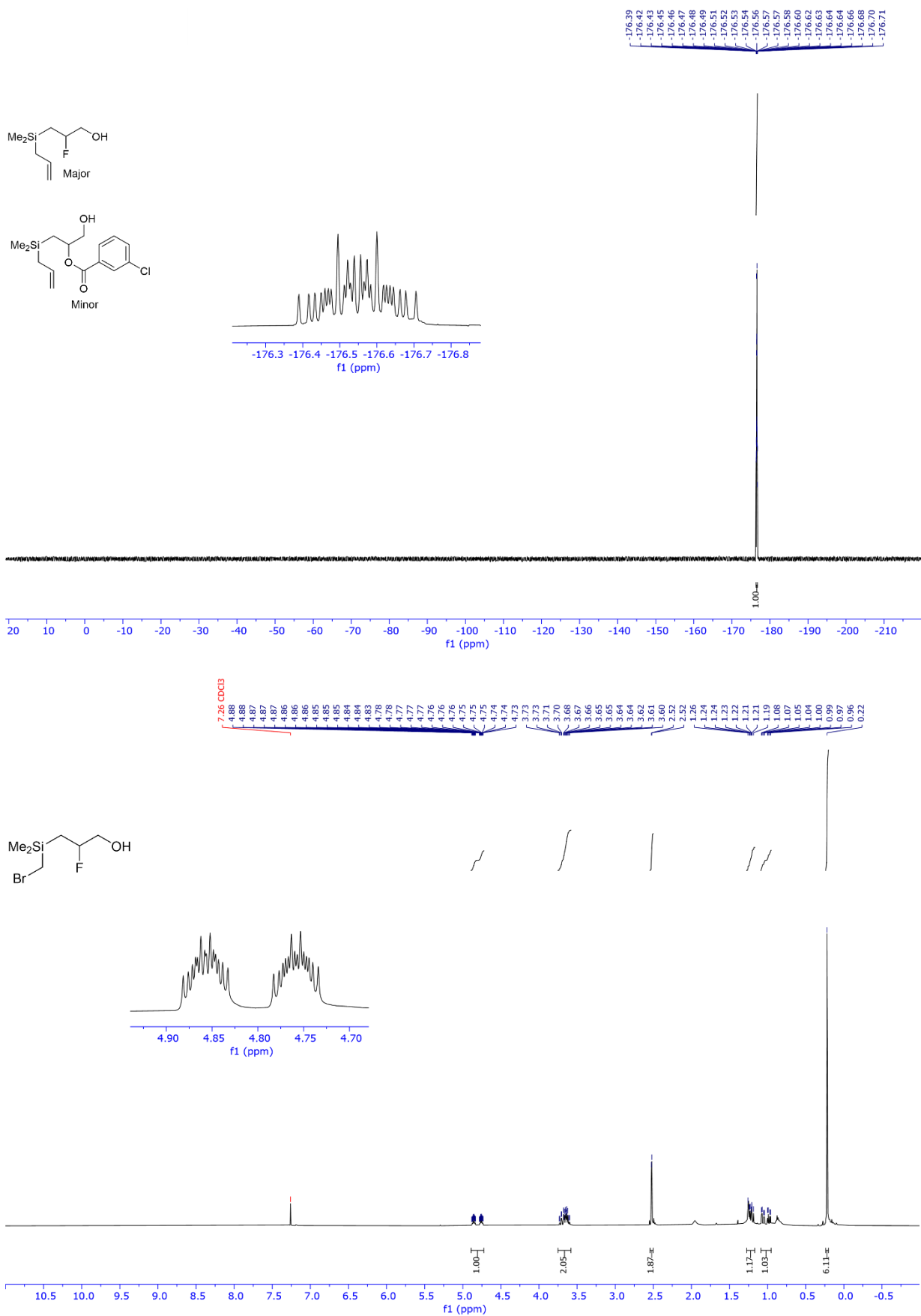


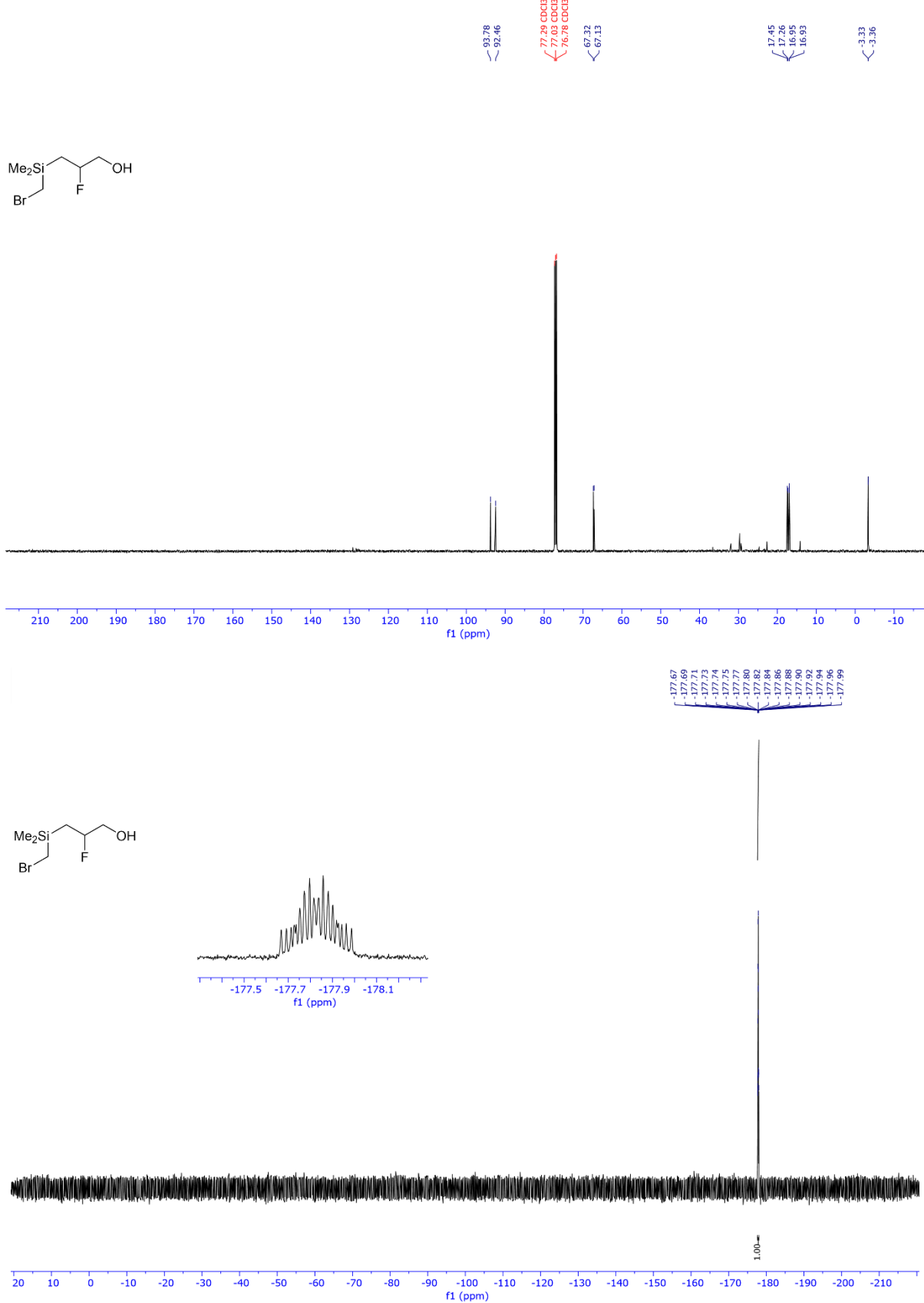


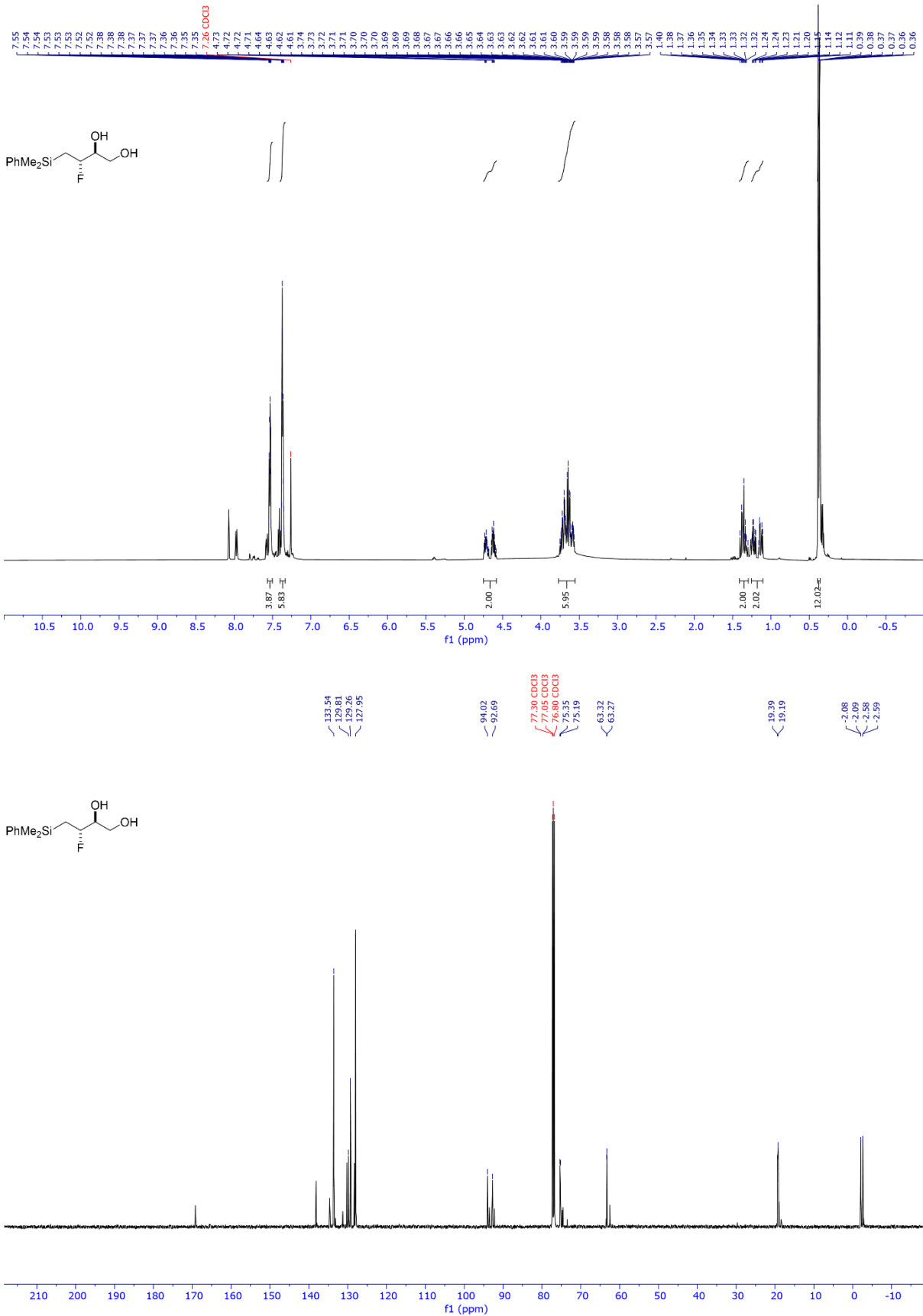


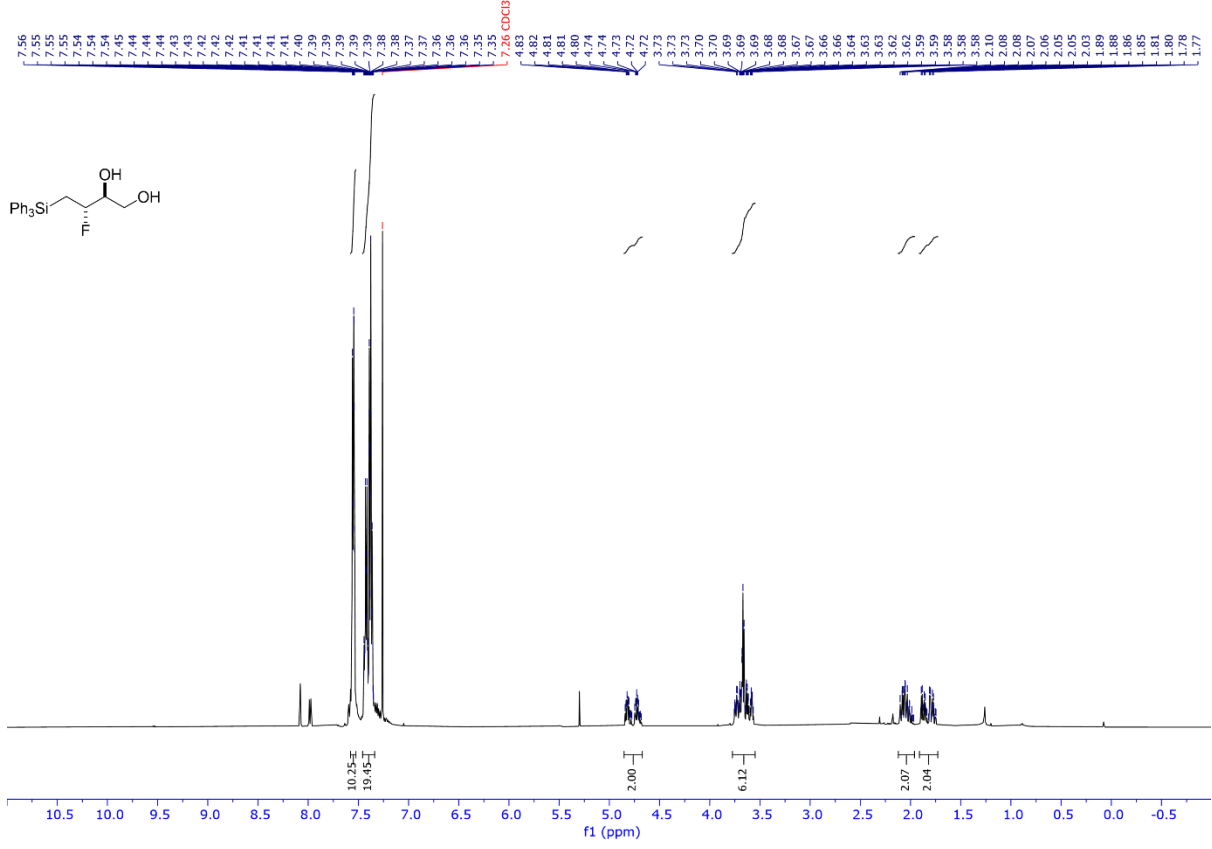
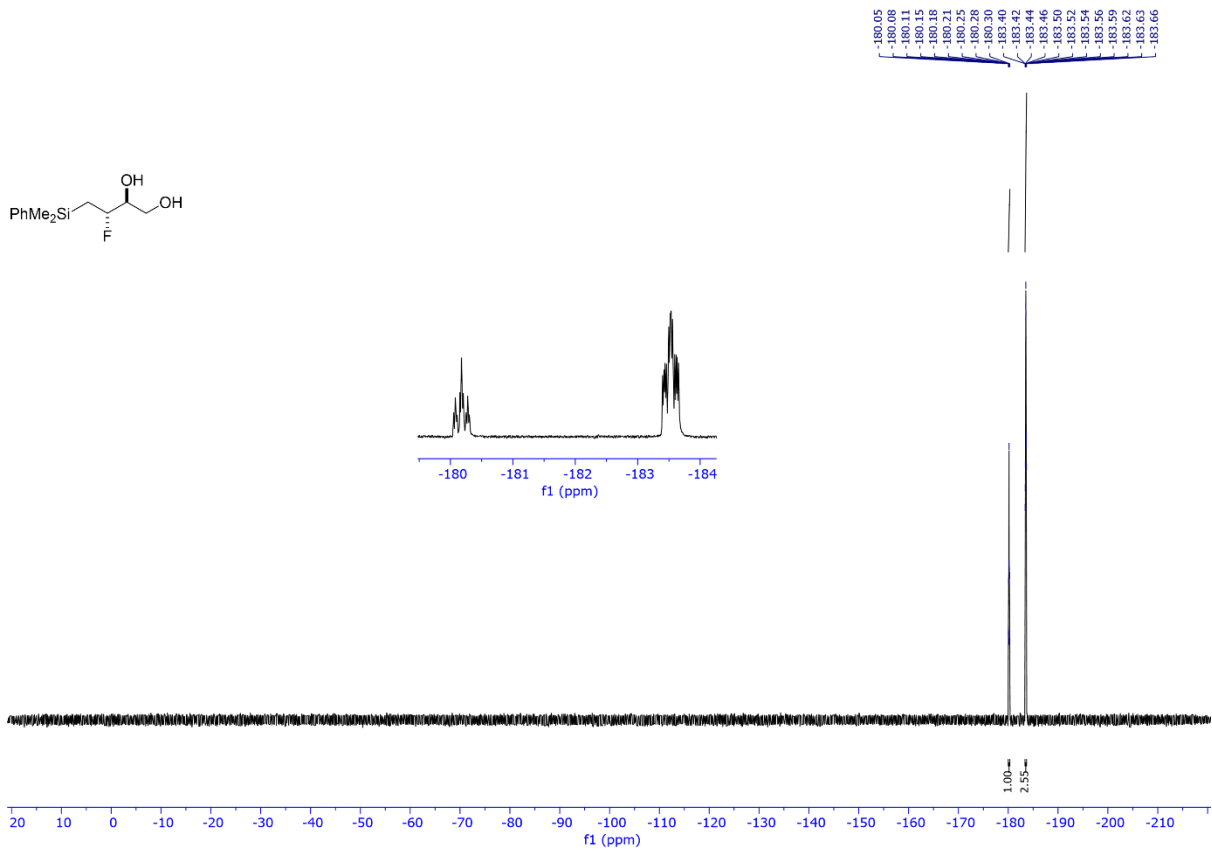


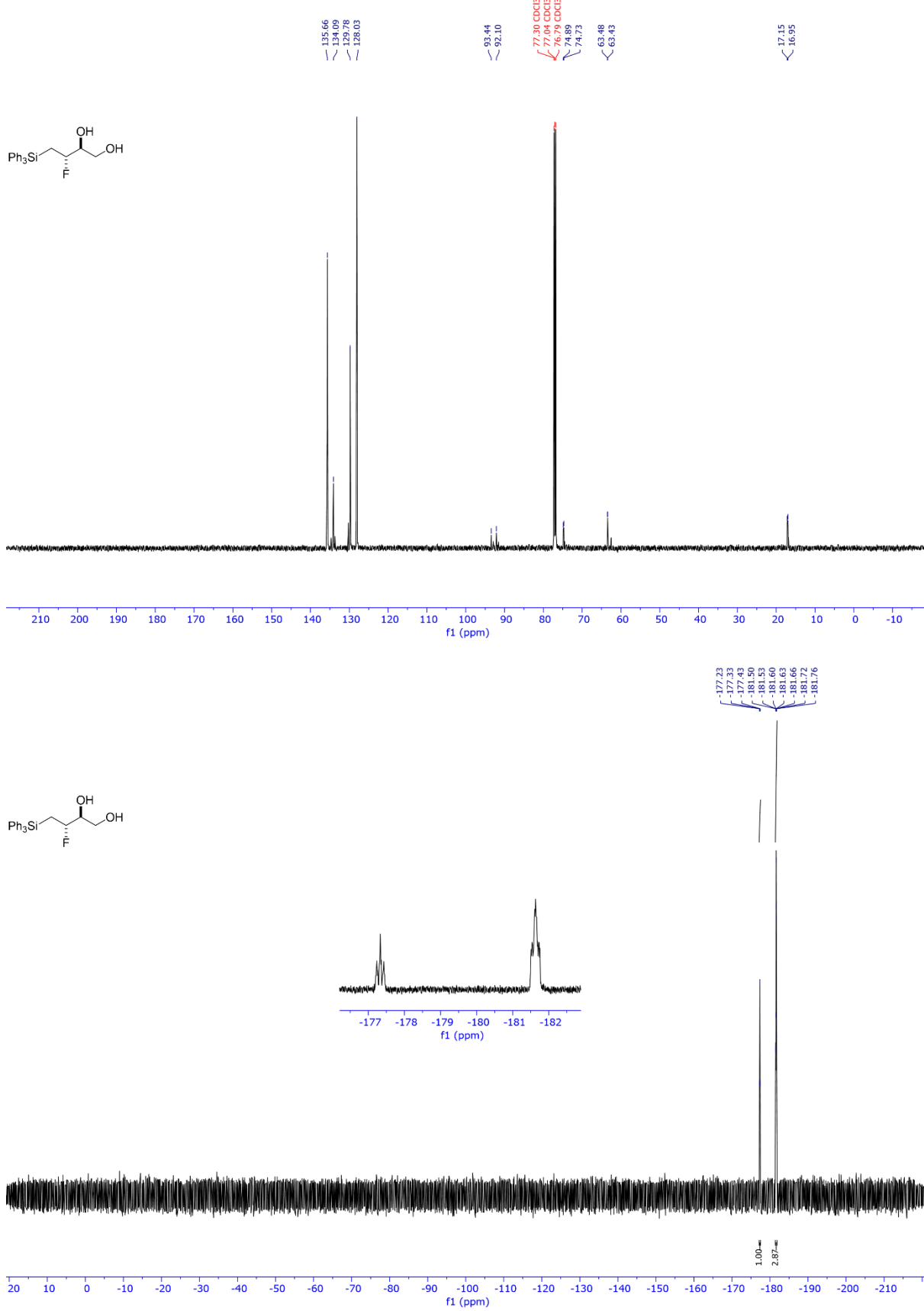


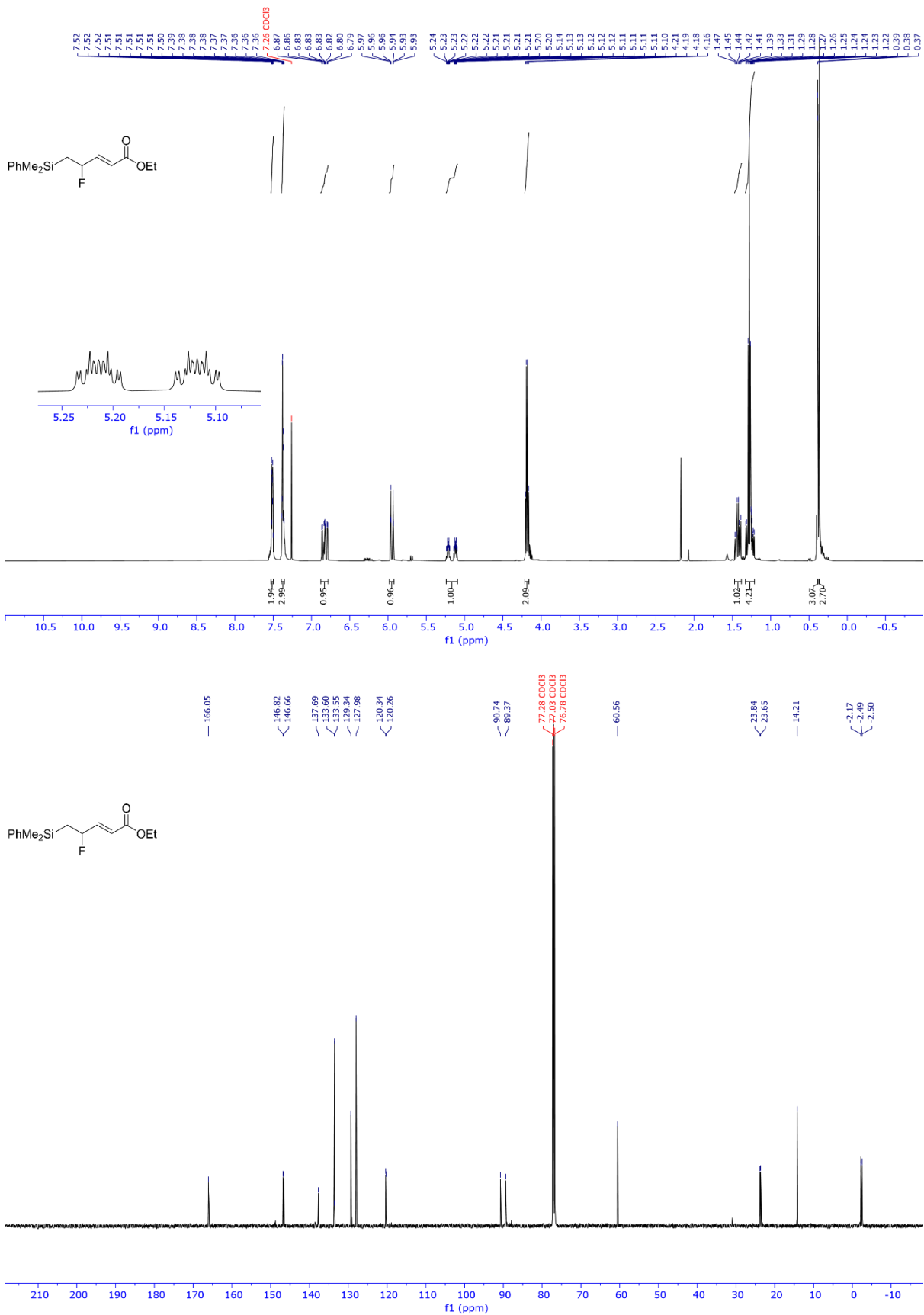


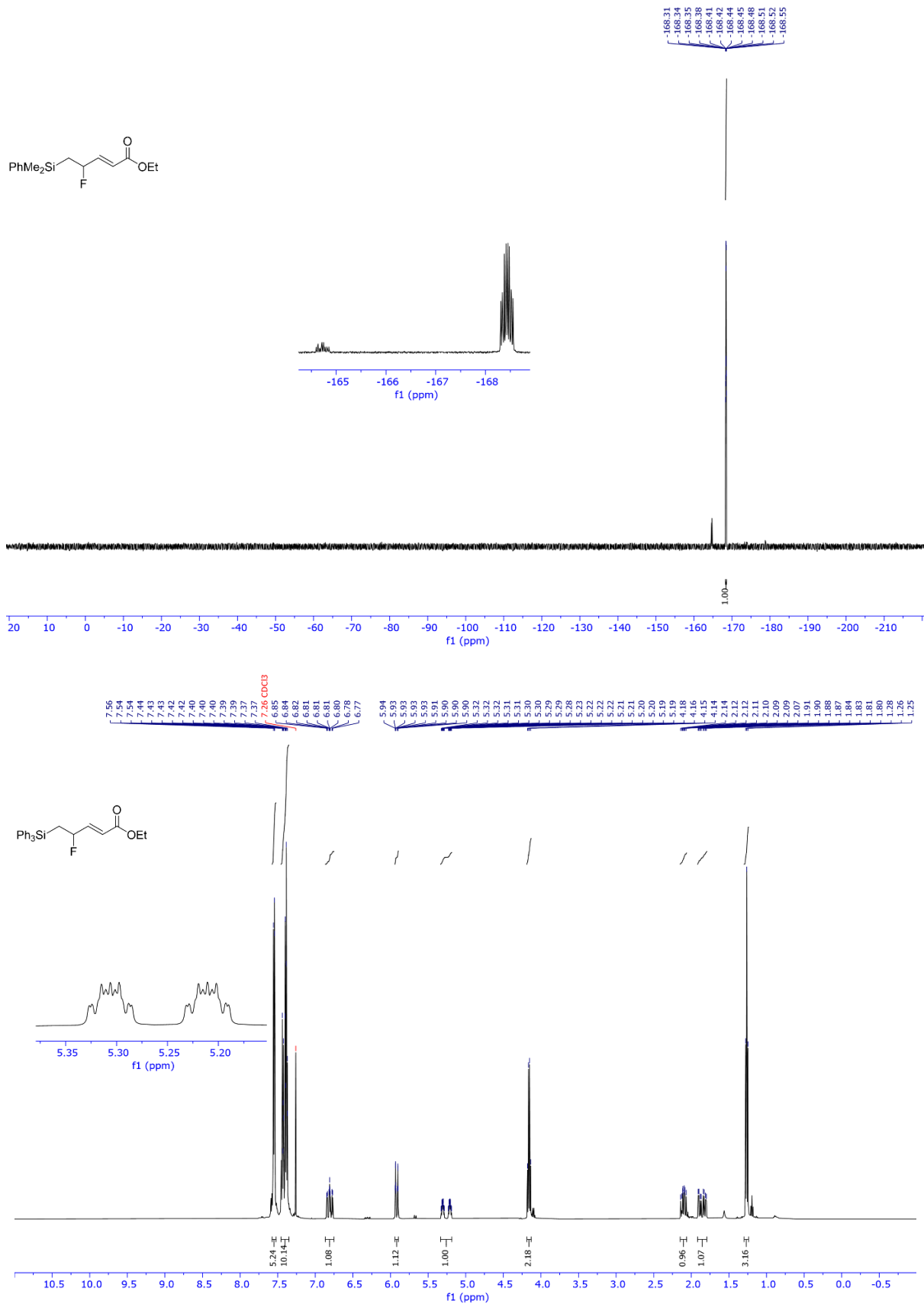


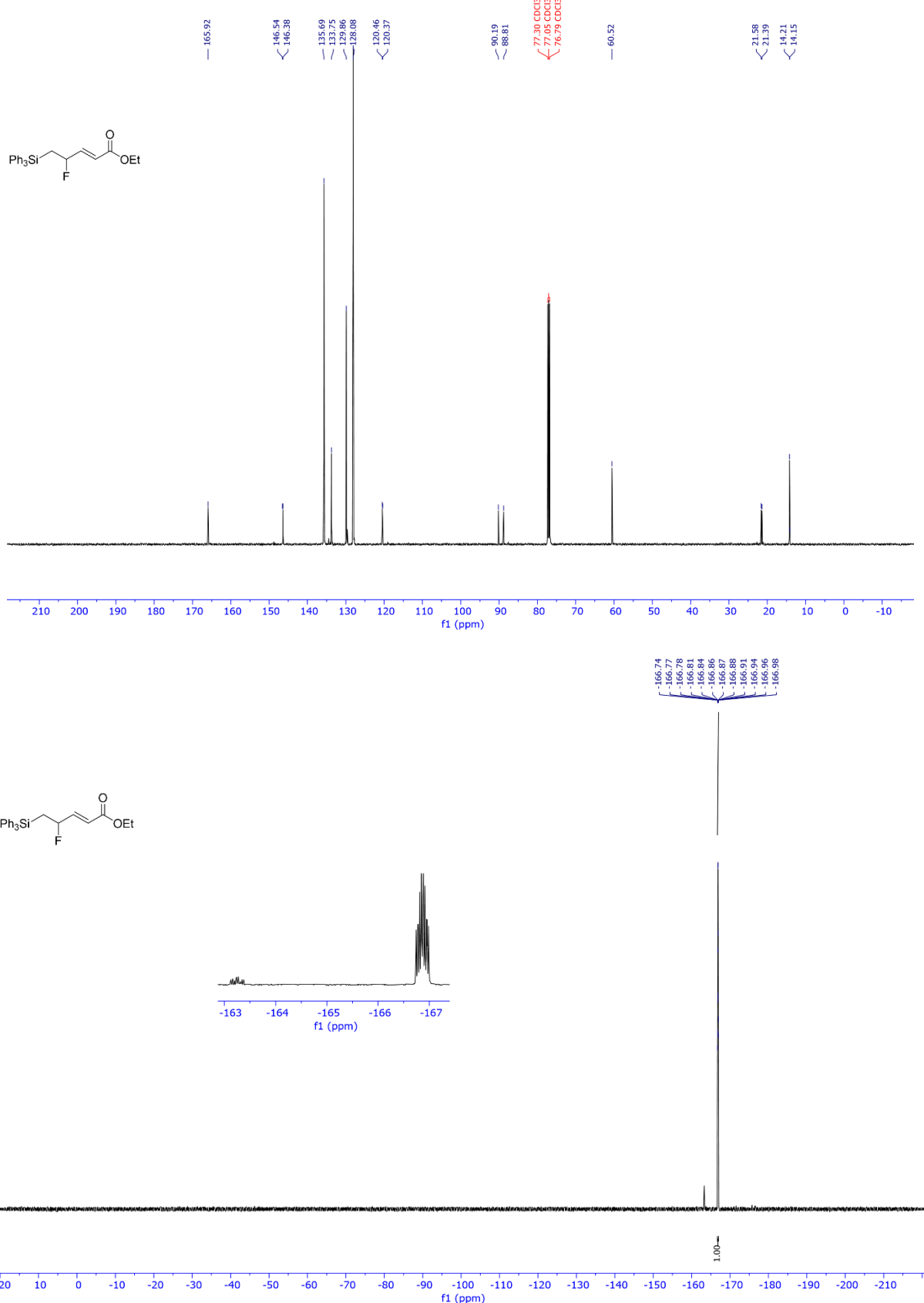


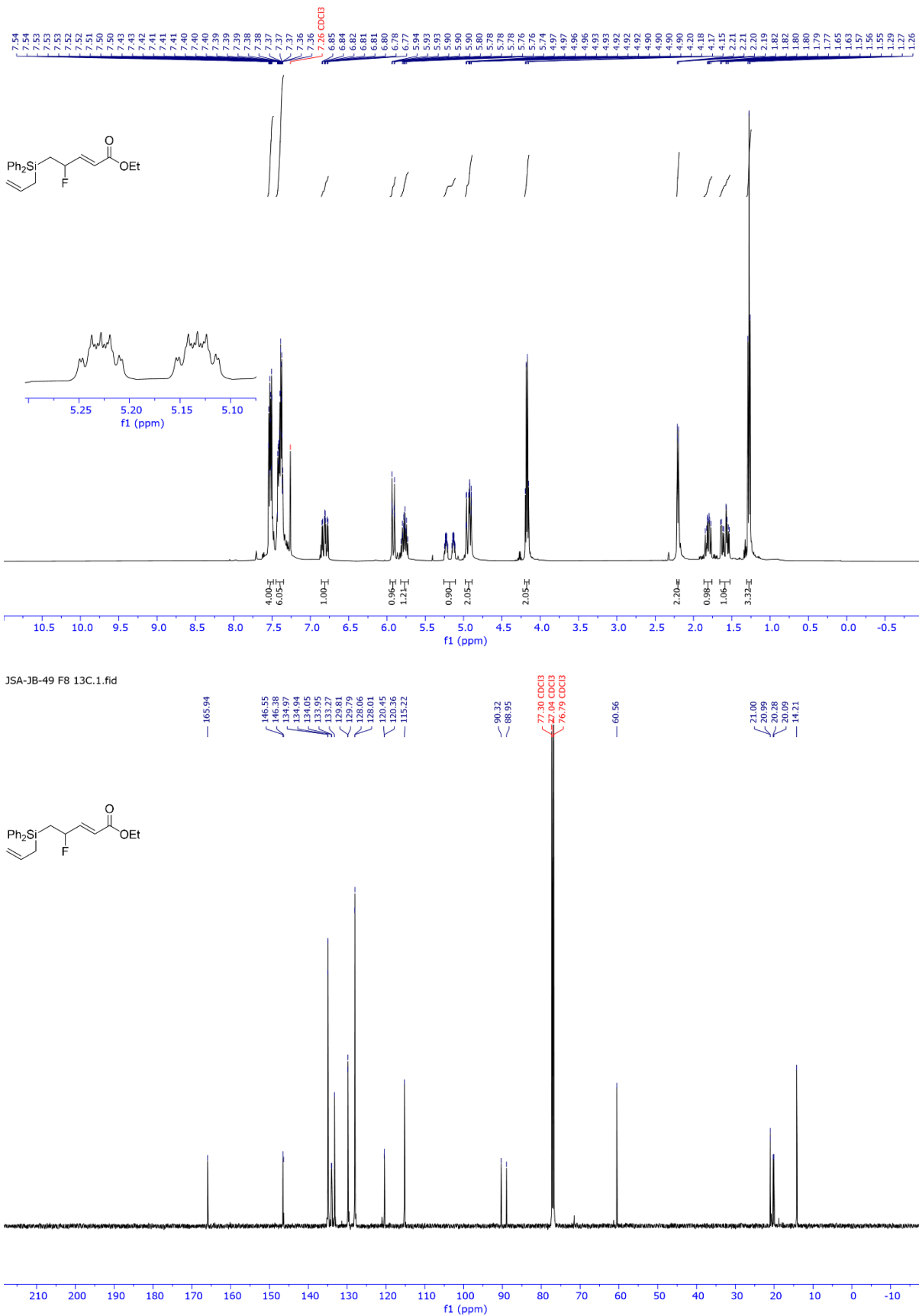


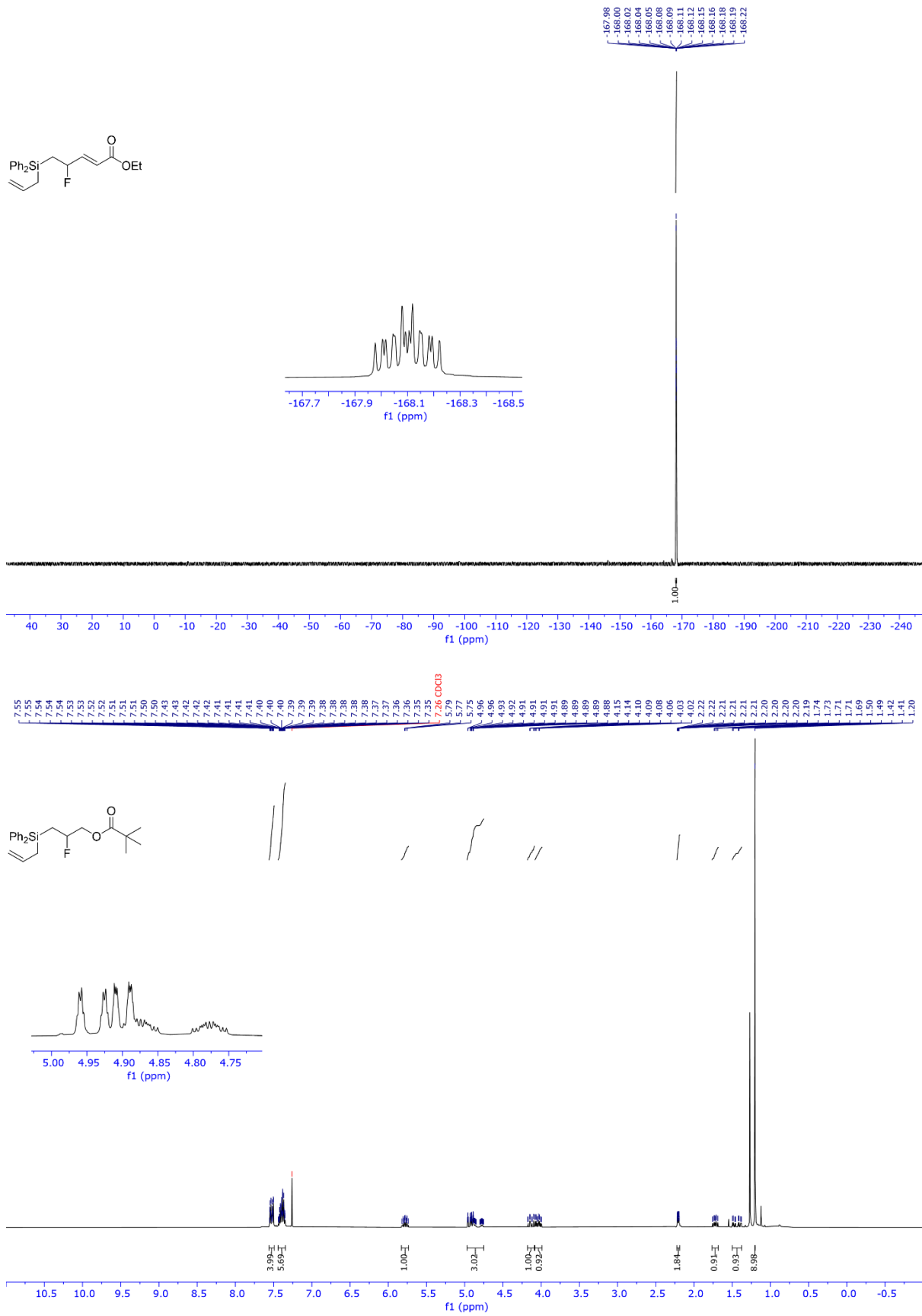


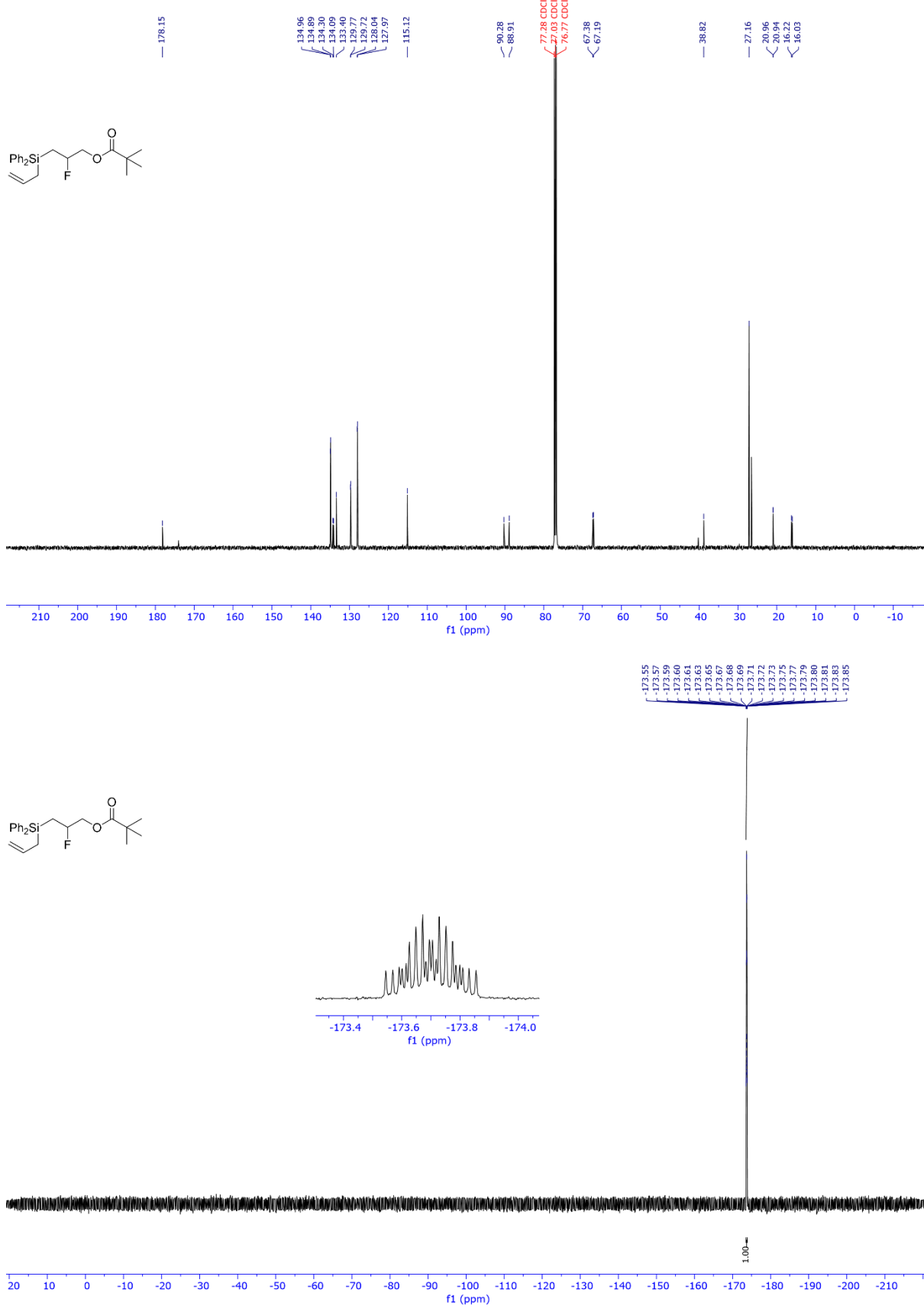


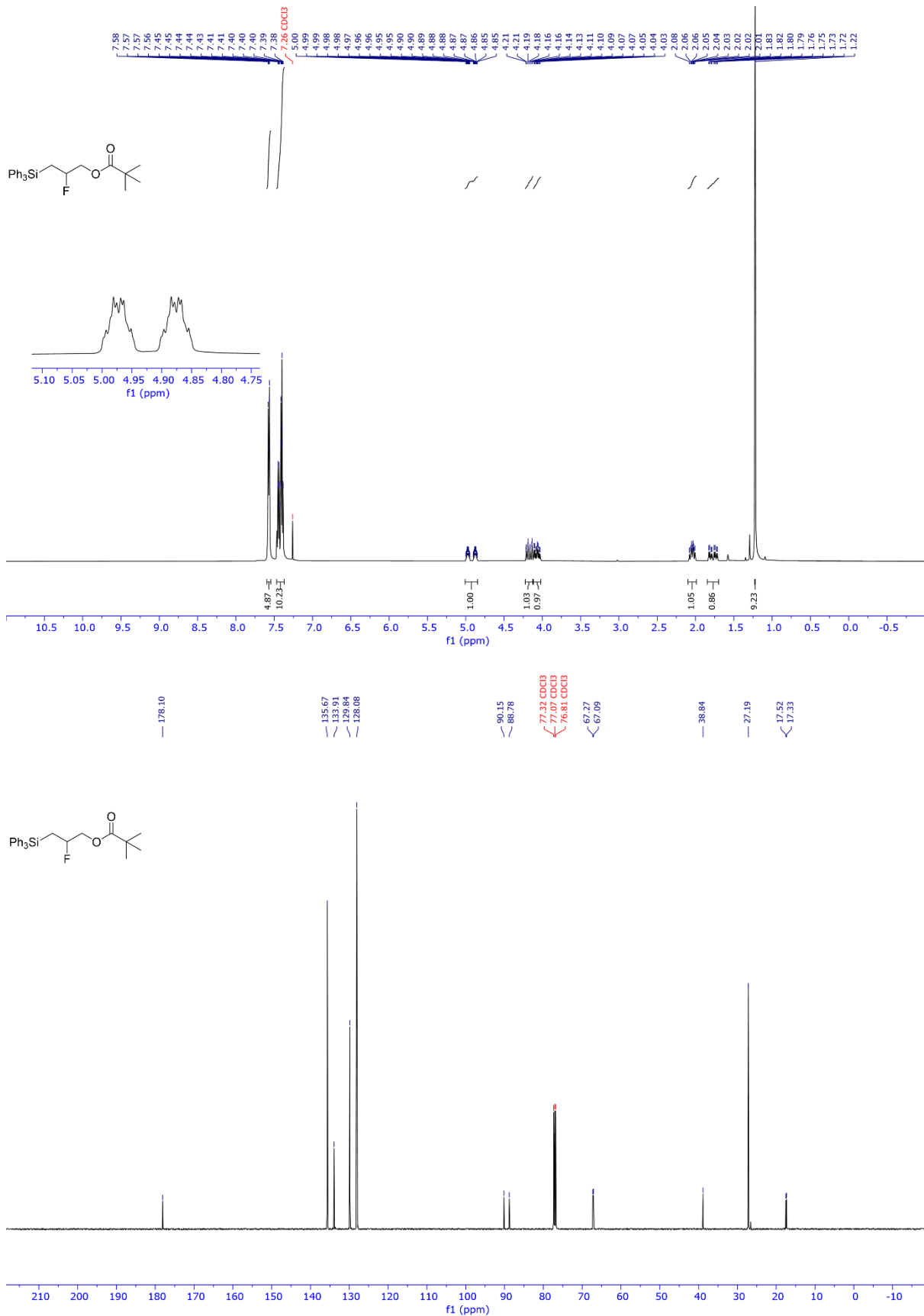


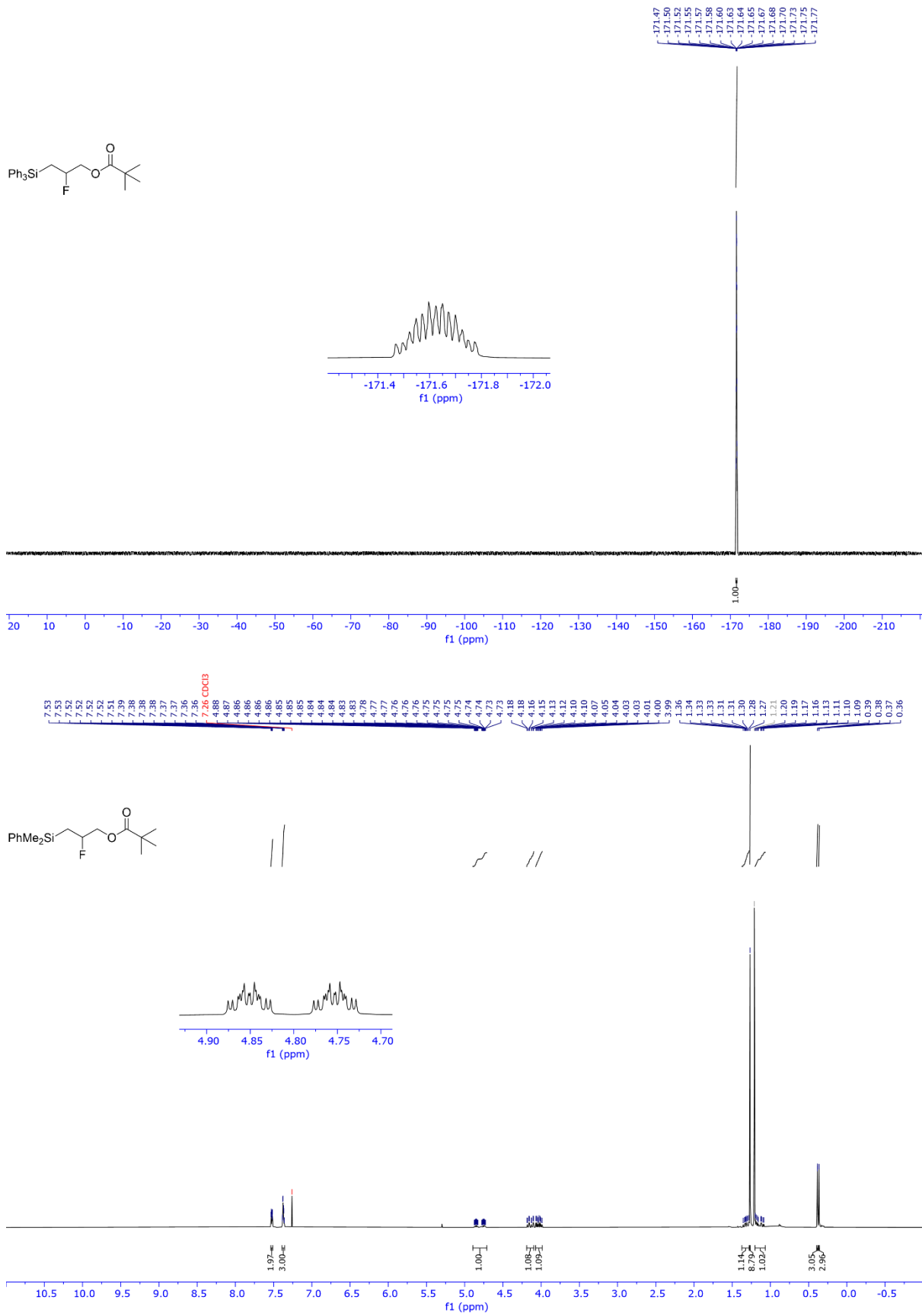


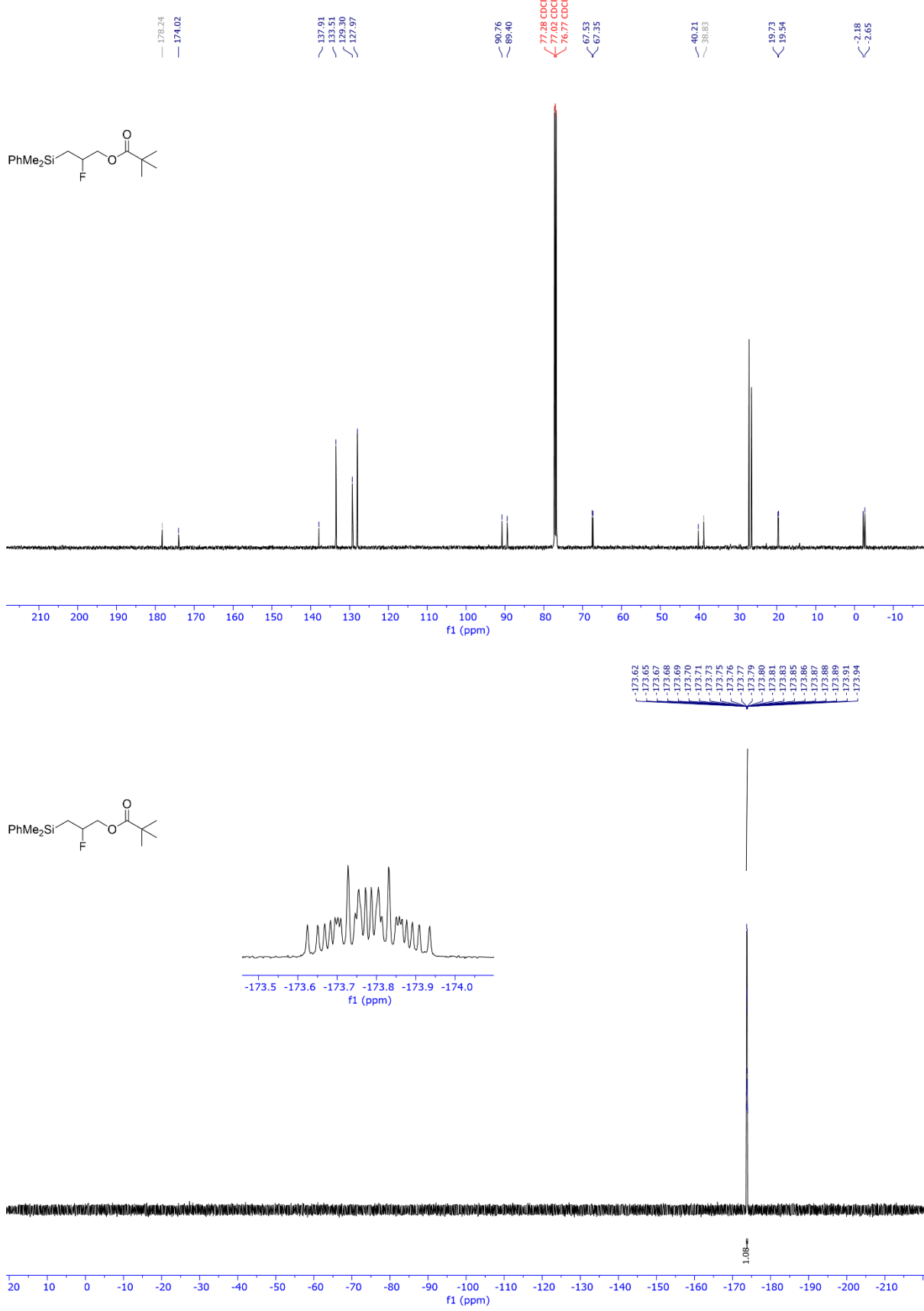


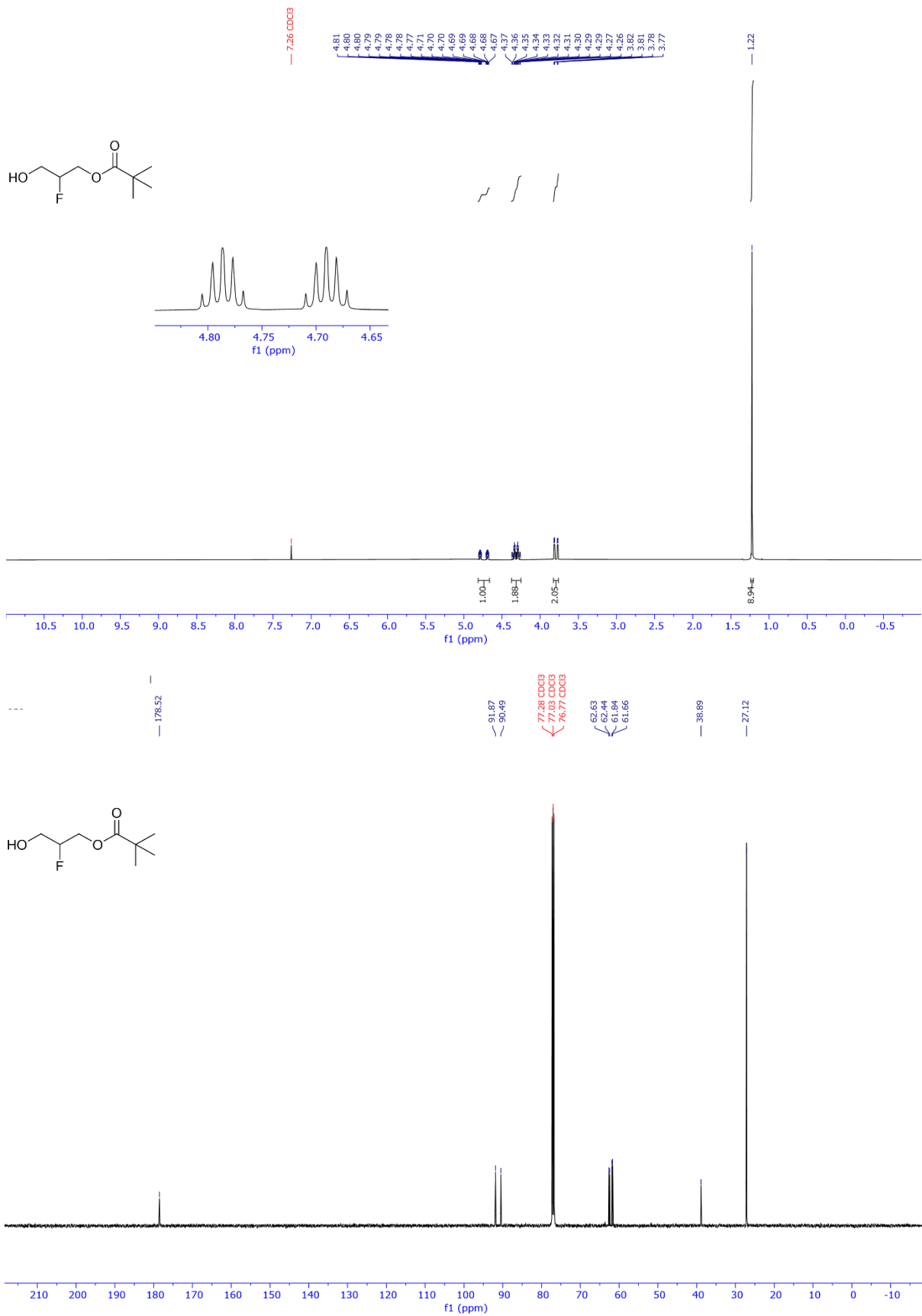


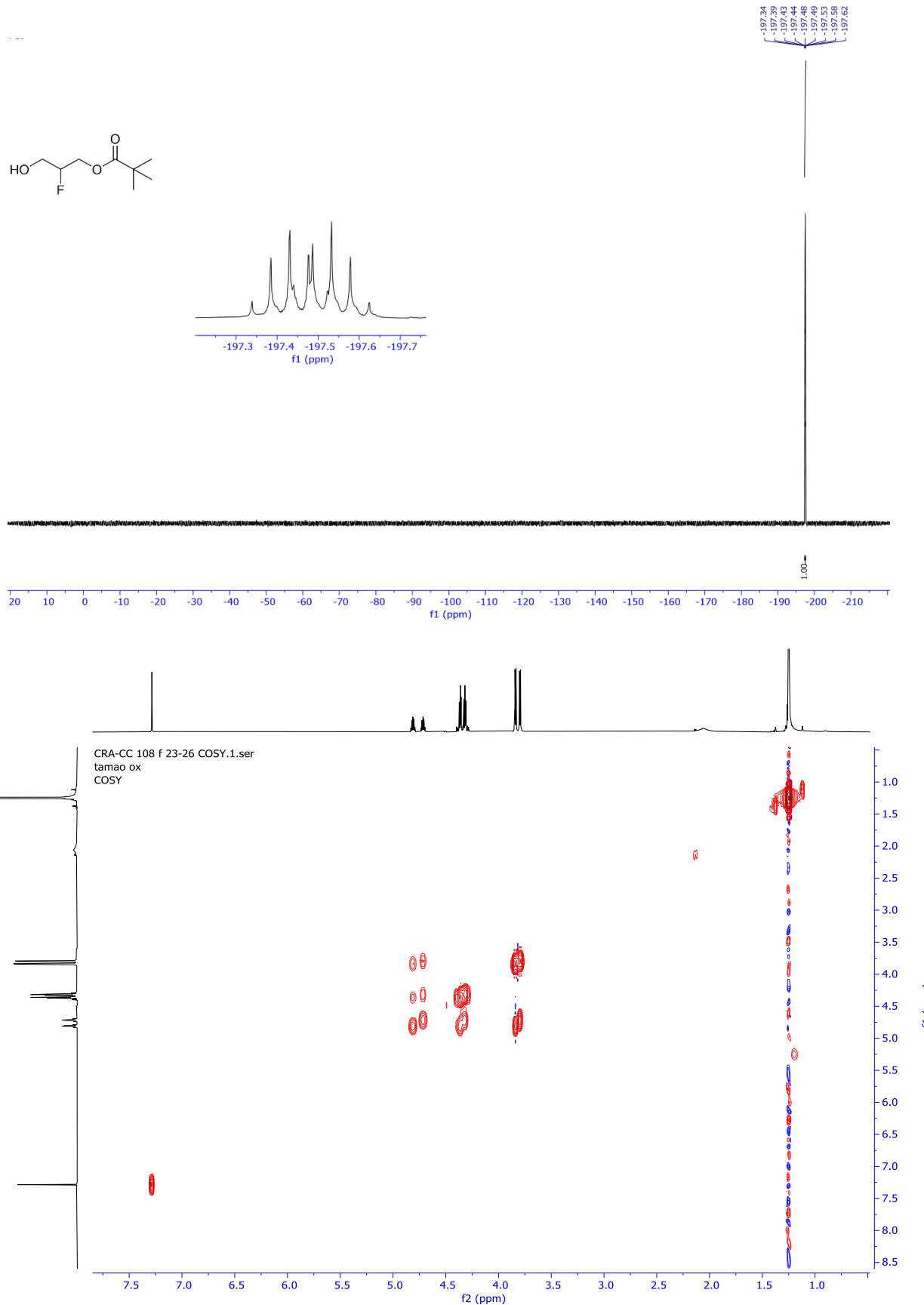


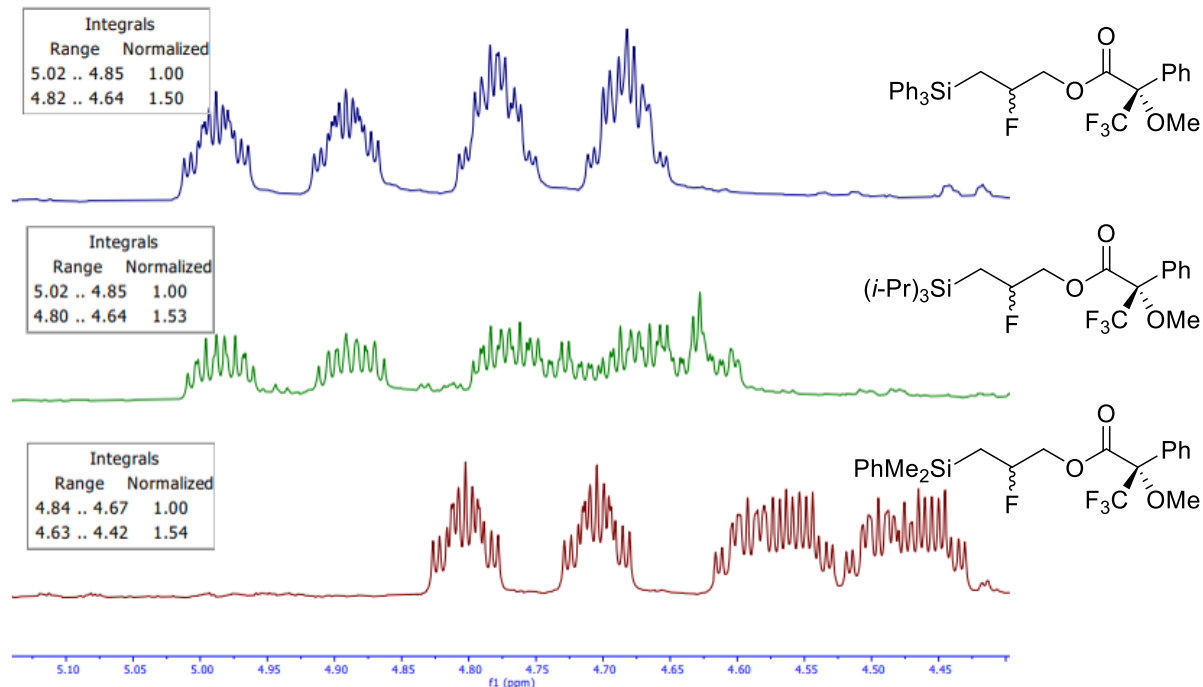












**General Procedure for Mosher Esterification.** Into a flame dried flask under nitrogen atmosphere the fluorohydrin (1 eq) and mosher acid (1.2 eq) were added followed by PhMe (0.02 M) and cooled to -78 °C. While stirring at -78 °C TEA (12 eq), DMAP (25 eq), and 2,4,6-TCBC (11.3 eq) were added and the reaction flask was allowed to stir overnight while warming to room temperature. The mixture was quenched with NaHCO<sub>3</sub> (30 mL) and extracted with EtOAc (3 x 20 mL). The combined organic extracts dried with MgSO<sub>4</sub> and filtered before removing the solvent under reduced pressure. The crude product was purified by flash column chromatography on silica (4:1 hexanes:ethyl acetate, R<sub>f</sub> ~ 0.6-0.7).

## Work Cited

1. Sai, M.; Yamamoto, H. Chiral Brønsted Acid as a True Catalyst: Asymmetric Mukaiyama Aldol and Hosomi-Sakurai Allylation Reactions. *J. Am. Chem. Soc.* **2015**, 137 (22), 7091–7094.
2. Matsuo, J.-I.; Murakami, M. The Mukaiyama Aldol Reaction: 40 Years of Continuous Development. *Angew. Chem. Int. Ed.* **2013**, 52 (35), 9109–9118.
3. Li, L.; Navasero, N. All-Carbon-Substituted Vinylsilane Stable to TBAF: Synthesis of Allyldimethylvinylsilane and Its Pd-Catalyzed Cross-Coupling under Mild Conditions. *Org. Lett.* **2006**, 8 (17), 3733–3736.
4. Landais, Y.; Mahieux, C.; Schenk, K.; Surange, S. S. A New Synthesis and Stereocontrolled Functionalization of Substituted Silacyclopent-3-Enes. *J. Org. Chem.* **2003**, 68 (7), 2779–2789.
5. BouzBouz, S.; Boulard, L.; Cossy, J. Ruthenium-Catalyzed Cross-Metathesis between Diallylsilanes and Electron-Deficient Olefins. *Org. Lett.* **2007**, 9 (19), 3765–3768.
6. Silicon in Organic Synthesis Colvin, E. Butterworth: London **1981**
7. Mayr, H.; Hagen, G. Kinetics of the Reactions of Allylsilanes, Allylgermanes, and Allylstannanes with Carbenium Ions. *J. Am. Chem. Soc.* **1991**, 113, 4954–4961.
8. Lambert, J. B.; Wang, G.; Finzel, R. B; Teramura, D. H. Stabilization of Positive Charge by  $\beta$  Silicon. *J. Am. Chem. Soc.* **1987**, 109, 7838–7845.
9. Akiyama T, Asayama K, Fujiyoshi S. J Chem Soc Perkin Trans 1. **1998**;3655–3656
10. Suslova, E. N.; Albanov, A. I.; Shainyan, B. A. Transformations of Diallylsilanes under the Action of Electrophilic Reagents. *J. Organomet. Chem.* **2009**, 694 (3), 420–426.
11. O’Neil, G. W.; Cummins, E. J. Iodine-Mediated Rearrangements of Diallylsilanes. *Tetrahedron Lett.* **2017**, 58 (35), 3406–3409.
12. Myers, C. R.; Spaltenstein, P.; Baker, L. K.; Schwans, C. L.; Clark, T. B.; O’Neil, G. W. Sequential Iodine-Mediated Diallylsilane Rearrangement/Asymmetric Dihydroxylation: Synthesis and Reactions of Enantioenriched Oxasilacycles. *Tetrahedron Lett.* **2021**, 82.
13. Halder, R.; Ritter, T. 18F-Fluorination: Challenge and Opportunity for Organic Chemists. *J. Org. Chem.* **2021**, 86, 13873–13884.
14. Molnár, I. G.; Gilmour, R. Catalytic Difluorination of Olefins. *J. Am. Chem. Soc.* **2016**, 138 (15), 5004–5007.
15. Banik, S. M.; Medley, J. W.; Jacobsen, E. N. Catalytic, Diastereoselective 1,2-Difluorination of Alkenes. *J. Am. Chem. Soc.* **2016**, 138, 5000–5003.
16. Inoue, M.; Sumii, Y.; Shibata, N. Contribution of Organofluorine Compounds to Pharmaceuticals. *ACS Omega* **2020**, 5 (19), 10633–10640.
17. Gillis, E. P.; Eastman, K. J.; Hill, M. D.; Donnelly, D. J.; Meanwell, N. A. Applications of Fluorine in Medicinal Chemistry. *J. Med. Chem.* **2015**, 58 (21), 8315–8359.
18. Maianti, J. P.; Kanazawa, H.; Dozzo, P.; Matias, R. D.; Feeney, L. A.; Armstrong, E. S.; Hildebrandt, D. J.; Kane, T. R.; Gliedt, M. J.; Goldblum, A. A.; Linsell, M. S.; Aggen, J. B.; Kondo, J.; Hanessian, S. Toxicity Modulation, Resistance Enzyme Evasion, and A-Site X-Ray Structure of Broad-Spectrum Antibacterial Neomycin Analogs. *ACS Chem. Biol.* **2014**, 9 (9), 2067–2073.
19. Walsh, R. Acc. Chem. Res. **1981**, 14, 246–252.
20. Kitamura, T.; Yoshida, K.; Mizuno, S.; Miyake, A.; Oyamada, J. Difluorination of Functionalized Aromatic Olefins Using Hypervalent Iodine/Hf Reagents. *J. Org. Chem.* **2018**, 83 (24), 14853–14860.

21. Centko, R. S.; Mohan, R. S. The Discovery-Oriented Approach to Organic Chemistry. 4. Epoxidation of p-Methoxy-Trans- $\beta$ [Beta]-Methylstyrene: An Exercise in NMR and IR Spectroscopy for Sophomore Organic Laboratories. *J. Chem. Educ.* **2001**, *78* (1), 77.
22. Badali, F.; Issa, W.; Pool, B.; White, J. M. Silicon-Directed Acid Ring-Opening of Allyltrimethylsilane Oxide. X-Ray Structures of 3-Triisopropylsilyl-2-(2,4-Dinitrobenzoyloxy)-1-Propanol and 3-Triisopropylsilyl-2-(2,4,6-Trinitrobenzoyloxy)-1-Propanol. *J. Organomet. Chem.* **1999**, *575* (2), 251–260.
23. Anxionnat, B.; Robert, B.; George, P.; Ricci, G.; Perrin, M.-A.; Gomez Pardo, D.; Cossy, J. Ring Expansion of Cyclic  $\beta$ -Amino Alcohols Induced by Diethylaminosulfur Trifluoride: Synthesis of Cyclic Amines with a Tertiary Fluorine at C3. *J. Org. Chem.* **2012**, *77* (14), 6087–6099.
24. Wang, Z. Meinwald Rearrangement. In: Comprehensive Organic Name Reactions and Reagents; Wiley: Hoboken, NJ, **2010**; pp 1880–1882.
25. Wang, W.; Xu, B.; Hammond, G. Synthesis of Fluorohydrins through Electrophilic Fluorination of Allyl Silanes. *Synthesis (Mass)* **2011**, *2011* (15), 2383–2386.
26. Wilkinson, J. A. Recent Advances in the Selective Formation of the Carbon-Fluorine Bond. *Chem. Rev.* **1992**, *92* (4), 505–519.
27. Dunitz, J. D.; Taylor, R. Organic Fluorine Hardly Ever Accepts Hydrogen Bonds. *Chem. Eur. J.* **1997**, *3* (1), 89–98.
28. Souza, F. R.; Freitas, M. P. Conformational Analysis and Intramolecular Interactions in 2-Haloethanols and Their Methyl Ethers. *Computational and Theoretical Chemistry* **2011**, *964* (1–3), 155–159.
29. Thiehoff, C.; Rey, Y. P.; Gilmour, R. The FluorineGauche Effect: A Brief History. *Isr. J. Chem.* **2017**, *57* (1–2), 92–100.
30. Thiehoff, C.; Holland, M. C.; Daniliuc, C.; Houk, K. N.; Gilmour, R. Can Acyclic Conformational Control Be Achieved via a Sulfur-Fluorine Gauche Effect? *Chem. Sci.* **2015**, *6* (6), 3565–3571.
31. Remete, A. M.; Kiss, L.; Kiss, L. Synthesis of Fluorine-Containing Molecular Entities through Fluoride Ring Opening of Oxiranes and Aziridines. *European J. Org. Chem.* **2019**.
32. Chen, J.-L.; Zheng, F.; Huang, Y.; Qing, F.-L. Synthesis of  $\gamma$ -Monofluorinated Goniothalamin Analogues via Regio- and Stereoselective Ring-Opening Hydrofluorination of Epoxide. *J. Org. Chem.* **2011**, *76* (16), 6525–6533.
33. Al-Maharik, N.; Kirsch, P.; Slawin, A. M. Z.; O'Hagan, D. The Influence of Vicinal Threo-Difluorination on Electro-Optic and Mesogenic Properties of Propyleneoxy-Linked Nematic Liquid Crystals. *Tetrahedron* **2014**, *70* (31), 4626–4630.
34. Brunet, V. A.; Slawin, A. M. Z.; O'Hagan, D. Three Step Synthesis of Single Diastereoisomers of the Vicinal Trifluoro Motif. *Beilstein J. Org. Chem.* **2009**, *5*, 61.
35. Frohn, M.; Wang, Z.-X.; Shi, Y. A Mild and Efficient Epoxidation of Olefins Using in Situ Generated Dimethyldioxirane at High pH. *J. Org. Chem.* **1998**, *63*, 6425–6426.
36. Clover, A. W.; Jones, A. P.; O'Neil, G. Regioselective Fluorohydrin Synthesis from Allylsilanes. **2023**. DOI: [10.26434/chemrxiv-2023-1ncv5](https://doi.org/10.26434/chemrxiv-2023-1ncv5).
37. Sedgwick, D. M.; López, I.; Román, R.; Kobayashi, N.; Okoromoba, O. E.; Xu, B.; Hammond, G. B.; Barrio, P.; Fustero, S. Metal-Free and User-Friendly Regioselective Hydroxyfluorination of Olefins. *Org. Lett.* **2018**, *20* (8), 2338–2341.
38. Wang, Z.-X.; Tu, Y.; Frohn, M.; Zhang, J.-R.; Shi, Y. An Efficient Catalytic Asymmetric Epoxidation Method. *J. Am. Chem. Soc.* **1997**, *119* (46), 11224–11235.

39. Finnegan, D.; Seigal, B. A.; Snapper, M. L. Preparation of Aliphatic Ketones through a Ruthenium-Catalyzed Tandem Cross-Metathesis/Allylic Alcohol Isomerization. *Org. Lett.* **2006**, *8* (12), 2603–2606.
40. Hamlin, T. A.; Kelly, C. B.; Cywar, R. M.; Leadbeater, N. E. Methylenation of Perfluoroalkyl Ketones Using a Peterson Olefination Approach. *J. Org. Chem.* **2014**, *79* (3), 1145–1155.
41. Ramesh, R.; Reddy, D. S. Quest for Novel Chemical Entities through Incorporation of Silicon in Drug Scaffolds. *J. Med. Chem.* **2018**, *61* (9), 3779–3798.
42. Jones, G. R.; Landais, Y. The Oxidation of the Carbon-Silicon Bond. *Tetrahedron* **1996**, *52* (22), 7599–7662.
43. Fleming, I.; Henning, R.; Parker, D. C.; Plaut, H. E.; Sanderson, P. E. J. The Phenyldimethylsilyl Group as a Masked Hydroxy Group. *J. Chem. Soc., Perkin Trans. 1* **1995**, No. 4, 317.
44. Yamashita, Y.; Minami, K.; Kobayashi, S. Catalytic Addition Reactions of Alkylazaarenes to Vinylsilanes. *Chem. Lett.* **2018**, *47* (5), 690–692.
45. Matsumura, Y.; Suzuki, T.; Sakakura, A.; Ishihara, K. Catalytic Enantioselective Inverse Electron Demand Hetero-Diels-Alder Reaction with Allylsilanes. *Angew. Chem. Int. Ed* **2014**, *53* (24), 6131–6134.
46. Fleming, I.; Winter, S. B. D. Controlling the Stereochemistry at C-15 in Prostaglandin Synthesis Using a Stereoconvergent Allylsilane Synthesis and a Silyl-to-Hydroxy Conversion. *Tetrahedron Lett.* **1995**, *36* (10), 1733–1734.
47. Hosomi, A.; Sakurai, H. Protection of Alcohols and Acids with Allylsilanes Catalyzed by Iodine or Iodotrimethylsilane in Chlorinated Hydrocarbon. *Chem. Lett.* **1981**, *10* (1), 85–88.
48. Ibrahim, S. M. S.; Banerjee, K.; Slater, K. A.; Friestad, G. K. A Tamao–Fleming Oxidation Route to Dipeptides Bearing N, O-Acetal Functionality. *Tetrahedron Lett.* **2017**, *58* (52), 4864–4866.
49. Li, Y.; Yao, Y.; Yu, L.; Tian, C.; Dong, M. Mechanistic Investigation of B12-Independent Glycerol Dehydratase and Its Activating Enzyme GD-AE. *Chem. Commun.* **2022**.
50. Linclau, B.; Ardá, A.; Reichardt, N.-C.; Sollogoub, M.; Unione, L.; Vincent, S. P.; Jiménez-Barbero, J. Fluorinated Carbohydrates as Chemical Probes for Molecular Recognition Studies. Current Status and Perspectives. *Chem. Soc. Rev.* **2020**.
51. R. Rablen, P.; W. Hoffmann, R.; A. Hrovat, D.; Thatcher Borden, W. Is Hyperconjugation Responsible for the “Gauche Effect” in 1-Fluoropropane and Other 2-Substituted-1-Fluoroethanes? †. *J. Chem. Soc., Perkin Trans. 2* **1999**, No. 8, 1719–1726.
52. Emenike, B. U.; Farshadmand, A.; Zeller, M.; Roman, A. J.; Sevimler, A.; Shinn, D. W. Electrostatic CH-π Interactions Can Override Fluorine Gauche Effects To Exert Conformational Control. *Chem. Eur. J* **2023**, *29* (6), e202203139.
53. Dolbier, W. R. *Guide to Fluorine NMR for Organic Chemists*. Chapter 2; John Wiley & Sons, Inc.: Hoboken, NJ, USA, **2009**.
54. Briggs, C. R. S.; O’Hagan, D.; Rzepa, H. S.; Slawin, A. M. Z. Solid State and Theoretical Evaluation of β-Fluoroethyl Esters Indicate a Fluorine-Ester Gauche Effect. *J. Fluor. Chem.* **2004**, *125* (1), 19–25.
55. Thacker, J. C. R.; Popelier, P. L. A. Fluorine Gauche Effect Explained by Electrostatic Polarization Instead of Hyperconjugation: An Interacting Quantum Atoms (IQA) and Relative Energy Gradient (REG) Study. *J. Phys. Chem. A* **2018**, *122* (5), 1439–1450.
56. Bruker (2007) APEX2 (Version 2.1-4), SAINT (version 7.34A), SADABS (version 2007/4), BrukerAXS Inc, Madison, Wisconsin, USA.
57. Sheldrick, G. M. (2005). CELL\_NOW. University of Goettingen, Germany.

58. Bruker (2007) APEX2 (Version 2.1-4), SAINT (version 7.34A), SADABS (version 2007/4), BrukerAXS Inc, Madison, Wisconsin, USA.
59. Sheldrick, G. M. (2007). TWINABS. University of Goettingen, Germany.
60. (a) Sheldrick GM. (2008) A short history of SHELX. *Acta Cryst. A*64, 112-122.  
(b) Sheldrick GM. (2015) SHELXT - Integrated space-group and crystal-structure determination. *Acta Cryst. A*71, 3-8.
61. (a) Altomare A, Burla C, Camalli M, Cascarano G L, Giacovazzo C, Guagliardi A, Moliterni AGG, Polidori G, Spagna R. (1999) SIR97: a new tool for crystal structure determination and refinement *Journal of Applied Crystallography*, 32, 115-119.  
(b) Altomare A, Cascarano G L, Giacovazzo C, Guagliardi A. (1993) Completion and refinement of crystal structures with SIR 92. *Journal of Applied Crystallography*, 26, 343-350.
62. (a) Sheldrick GM. (1997) SHELXL-97, Program for the Refinement of Crystal Structures. University of Göttingen, Germany.  
(b) Sheldrick GM. (2015) Crystal structure refinement with SHELXL. *Acta Cryst. C*71, 3–8
63. Waasmaier, D.; Kirsch, A. (1995) New Analytical Scattering Factor Functions for Free Atoms and Ions. *Acta Crystallographica A.*, 51, 416-430.
64. Farrugia LJ. (1997) Ortep-3 for Windows. *Journal of Applied Crystallography*, 30, 56.